NASA TECHNICAL MEMORANDUM

NASA TM X-64841
Revision A

SSME/SIDE LOADS ANALYSIS FOR FLIGHT CONFIGURATION

By Wayne Holland
Systems Dynamics Laboratory

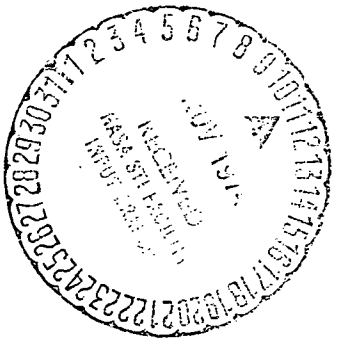

September 1974

NASA

George C. Marshall Space Flight Center
Marshall Space Flight Center, Alabama

MSFC - Form 3190 (Rev June 1971)

TECHNICAL REPORT STANDARD TITLE PAGE

1. REPORT NO.	2. GOVERNMENT ACCESSION NO.	3. RECIPIENT'S CATALOG NO.
NASA TM X-64841, Revision A		

4. TITLE AND SUBTITLE	5. REPORT DATE
SSME/Side Loads Analysis for Flight Configuration	September 1974
	6. PERFORMING ORGANIZATION CODE

7. AUTHOR(S)	8. PERFORMING ORGANIZATION REPORT #
Wayne Holland	

9. PERFORMING ORGANIZATION NAME AND ADDRESS	10. WORK UNIT NO.
George C. Marshall Space Flight Center Marshall Space Flight Center, Alabama 35812	11. CONTRACT OR GRANT NO.
	13. TYPE OF REPORT & PERIOD COVERED
12. SPONSORING AGENCY NAME AND ADDRESS	Technical Memorandum
National Aeronautics and Space Administration Washington, D. C. 20546	14. SPONSORING AGENCY CODE

15. SUPPLEMENTARY NOTES

Prepared by Systems Dynamics Laboratory, Science and Engineering

16. ABSTRACT

This document describes the dynamic loads analysis accomplished for the Sapce Shuttle Main Engine (SSME) considering the side load excitation associated with transient flow separation on the engine bell during ground ignition. The results contained herein pertain only to the flight configuration. A Monte Carlo procedure was employed to select the input variables describing the side load excitation and the loads were statistically combined. This revision includes an active thrust vector control system representation and updated orbiter thrust structure stiffness characteristics. No future revisions are planned but may be necessary as system definition and input parameters change.

17. KEY WORDS	18. DISTRIBUTION STATEMENT
	Unclassified-unlimited

19. SECURITY CLASSIF. (of this report)	20. SECURITY CLASSIF. (of this page)	21. NO. OF PAGES	22. PRICE
Unclassified	Unclassified	90	NTIS

For sale by National Technical Information Service, Springfield, Virginia 22151

TABLE OF CONTENTS

	Page
INTRODUCTION	1
STRUCTURAL MODEL	1
TVC ACTUATOR MODEL	2
SIDE LOAD FORCING FUNCTIONS	2
MONTE CARLO LOADS ANALYSIS	4
OUTPUT	8
RESULTS	9
APPENDIX: METHODOLOGY	61

LIST OF ILLUSTRATIONS

Figure	Title	Page
1.	SSME-orbiter configuration	11
2.	Node points and coordinate system	12
3.	SSME structural model	13
4.	Element coordinate system	14
5.	Servoactuator schematic	15
6.	Distribution of J-2S rms amplitude for 1.6 Hz bandwidth F*	16
7.	Side load transient no. 1	18
8.	Side load transient no. 2	19
9.	Side load transient no. 3	20
10.	Side load transient no. 4	21
11.	Side load transient no. 5	22
12.	Side load transient no. 6	23
13.	Side load transient no. 7	24
14.	Side load transient no. 8	25
15.	Side load transient no. 9	26
16.	Side load transient no. 10	27
17.	Side load transient no. 11	28
18.	Side load transient no. 12	29
19.	Side load transient no. 13	30

LIST OF ILLUSTRATIONS (Concluded)

Figure	Title	Page
20.	Side load transient no. 14	31
21.	Side load transient no. 15	32
22.	Side load transient no. 16	33
23.	Side load transient no. 17	34
24.	Side load transient no. 18	35
25.	Side load transient no. 19	36
26.	Side load transient no. 20	37
27.	Side load transient no. 21	38
28.	Side load transient no. 22	39
29.	Side load transient no. 23	40
30.	Side load transient no. 24	41
31.	Actuator no. 1 load time history engine 2, start position, excitation case 1 peak side load excitation = 13 613.3 lb	42
32.	Actuator no. 2 load time history engine 2, start position, excitation case 1 peak side load excitation = 13 613.3 lb	43
A-1.	Applied forces for engine without actuators	62
A-2.	Actuator geometry	72

LIST OF TABLES

Table	Title	Page
1.	Degree of Freedom Table	44
2.	Identification of SSME Ducts	45
3.	Identification of Structural Elements Selected for Loads Output	45
4.	Servoactuator Parameters	46
5.	Randomly Selected Input Data	47
6.	Peak Force of Side Load Transients	49
7.	Identification of Output Set A	50
8.	Identification of Output Set B	53
9.	Statistical Values — Output Set A, Engine 1 — Start Position	55
10.	Statistical Values — Output Set B, Engine 1 — Start Position	57
11.	Statistical Values — Output Set A, Engine 2 — Start Position	58
12.	Statistical Values — Output Set B, Engine 2 — Start Position	60

ABBREVIATIONS

C.G.	center of gravity
C. L.	centerline
FORMA	Fortran matrix analysis computer subroutine library
HPFTP	high pressure fuel turbo pump
HPOTP	high pressure oxidizer turbo pump
LPFTP	low pressure fuel turbo pump
LPOTP	low pressure oxidizer turbo pump
NASTRAN	NASA structural analysis program
TVC	thrust vector control
SSME	Space Shuttle Main Engine

TECHNICAL MEMORANDUM X-64841

SSME/SIDE LOADS ANALYSIS FOR FLIGHT CONFIGURATION

INTRODUCTION

This memorandum presents the results of a comprehensive Monte Carlo dynamic loads analysis of the Space Shuttle Main Engine (SSME) for the side load transients produced by flow separation in the engine bell during ground ignition. The side load excitation is a transient phenomenon which occurs during ignition of an engine that has a high expansion ratio nozzle like the SSME. The previous publication of this document is revised herein to include a more refined structural model of the engine and the orbiter thrust structure and to include an active thrust vector control system (in the previous analysis the actuators were simulated with "equivalent" springs). The results presented herein pertain only to the flight configuration; test configurations that include constraints on the engine different from the flight configuration will require additional analysis.

STRUCTURAL MODEL

The structural modeling and vibration analysis were accomplished by the Structural Dynamics Section, S&E-ASTN-ADS, MSFC. The dynamic response of the engines is greatly influenced by the stiffness characteristics of the orbiter thrust structure at the interfaces with the engine. The orbiter thrust structure flexibility matrix was supplied by Rockwell International, Space Division. The flexibility coefficients are different for each engine and for each engine/thrust structure interface point. This necessitates a structural model for each engine. The engine locations, their orientations, and coordinate axes are shown in Figure 1. The description of the structural models and their vibration analyses are documented in MSFC memorandums S&E-ASTN-ADS (74-23) and S&E-ASTN-ADS (74-25). The frequency of the pendulum mode (first mode) was determined to be 8.49 Hz, 9.42 Hz, and 8.15 Hz for engine numbers 1, 2, and 3, respectively.

Figure 2 presents the NASTRAN node points and coordinate system for the structural idealization. Table 1 shows the degrees of freedom and grid

point coordinates. The structural models of all the engines are identical; only the backup structure differs for each engine. Two coordinate systems are identified in Table 1. Coordinate system no. 4 is fixed with its origin at the gimbal point. Coordinate system no. 3 is rotated with respect to coordinate system no. 4 to obtain the various start positions specified for each engine. Five propellant ducts were included in the structural model and are identified in Table 2. A sketch indicating the most pertinent nodes for this analysis is shown in Figure 3. It is noted that the actuators are not included as part of the structural model. For this analysis the mode shapes of the "dangling" engine (engine without actuators) are used. The actuators are simulated as feedback control systems via the transient response equations (see Appendix for details).

The structural elements monitored for loads are identified in Table 3. The NASTRAN sign convention is used for element loads and is shown on Figure 4. A model damping value of $\zeta = 0.01$ was used in all the "dangling" modes. Modes were retained through 100 Hz in the transient response analysis.

TVC ACTUATOR MODEL

All actuators in the orbiter thrust vector control system are not identical. However, for this study all were assumed to be identical to the pitch actuator on engine 1. The actuator locations are shown in Figure 1. The pitch actuator on engine 1 is being developed by MSFC and presently is the only one for which a dynamic model is available. All the actuators are expected to behave in approximately the same way, dynamically. A description of the actuator model is provided in MSFC memorandum, S&E-ASTR-GM-140-74, SSME TVC Actuator Block Diagram for Transient Load Analysis, dated April 16, 1974. The block diagram is shown on Figure 5 and the actuator parameters are tabulated in Table 4. The procedure used to couple the actuator model to the structural model is explained in the Appendix.

SIDE LOAD FORCING FUNCTIONS

The SSME side load forcing functions were obtained by scaling J-2S side load data to the SSME. The J-2S data were gathered and analyzed by Rocketdyne from J-2S firing data and J-2S dynamic shake test data. Rocketdyne supplied an analog tape containing 24 side load transients and a 40 Hz bandwidth white noise signal from which the transients were obtained. These transients were derived by shaping the white noise signal as indicated in the following block diagram.

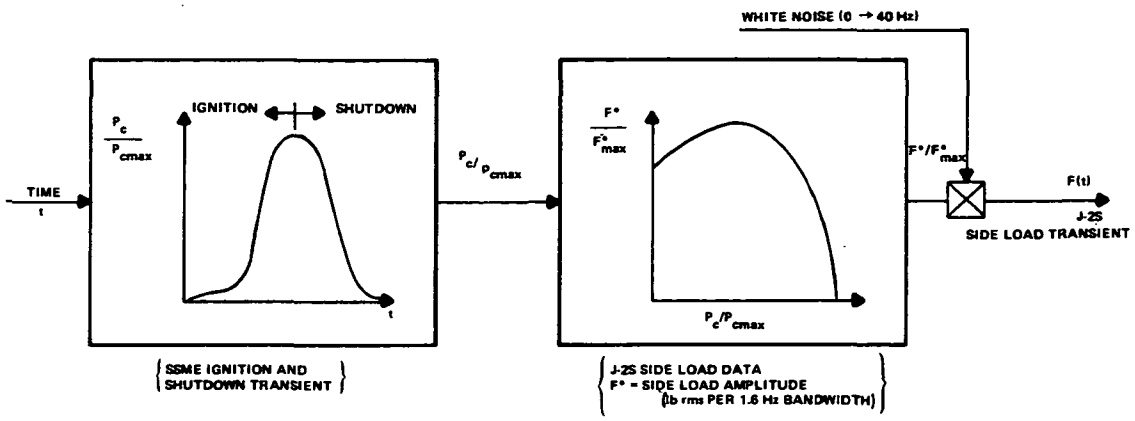

The J-2S side load data were extracted at the bell exit; i.e., grid point 33 on Figure 2. It is observed that the magnitude of the side load transient is directly related to F^*_{max}, the rms force per 1.6 Hz bandwidth of the white noise. Data scatter was observed in determining F^*_{max} from various measurements (load cells and accelerometers). Thus this parameter is treated as a random variable in the Monte Carlo analysis. The statistical distribution for F* was generated from test data supplied by Rocketdyne.[1] The data were taken from test 043 for the time slice corresponding to the operating point for maximum side loads. The data points included measurements from both load cells and accelerometers. The distribution is presented in Figure 6. Rocketdyne's assessment of all valid test data had previously yielded a mean $+3\sigma$ value of 1600 lb rms per 1.6 Hz bandwidth for J-2S side load. Correspondingly, the distribution in Figure 6 was adjusted to yield the same mean $+3\sigma$ value.

The analog data tape supplied by Rocketdyne was digitized by R-COMP-RRV at MSFC. Plots of the digitized transients are presented in Figures 7 through 30. The digitized transients are referenced to F^*_{max} = 1432 lb rms per 1.6 Hz resolution bandwidth. It was observed that the digitization at 400 samples per second tended to generally decrease the peak value of the transient by about 10 percent.

Information with regard to directionality of the side load excitation was not available from J-2S data. For this analysis the direction of the side load excitation, θ, (Fig. 1) is assumed variable from 0 deg to 360 deg and is considered to be constant for each side load transient. Thus, θ is a random variable for the Monte Carlo analysis with uniform distribution between 0 deg and 360 deg.

1. Internal Letter SSME 73-3199, Statistical Evaluation of J-2S Side Load Data for SSME, November 15, 1973.

To obtain side load excitation applicable for the SSME, the J-2S data are multiplied by a scale factor, $R_{SSME/J-2S}$. This scaling factor is also treated as a random variable. The distribution for the scaling factor is normal with mean equal to 1.53 and a standard deviation of 0.06. This information was supplied by S&E-ASTN-PPT, MSFC.

In view of the above discussion the x and y components of a side load excitation acting on grid point 33 are expressed as

$$F_x(t) = \left(\frac{F^*}{1432}\right) (\cos\theta) (R_{SSME/J-2S}) (1.1) F_i(t) \qquad (1)$$

and

$$F_y(t) = \left(\frac{F^*}{1432}\right) (\sin\theta) (R_{SSME/J-2S}) (1.1) F_i(t) \quad , \qquad (2)$$

where $F_i(t)$ is one of the 24 side load transients presented in Figures 7 through 30; i.e., i = 1, 2, 3, . . . 24. The transient number, i , is also treated as a random variable uniformly distributed between 1 and 24. The factor 1.1 is included to account for the decrease in peak values associated with digitization of the analog tape.

It is observed that this description of the side load forcing function involves four variables F*, θ, $R_{SSME/J-2S}$, and $F_i(t)$. Considering the ranges and various combinations of these variables, an infinitude of side load forcing functions can be defined.

MONTE CARLO LOADS ANALYSIS

There are at least two methods for determining dynamic loads and responses. One method is to calculate loads based upon discrete values of the input parameters selected by judgment from the entire range of possible input data. If judgment and experience are sufficient to identify the combination of parameters yielding maximum loads, the resulting maximum load may be

unduly conservative. For example, if the worst combination of the four variables involved in the SSME side loads analysis is selected as input, the resulting loads will exceed the design values. A second method is to utilize the Monte Carlo technique. This involves drawing samples of the input parameters from their parent populations through sampling procedures governed by specified probability laws.

For this analysis the input parameters which define the side load excitation are treated as random variables. These parameters are as follows:

1. F*, the amplitude of the J-2S side load, lb rms per 1.6 Hz bandwidth.

2. θ, the direction of the side load excitation.

3. $R_{SSME/J-2S}$, the scaling factor from J-2S data to SSME.

4. $F_i(t)$, the side load transient number, i, from the set of 24 available.

Values of the above variables were drawn to define 100 side load forcing functions. The procedure used herein for drawing the variables according to their probability laws is based upon a sequence of random numbers, ρ_i, uniformly distributed in the unit interval $0 \leq x \leq 1$. UNIVAC library subroutine RANDOM was used to generate 400 random numbers uniformly distributed between 0 and 1. Four of these are used to determine values of the input variables for each of the 100 cases. Having determined the random numbers, ρ_i, to select samples of random variable, ξ, with distribution $F(x)$ one must solve the equation

$$\rho = F(x) \tag{3}$$

for x as a function of ρ. The solution is

$$x = \phi(\rho) \quad . \tag{4}$$

Substitute the random numbers ρ_i into the right side of equation (4) and obtain a set of numbers, t_i, as

$$t_i = \phi(\rho_i) \quad . \tag{5}$$

The numbers t_i are distributed according to the distribution $F(x)$.[2] The input variables for this study defined using this random selection technique are presented in Table 5. The peak values of the resulting side load forcing functions are presented in Table 6.

Using the 100 side load forcing functions generated by the random selections procedure, 100 transient response cases were run resulting in peak loads and accelerations for each case. The peak loads and acceleration data are combined statistically, resulting in a single set of loads to be used for strength assessment purposes. The combination of load is

$$L = \bar{L} \pm KS,$$

where

L = statistical load,

K = number of standard deviations desired,

S = sample standard deviation of the load

$$= \left[\frac{\sum_{i=1}^{N} (\bar{L} - L_i)^2}{N} \right]^{1/2} ,$$

2. Monte Carlo Principles and Neutron Transport Problems, by Jerome Spanier and Ely Gelbard.

$\bar{L}$ = mean value of the N cases, $= \frac{1}{N} \sum_{i=1}^{N} L_i$,

N = number of cases, (100 for this analysis) ,

and

L_i = peak value (maximum or minimum) for case i.

Since a finite sample size is used to form the statistical load (100 cases in this analysis), confidence limits are applied to obtain an estimate of the upper limit on the true value of the statistical load. The confidence limits are determined by modifying the K value to assure that a load having K sigma probability will not be exceeded. This new modified value of K is designated K_p.[3] The load combination thus becomes

$$L = \bar{L} \pm K_p S$$

where

$$K_p = \frac{K \pm \left[K^2 - \left(1 - \frac{Z_p^2}{2(N-1)} \right) \left(K^2 - \frac{Z_p^2}{N} \right) \right]^{1/2}}{\left[1 - \frac{Z_p^2}{2(N-1)} \right]} ,$$

K = number of standard deviations (three for this analysis),

3. The expression for K_p is explained in Monte Carlo Dynamic Analysis for Lunar Module Loads, by Merchant and Sandy, Journal of Spacecraft and Rockets, Vol. 8, No. 1, January 1971.

Z_p = point on the normal density curve corresponding to the desired confidence level,

Z_p = 1.645 for 95 percent confidence level (used in this analysis)

and

N = number of cases (100 in this analysis).

Summarizing, the following steps were taken to determine the statistical loads and accelerations for the SSME side load excitation problem:

1. 100 sets of randomly selected input parameters are chosen.

2. 100 transient analyses are accomplished to obtain 100 cases of loads.

3. Peak (maximum and minimum) loads are obtained and are assumed to have a Gaussian distribution.

4. A mean and standard deviation are computed.

5. A statistical load is computed for strength analysis. This load is defined to be the upper confidence limit on the 3σ load corresponding to a 95 percent confidence level.

OUTPUT

Since the three dynamic models of the engines are different, because of differing backup structure and orientations, they will necessarily yield different load responses. For expediency engine 3 was not considered; the justification for this is as follows:

Previous analysis indicates that in general the loads tend to increase as the pendulum frequency increases. Engine 2 has the highest pendulum frequency and thus must be considered. Engine 1 being the upper engine is also considered for completeness and comparison. Thus one has loads for both a lower engine, engine 2, and the upper engine, engine 1.

The transient response analysis was accomplished using the 100 forcing functions generated as described above. The engines were in the start positions,[4] which are identified in Figure 1.

The response data for each engine was divided into two sets, output set A and output set B. The actuator loads and element loads are presented in output set A. Displacement and acceleration responses are in output set B. The coordinates (or rows) of output sets A and B are identified in Tables 7 and 8, respectively. The statistical values of output set A and output set B for engine 1 are presented in Tables 9 and 10, respectively. Similarly, output set A and output set B data for engine 2 are presented in Tables 11 and 12, respectively. The statistical values represent the upper confidence limit on the 3σ value for a 95 percent confidence level as determined from the 100 case samples. The mean values and standard deviations are included for information only. For strength assessment the statistical values should be used.

RESULTS

Results of particular interest are extracted from the output tables and tabulated below.

1. Actuator Load:

   Maximum = 69 980 lb (Compression), Table 9, row 2

   Minimum = 73 020 lb (Tension), Table 9, row 2

2. Throat Bending Moment Load:

   Peak = 2 672 000 in.-lb, Table 9, row 43

3. Gimbal Bearing Center Torsion Load:

   Peak = 598 200 in.-lb, Table 11, row 13

4. Rockwell Internal Letter, P&PS-GHC-73-029, April 26, 1973.

4. High Pressure Fuel Pump Acceleration:

   Translational:

   Peak = 25.5 g, Table 10, row 22

   Rotational:

   Peak = 1.23 g/in., Table 10, row 26

5. High Pressure Oxidizer Pump Acceleration

   Translational:

   Peak = 33.06 g, Table 10, row 30

   Rotational:

   Peak = 1.16 g/in., Table 10, row 34

6. Nozzle Exit Displacement

   Peak = 2.19 in., Table 12, row 3

The actuator incorporates a bypass which opens at an actuator load of 90 000 lb. The 3σ actuator load (73 020 lb) is well below the bypass value. It is interesting that for each engine only one case out of the 100 cases resulted in an actuator load exceeding the bypass value.

The nozzle exit displacement of 2.2 in. is well within the available rattle space of approximately 18 in. To demonstrate the transient character of the response data, time histories of actuator loads for a specific case are presented in Figures 31 and 32. These time histories are typical of those obtained for all cases examined.

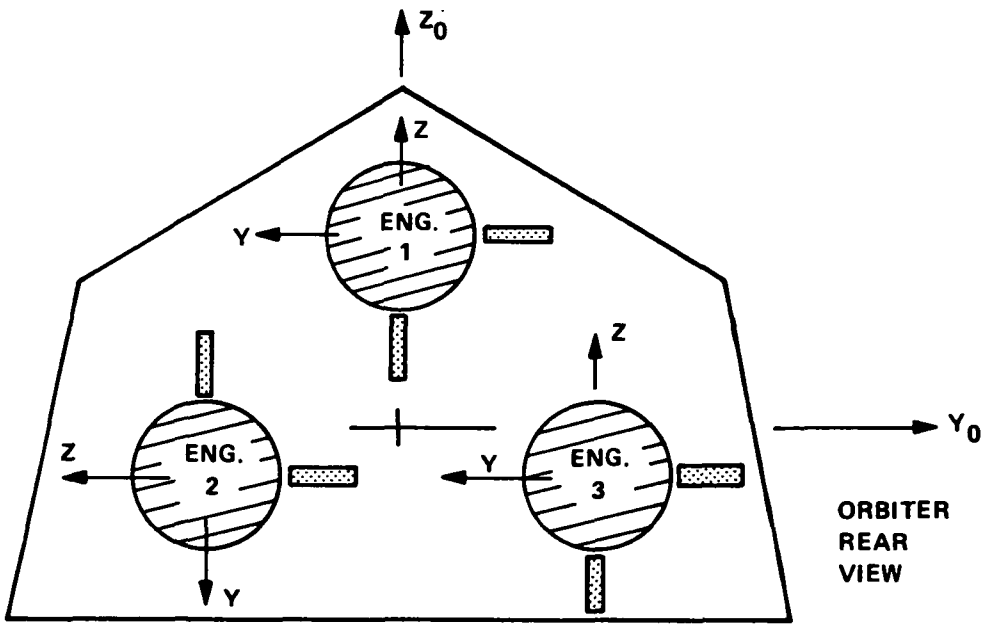

ACTUATOR

X_0, Y_0, Z_0 ORBITER COORDINATE AXES

X, Y, Z ENGINE COORDINATE AXES

ENGINE NUMBER	NULL POSITION		START POSITION	
	PITCH	YAW	PITCH	YAW
1	16 DEG	0 DEG	18 DEG	0 DEG
2&3	10 DEG	3.5 DEG	7 DEG 40 MIN	5 DEG 10 MIN

NOTES: ENGINES CANTED OUTBOARD IN YAW
ENGINES CANTED BELL UP IN PITCH

Figure 1. SSME-orbiter configuration.

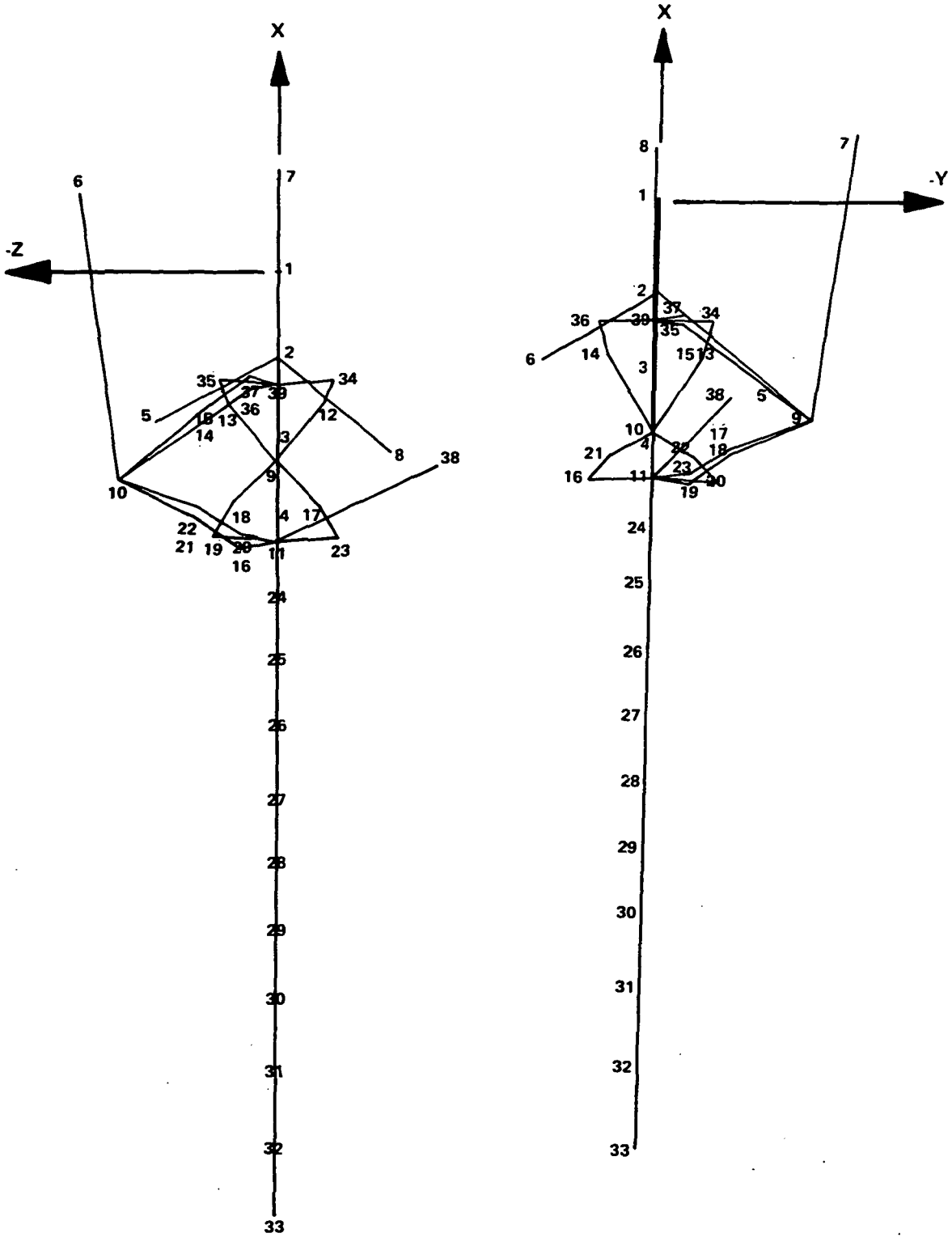

Figure 2. Node points and coordinate system.

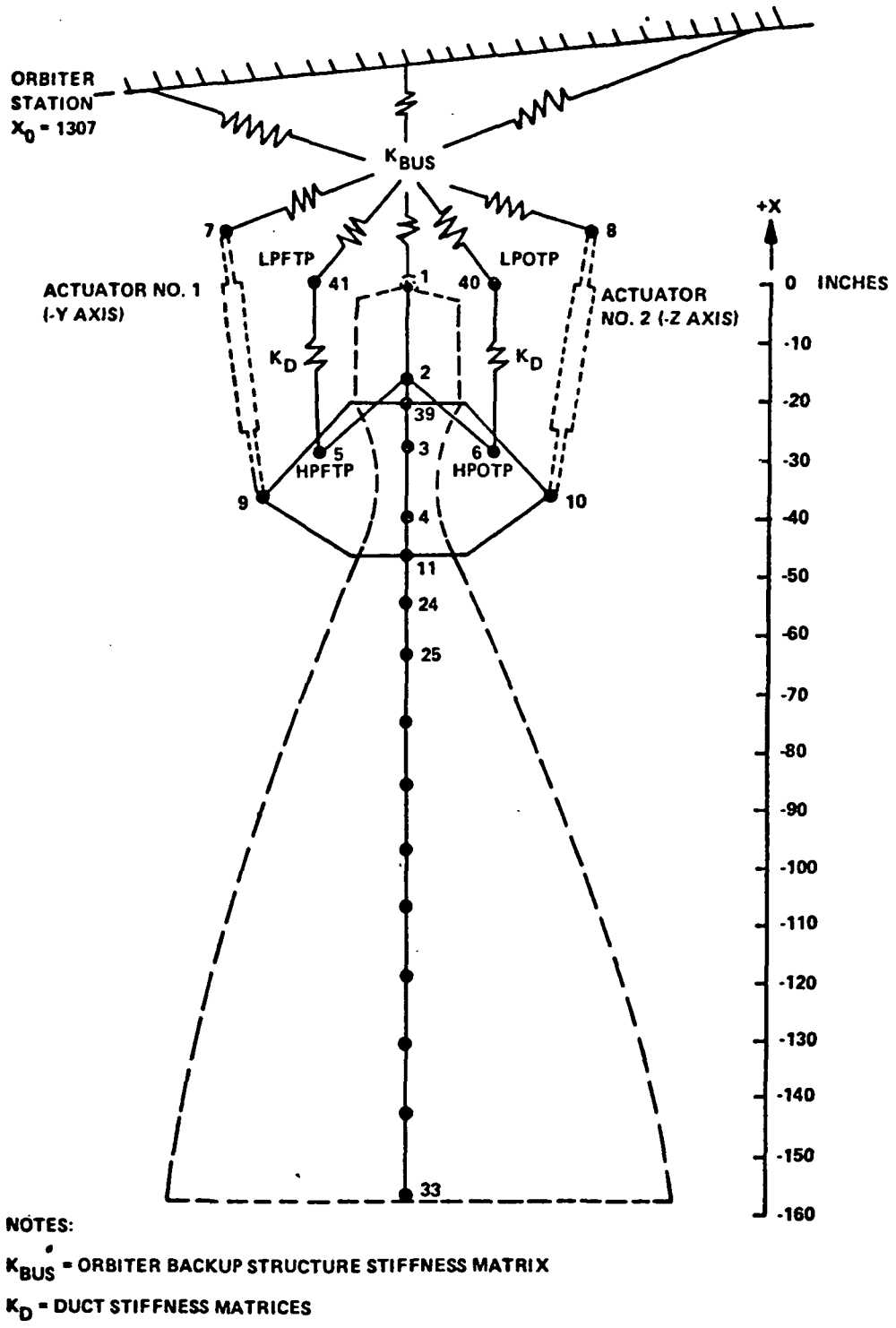

Figure 3. SSME structural model.

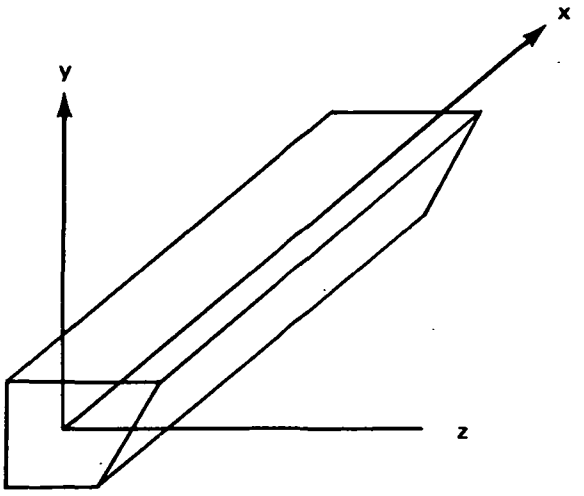

(a) ELEMENT COORDINATE SYSTEM

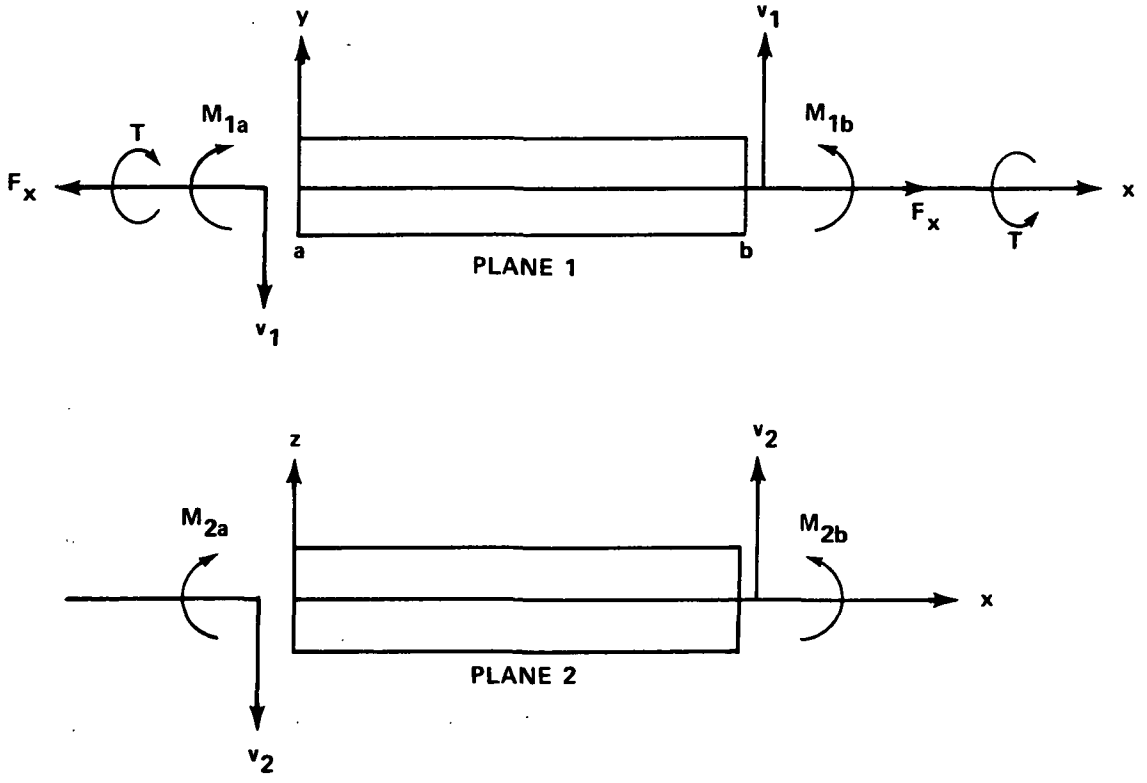

(b) ELEMENT FORCES

Figure 4. Element coordinate system.

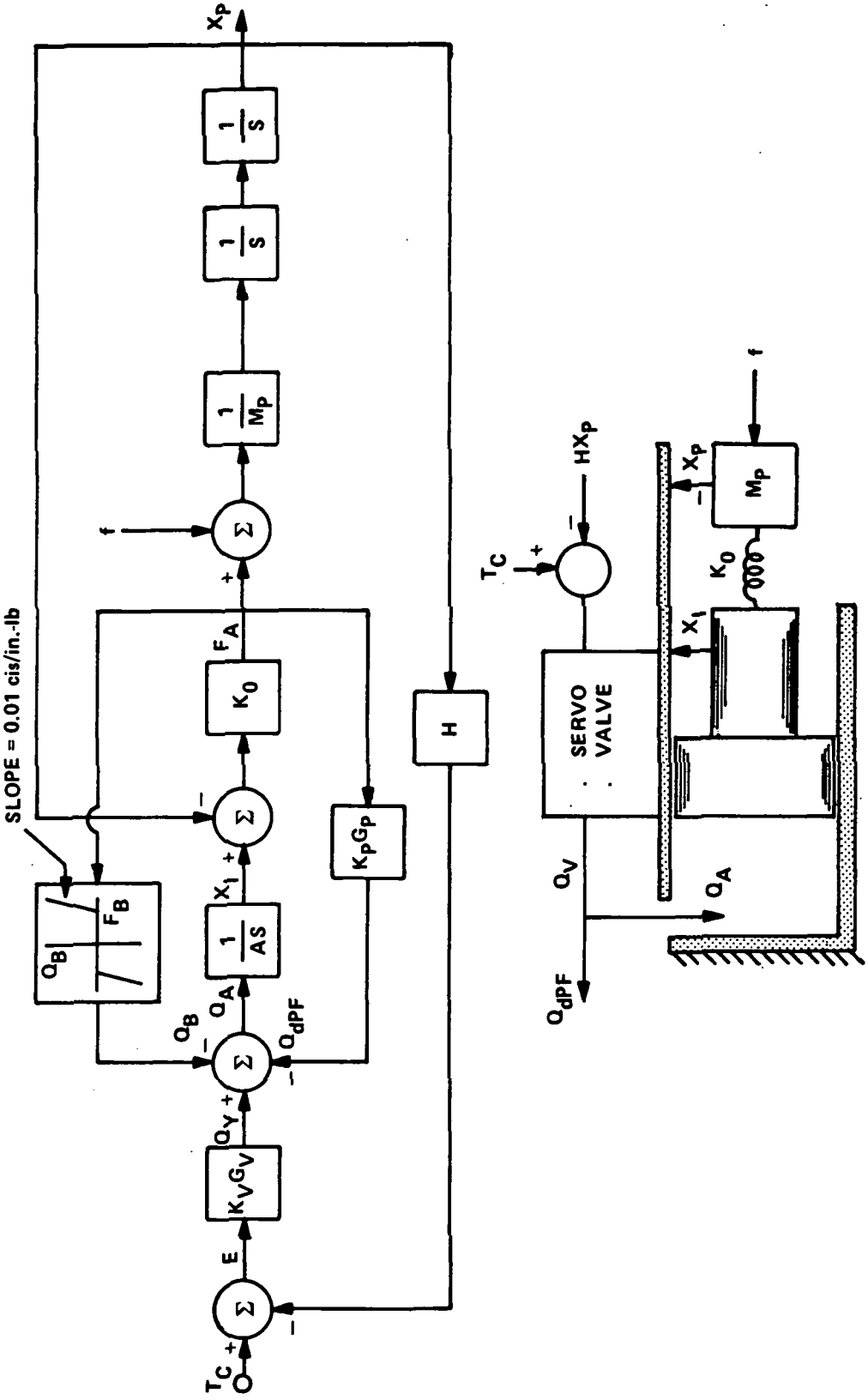

Figure 5. Servoactuator schematic.

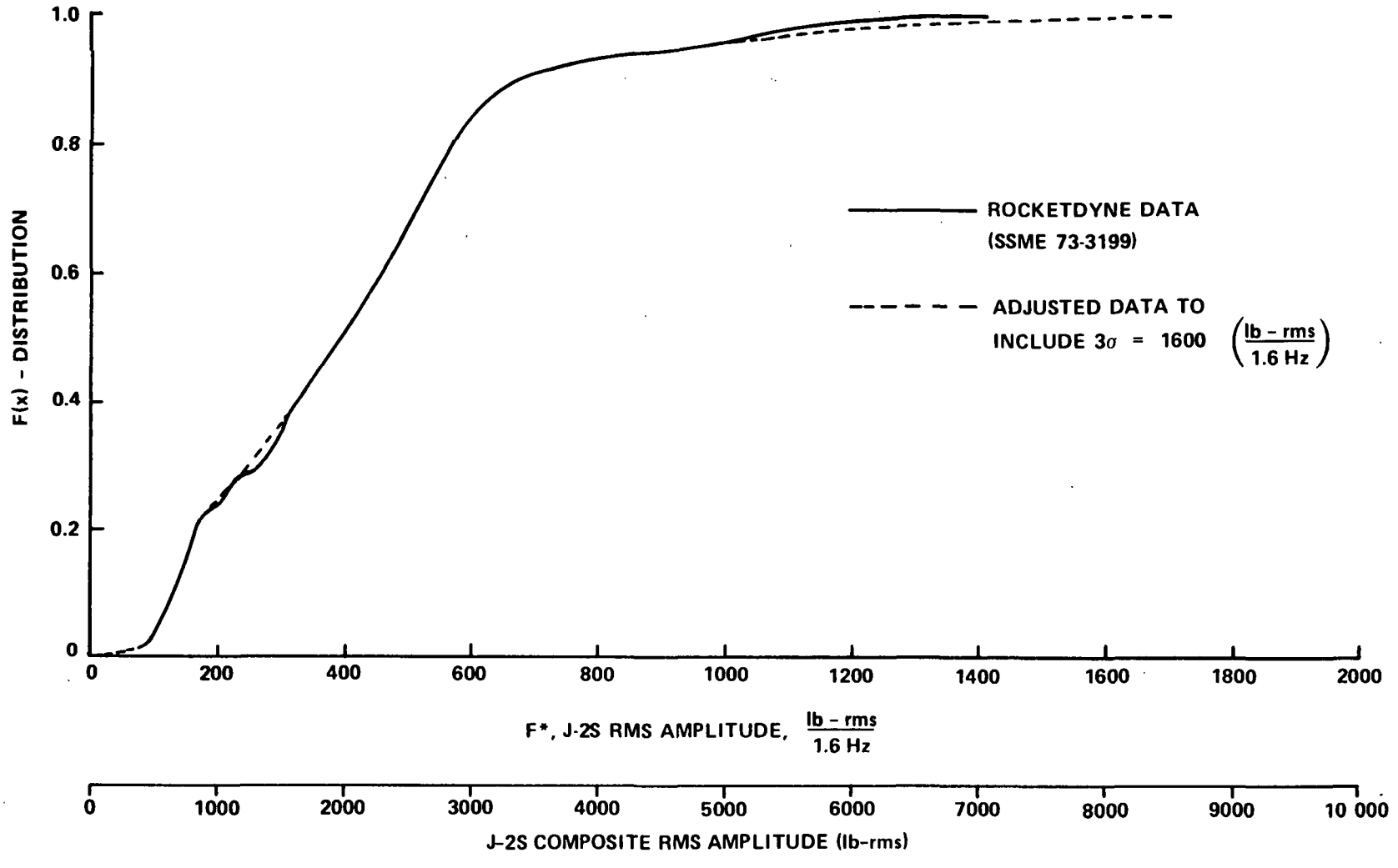

Figure 6. Distribution of J-2S rms amplitude for 1.6 Hz bandwidth, F*.

Side Load Forcing Functions are generated using from this set of 24 transients (Figs. 7 through 30) as follows:

$$F_j(t) = \frac{F_j^*}{1432} \left(R_{SSME/J2\text{-}S}\right) (1.1)\, F_i(t) \; ; \; i = 1, 2, 3, \ldots, 24$$

$$j = 1, 2, 3, \ldots \infty$$

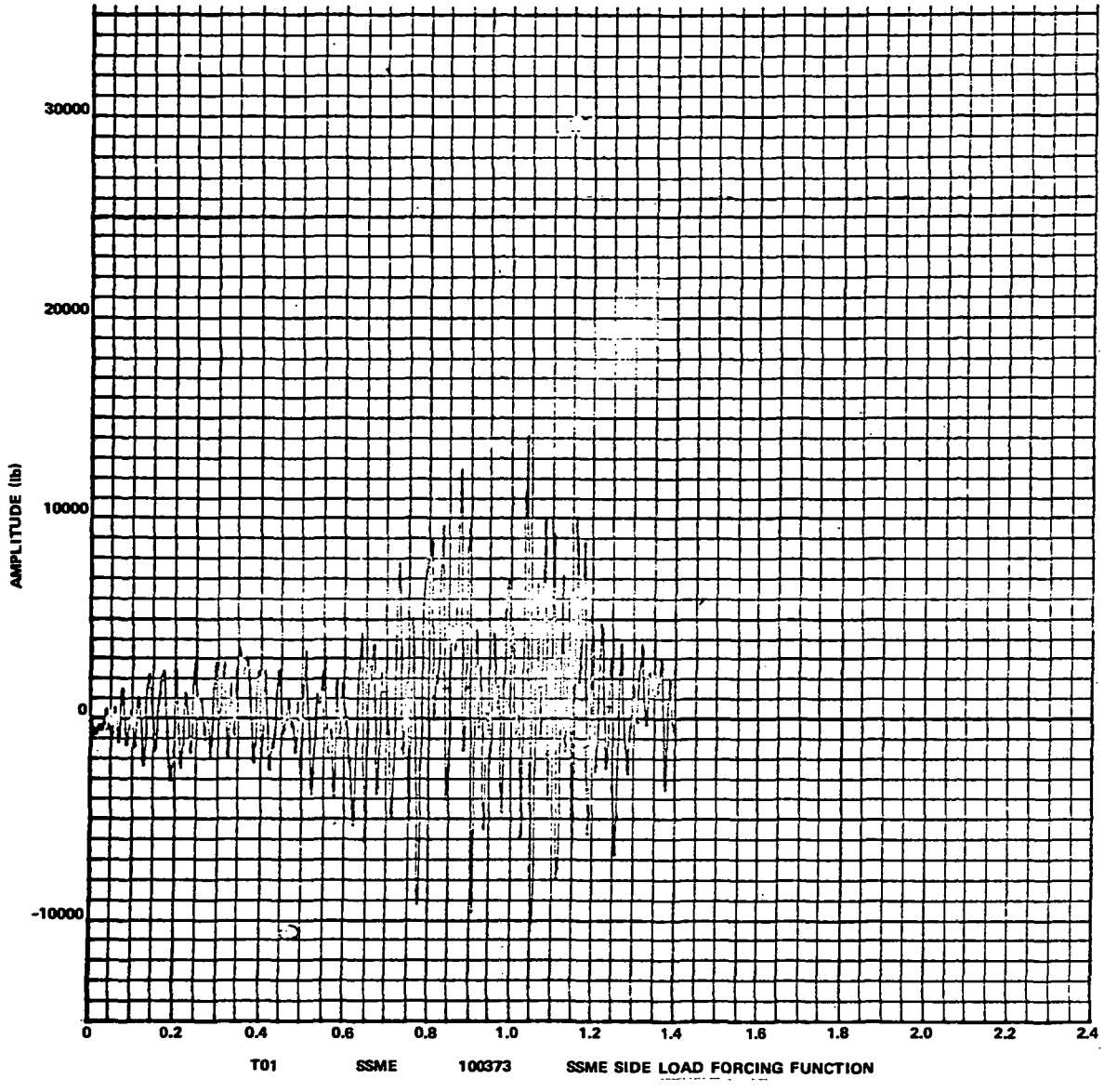

Figure 7. Side load transient no. 1.

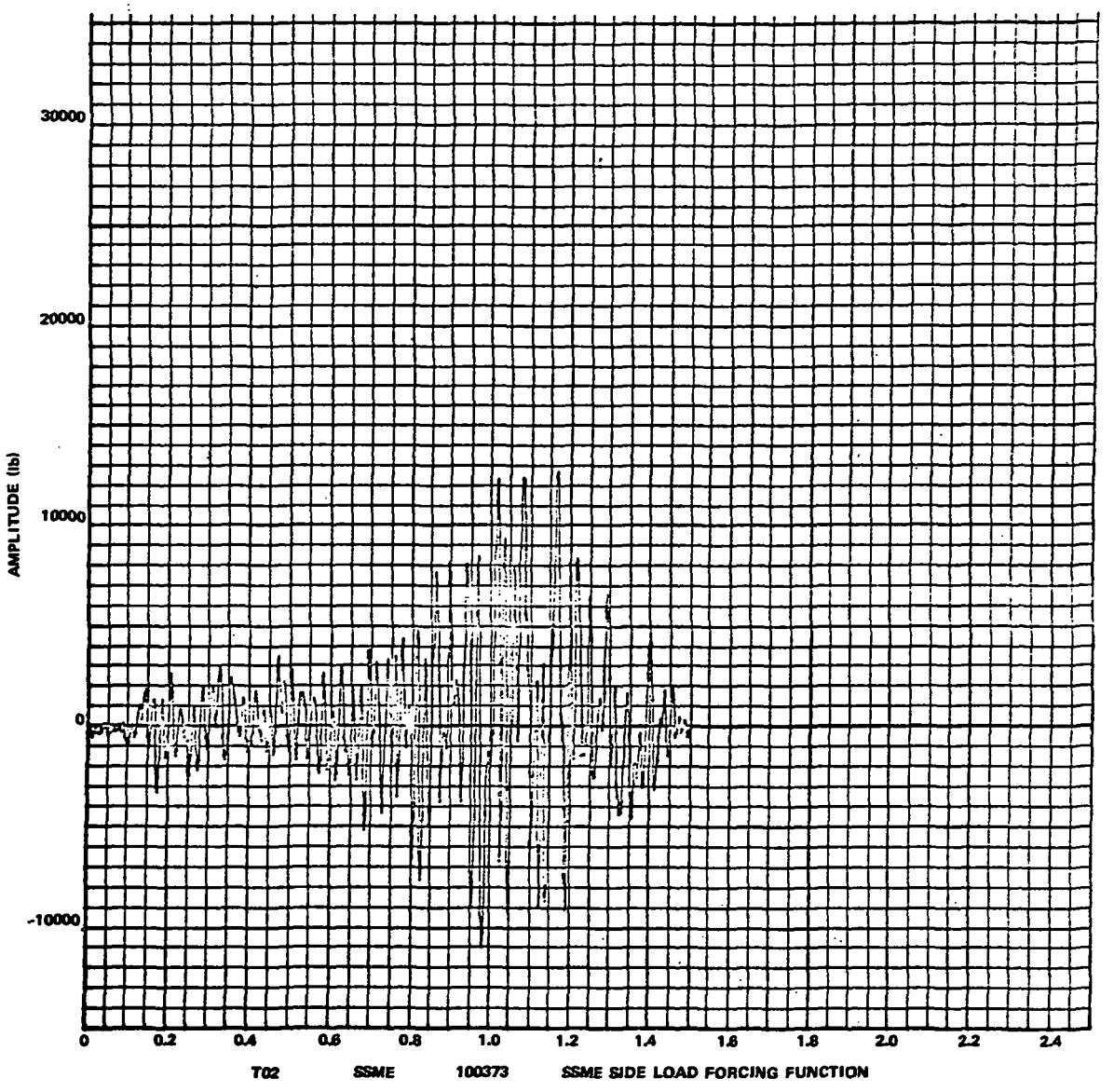

Figure 8. Side load transient no. 2.

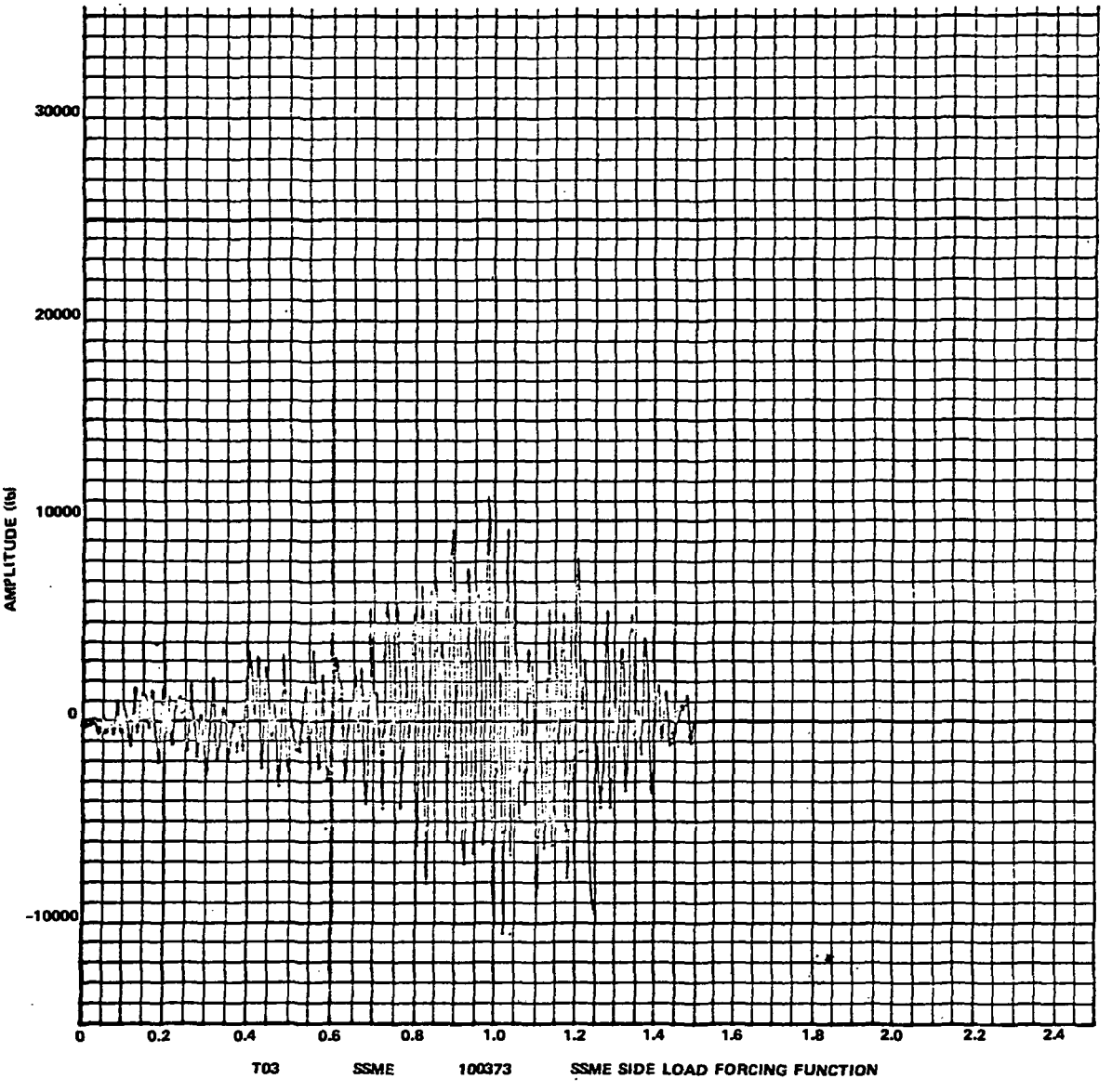

Figure 9. Side load transient no. 3.

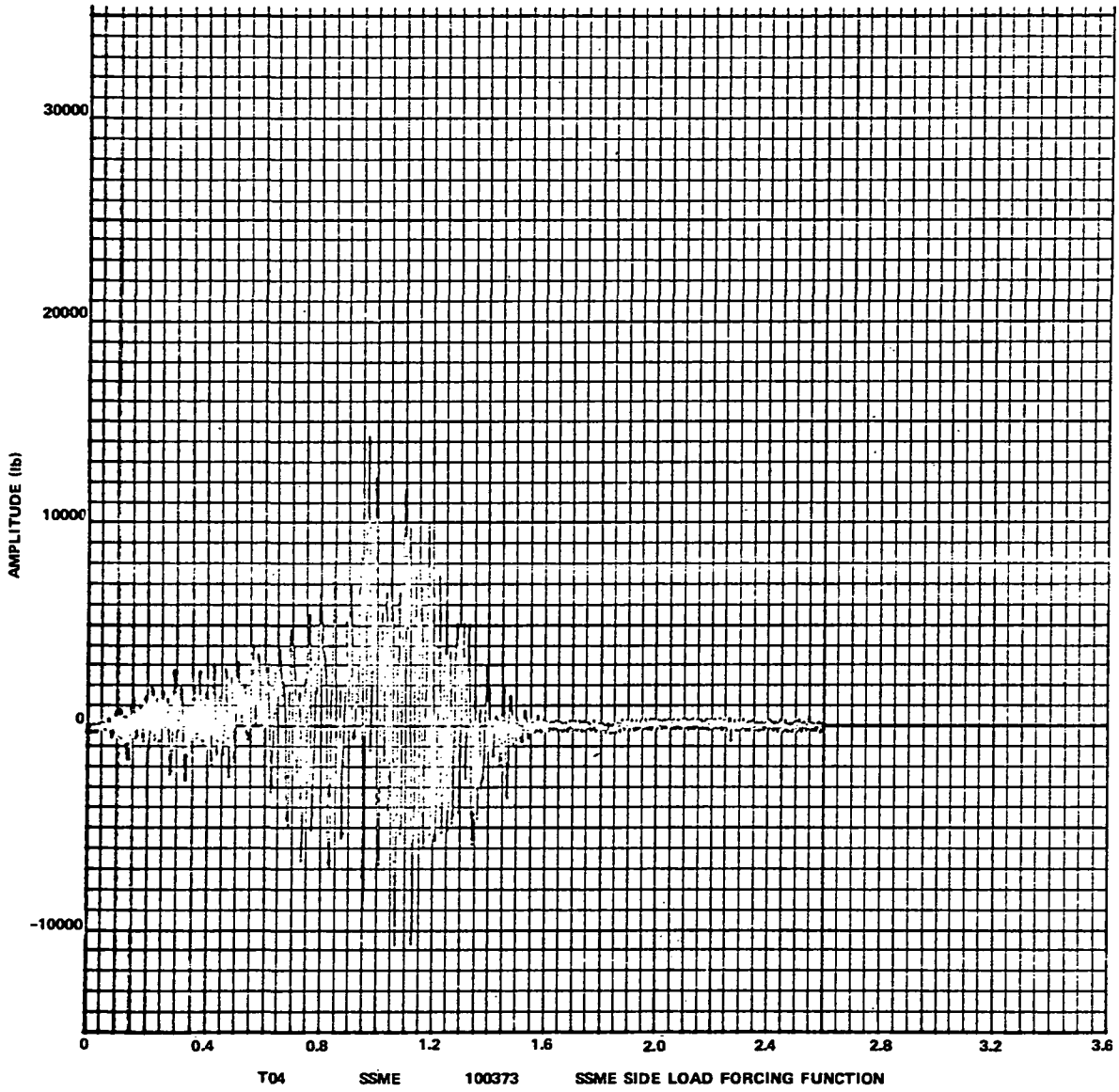

Figure 10. Side load transient no. 4.

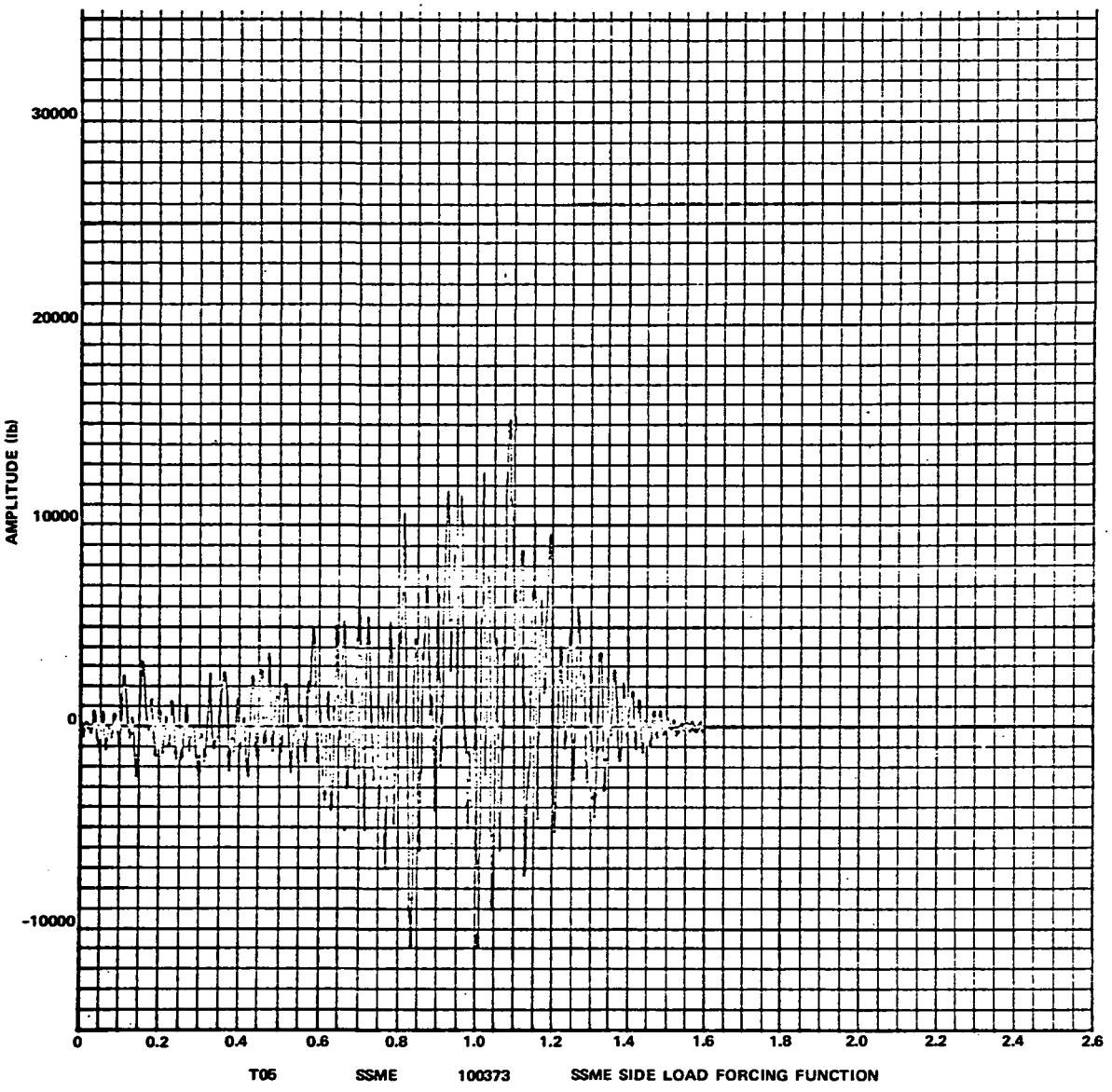

Figure 11. Side load transient no. 5.

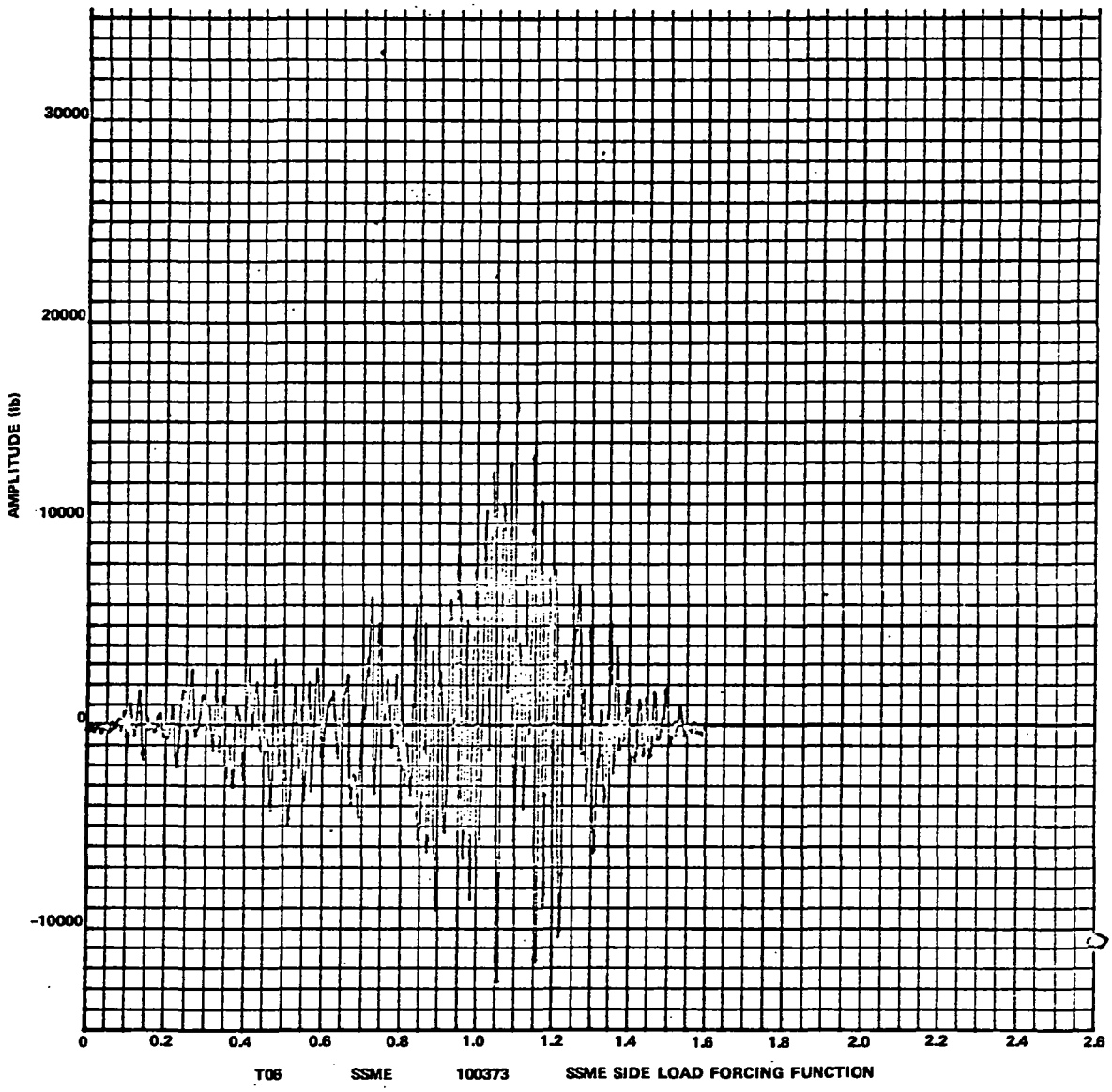

Figure 12. Side load transient no. 6.

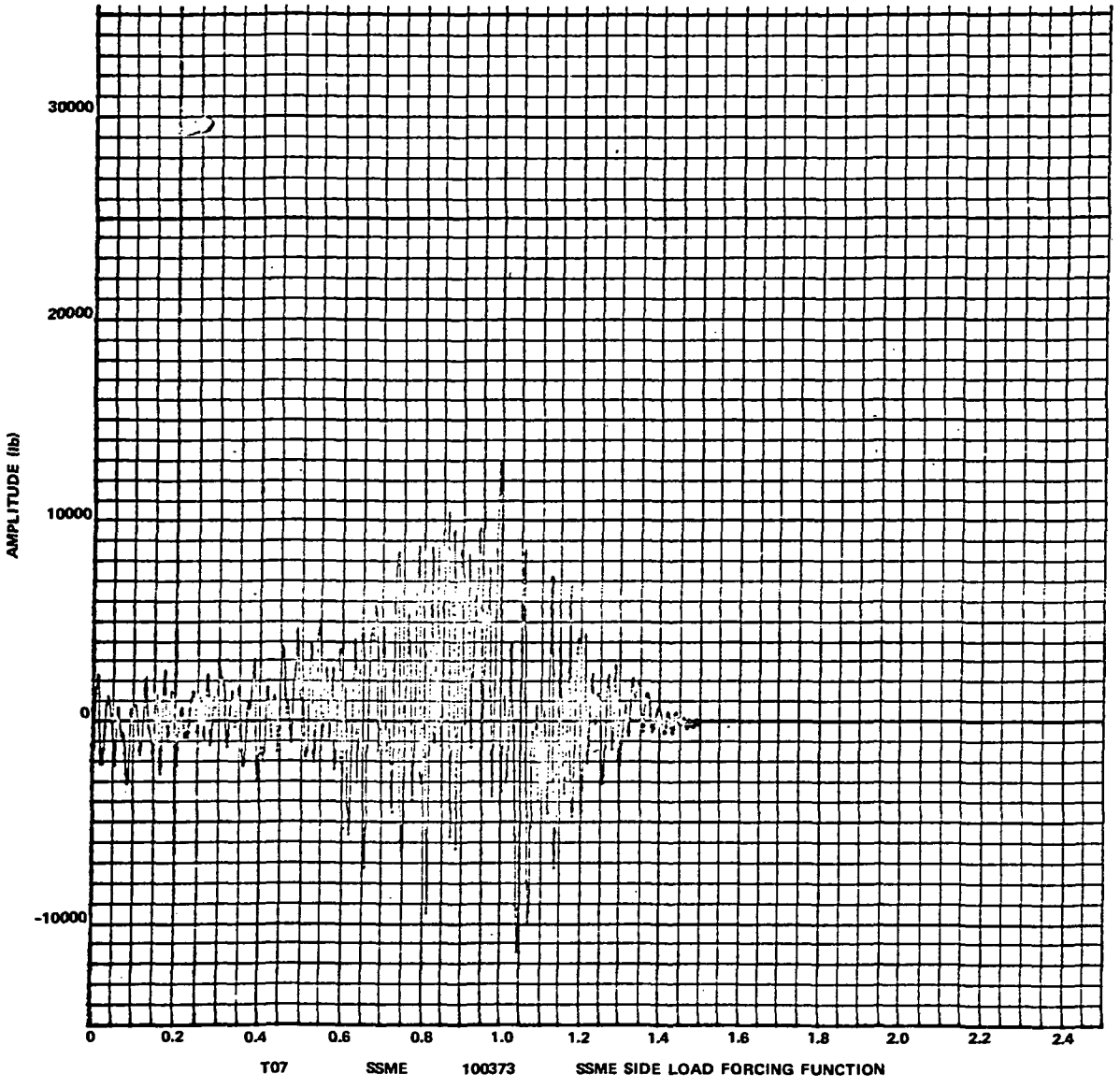

Figure 13. Side load transient no. 7.

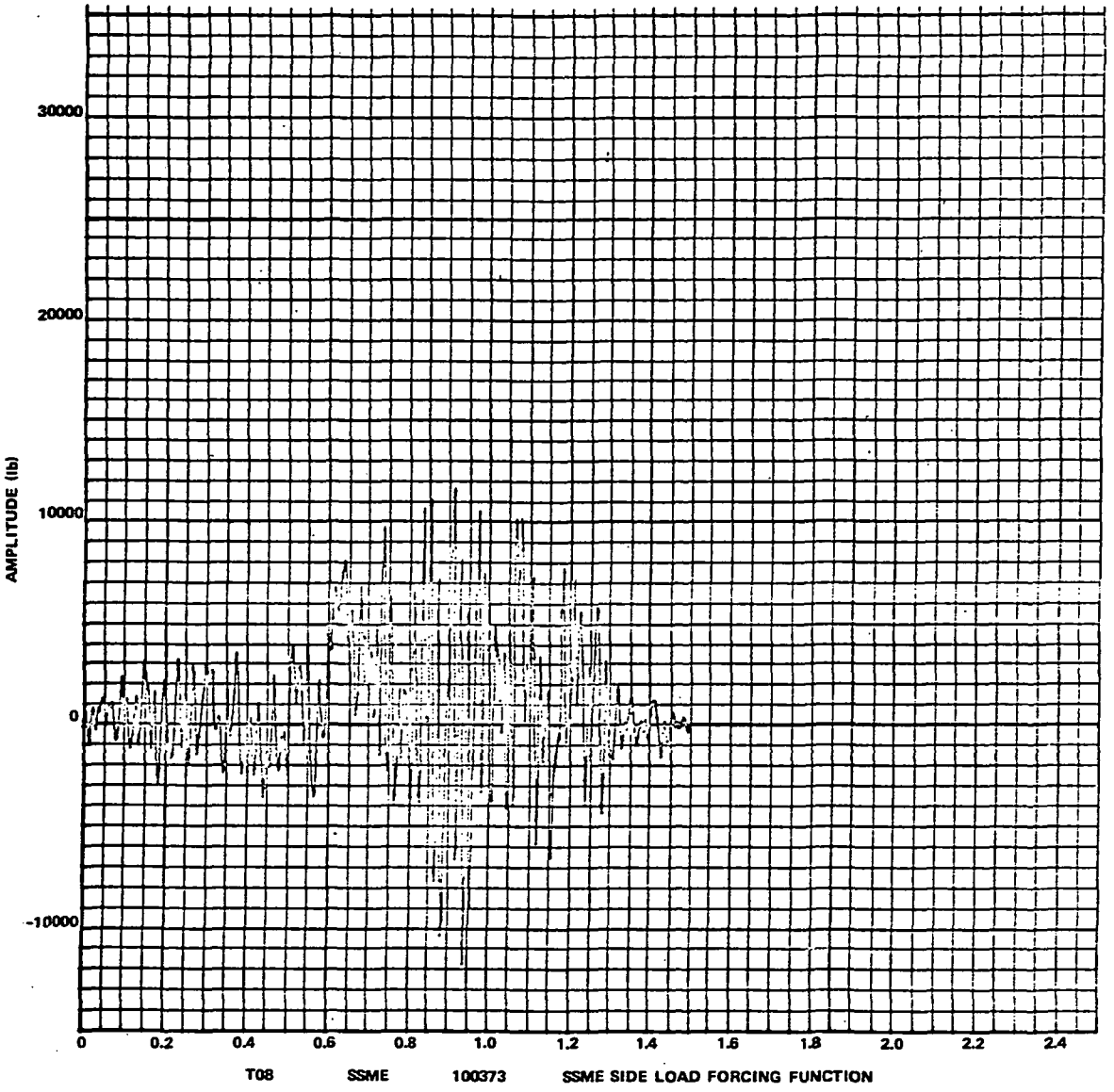

Figure 14. Side load transient no. 8.

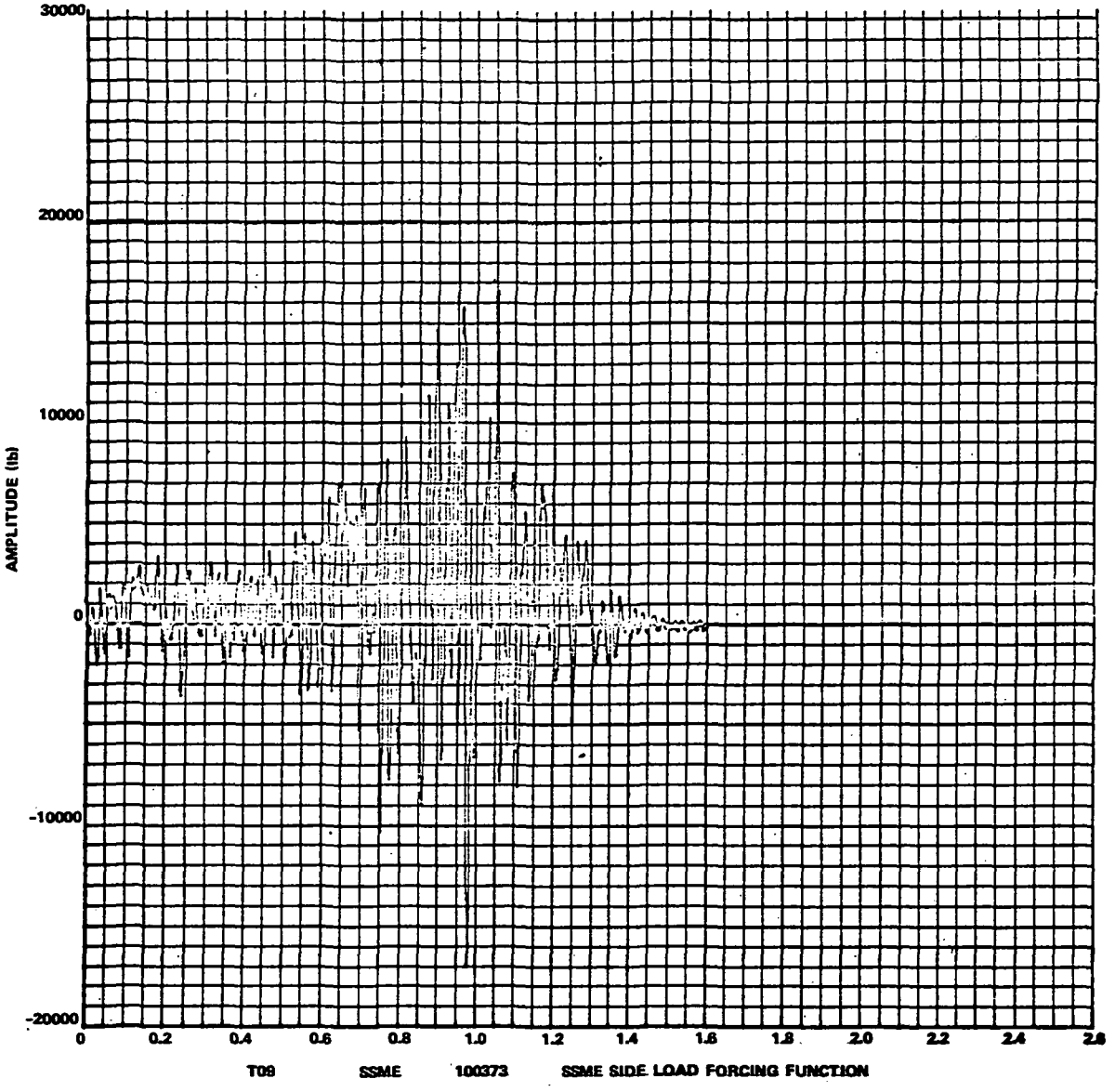

Figure 15. Side load transient no. 9.

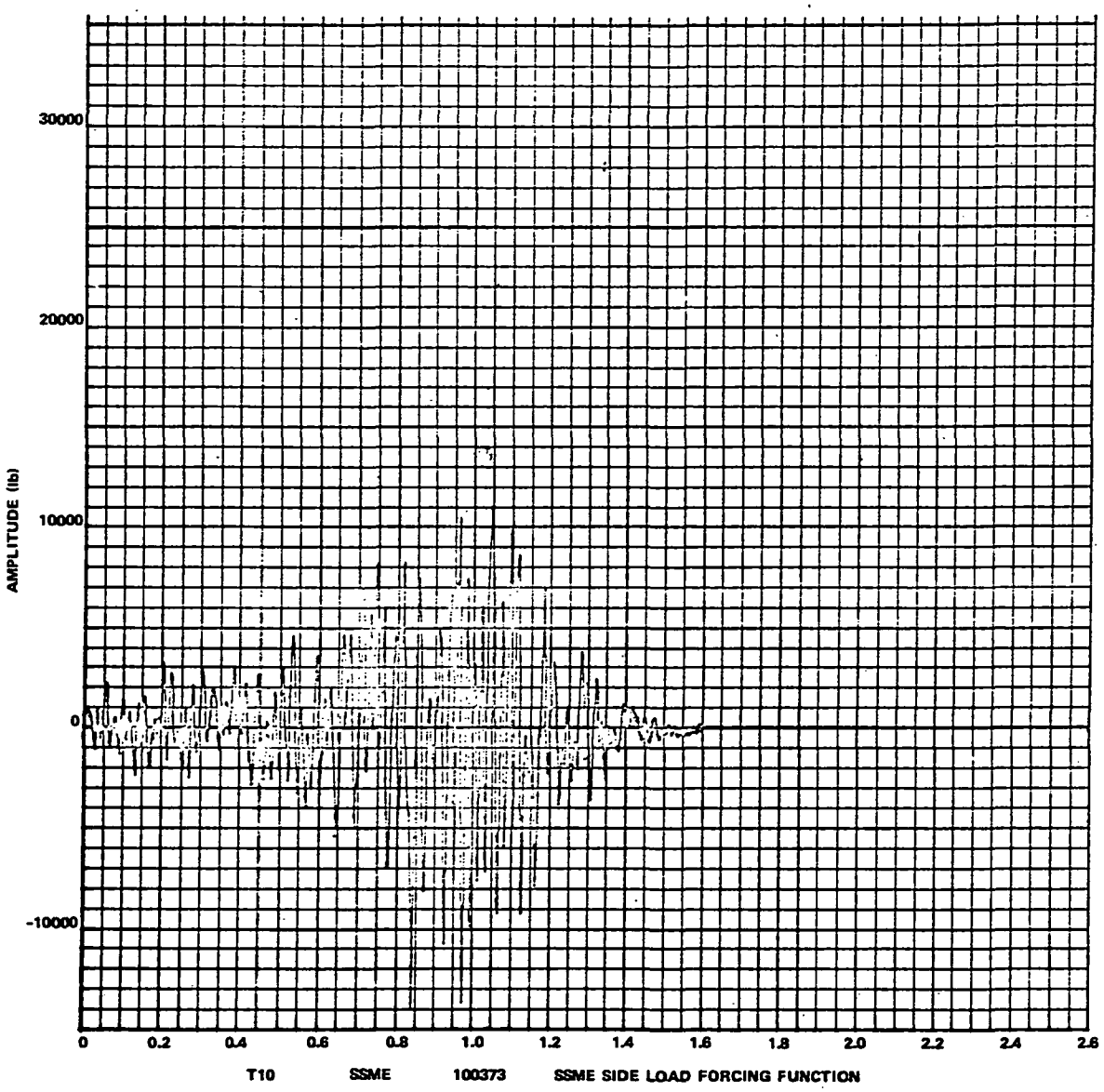

Figure 16. Side load transient no. 10.

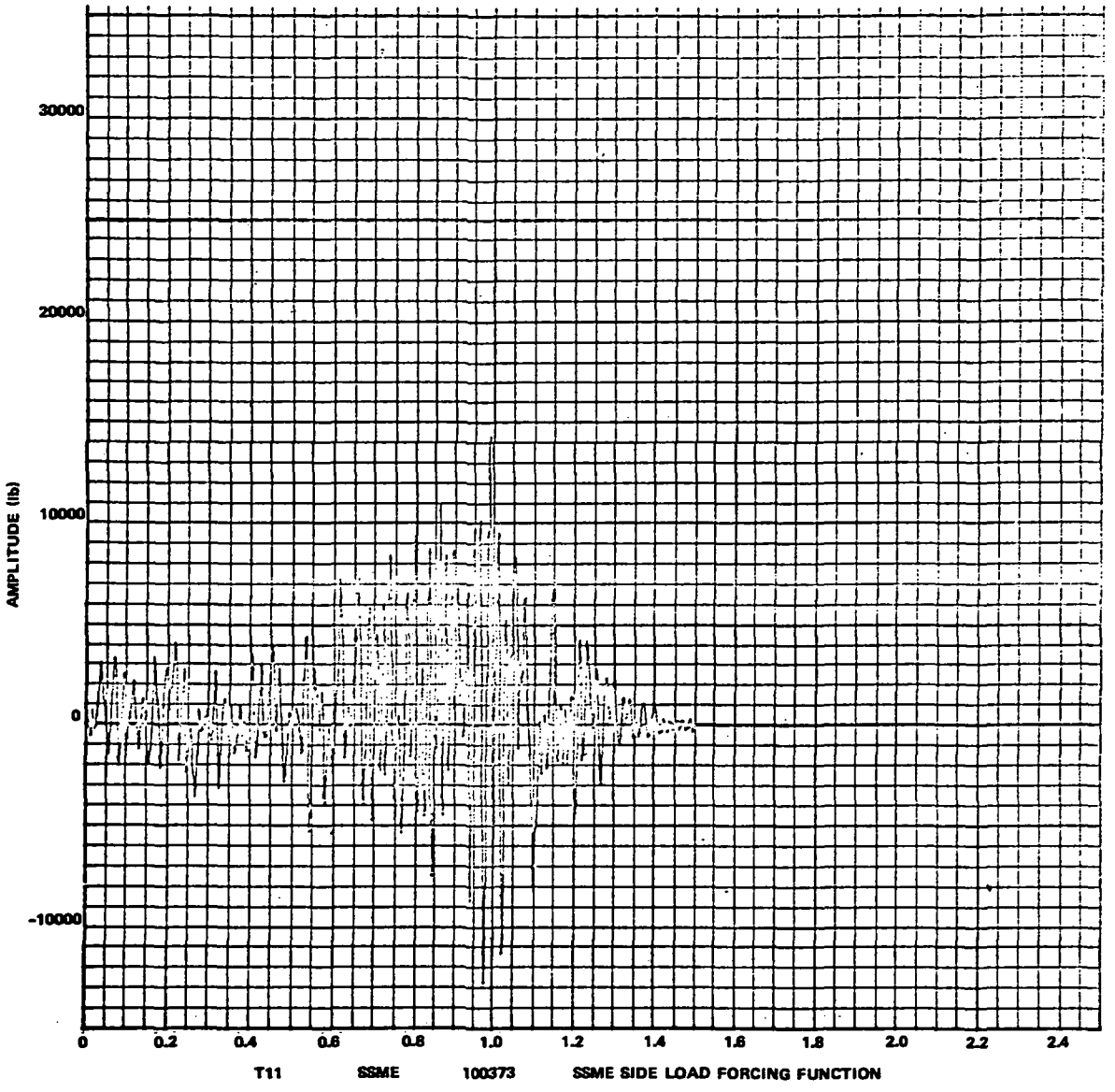

Figure 17. Side load transient no. 11.

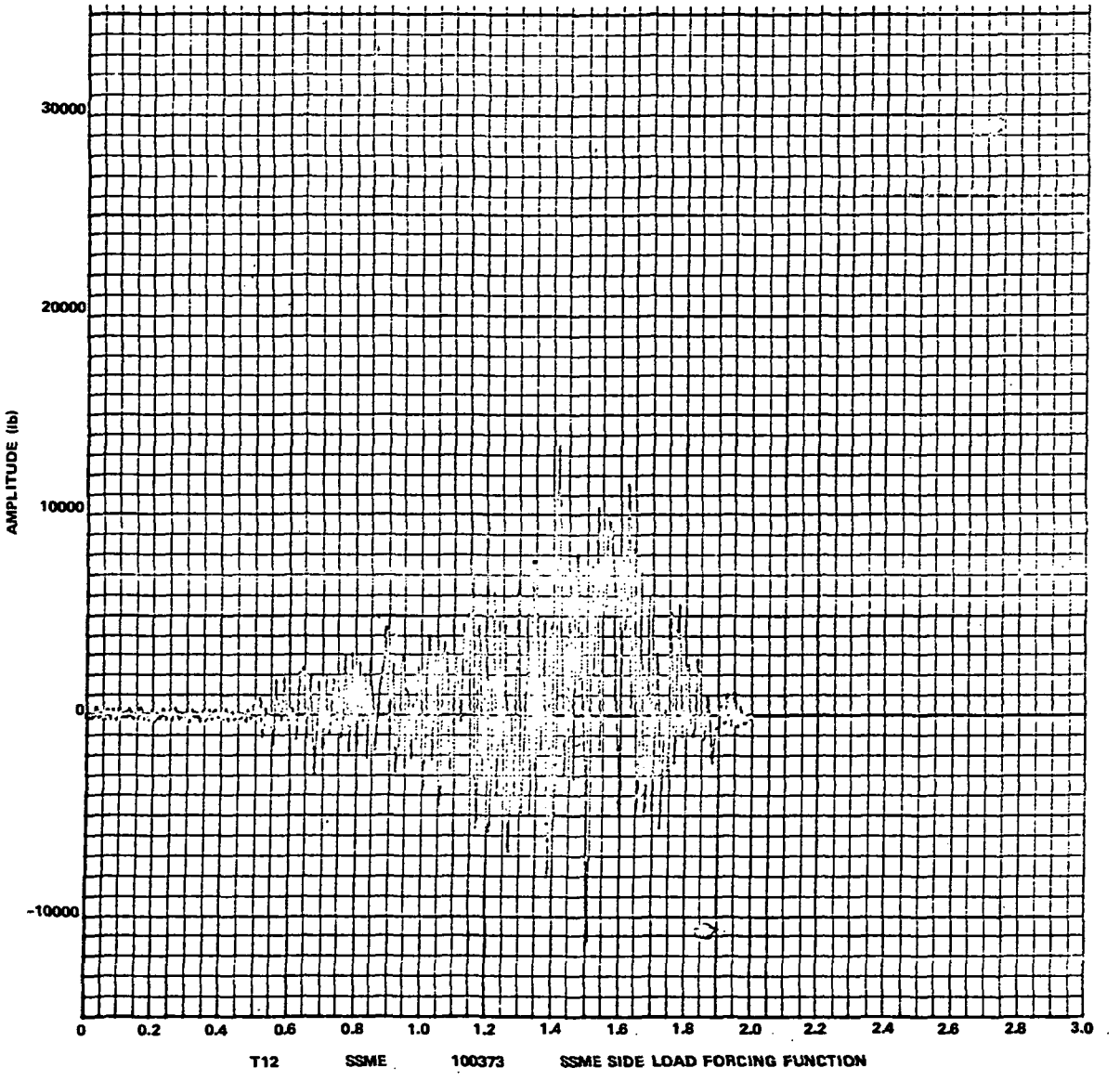

Figure 18. Side load transient no. 12.

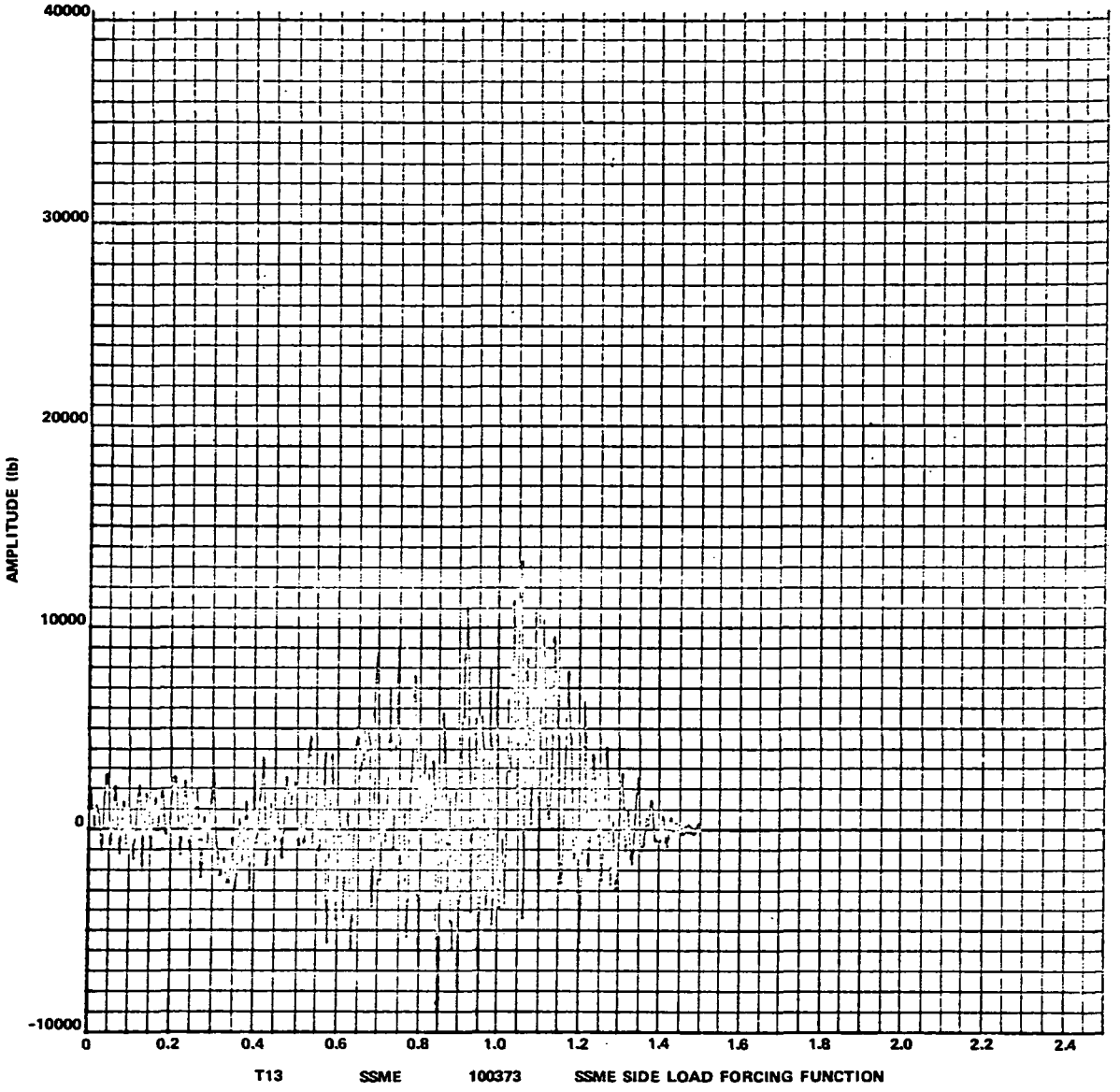

Figure 19. Side load transient no. 13.

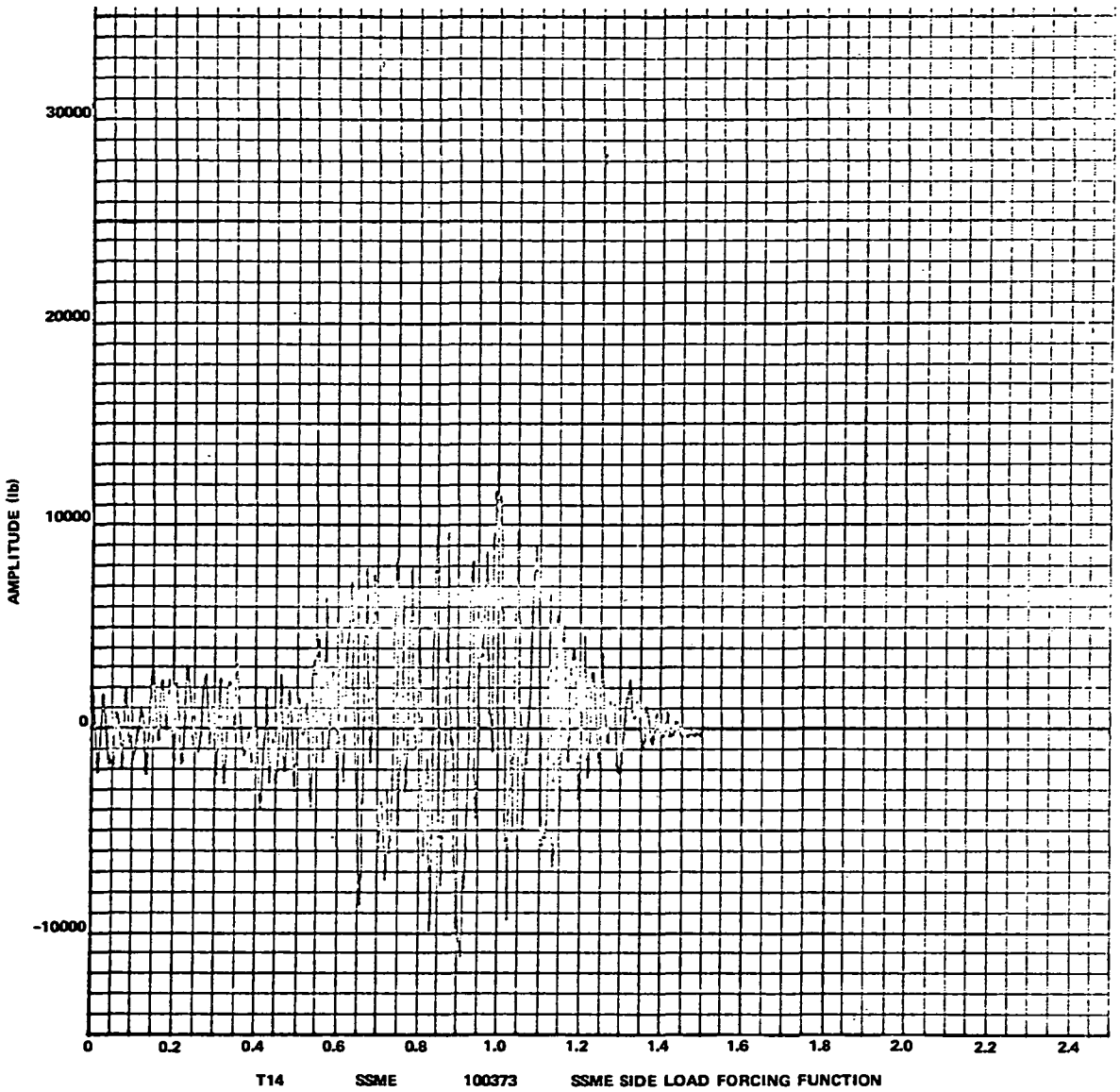

Figure 20. Side load transient no. 14.

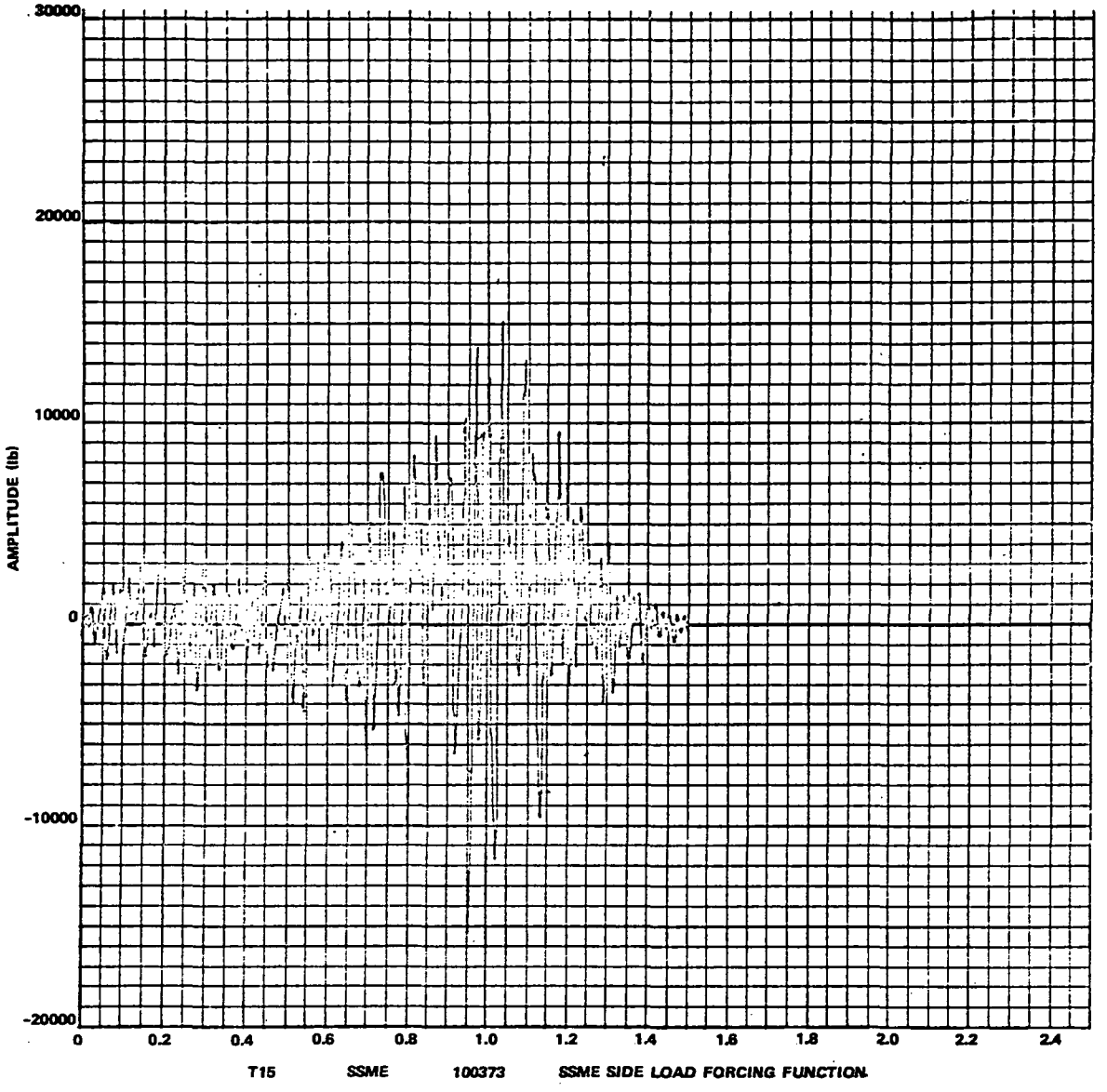

Figure 21. Side load transient no. 15.

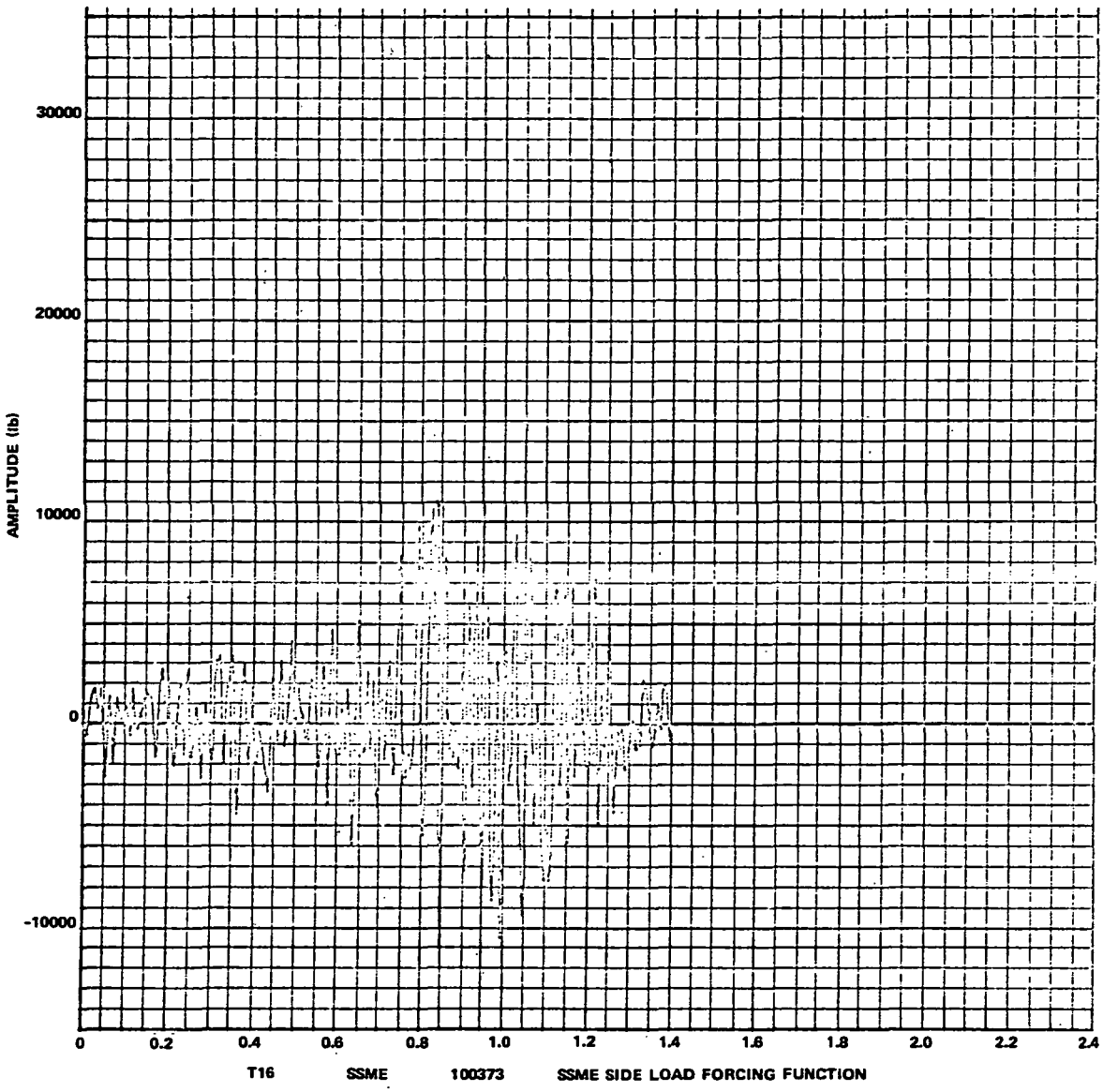

Figure 22. Side load transient no. 16.

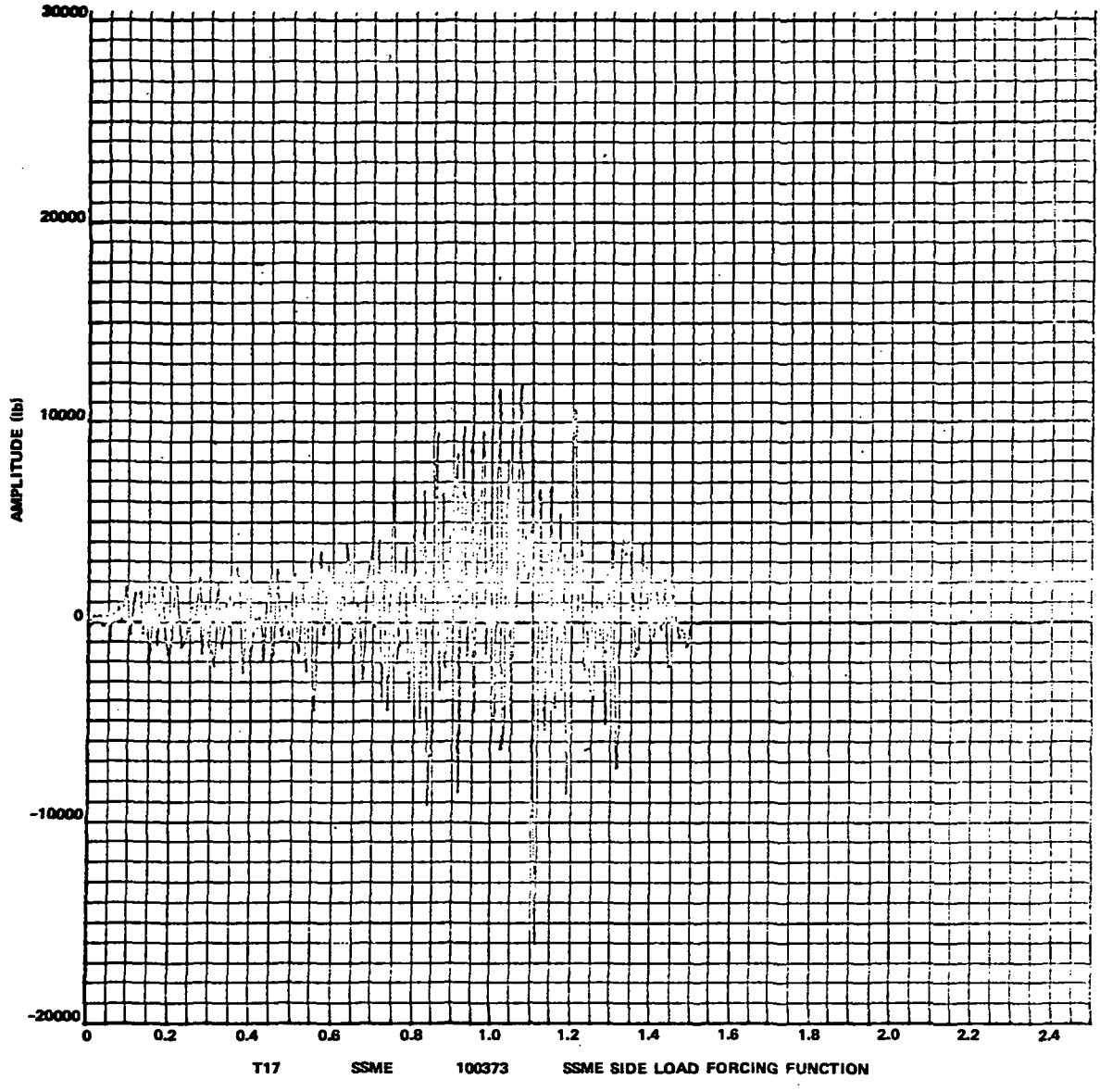

Figure 23. Side load transient no. 17.

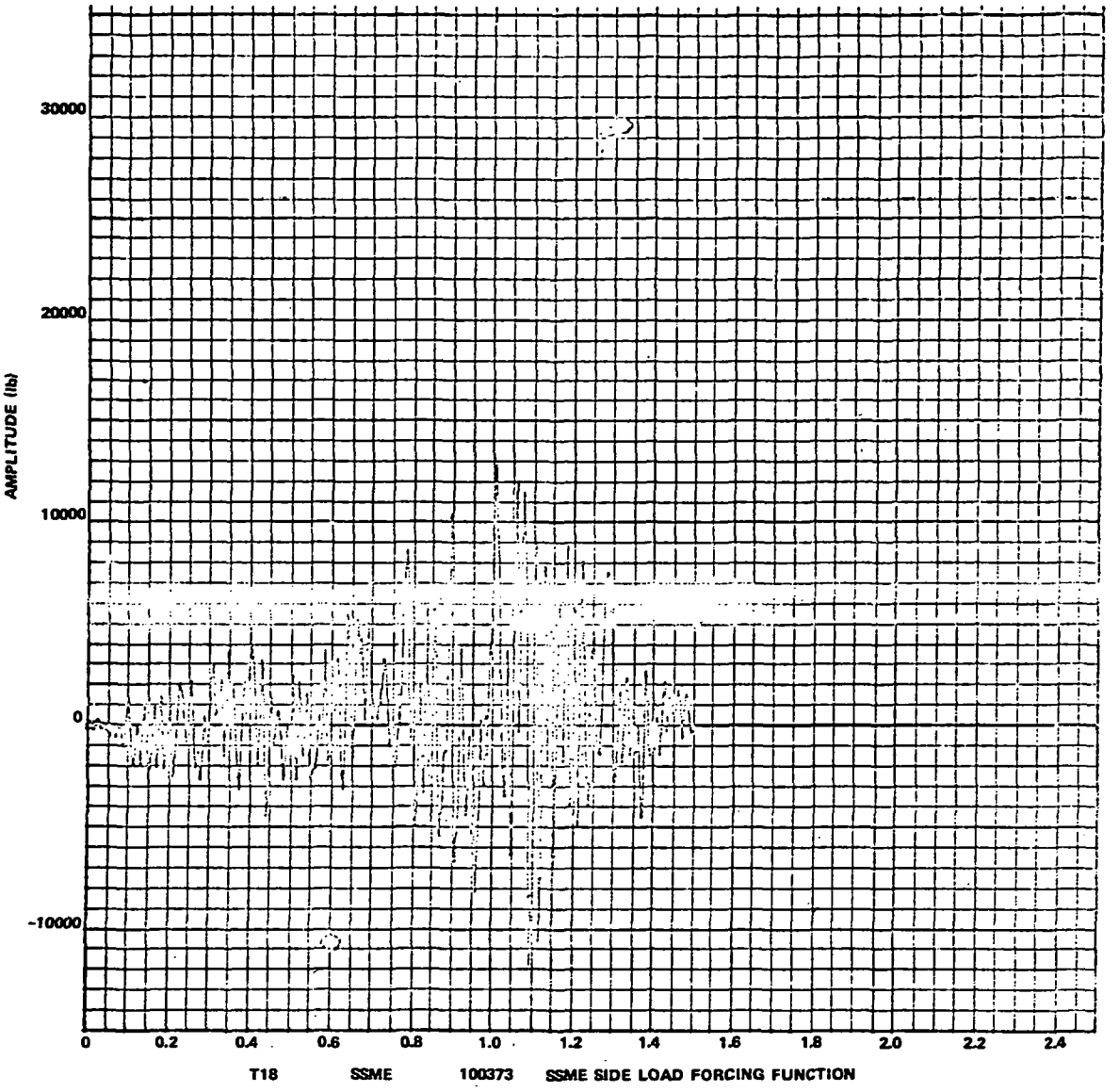

Figure 24. Side load transient no. 18.

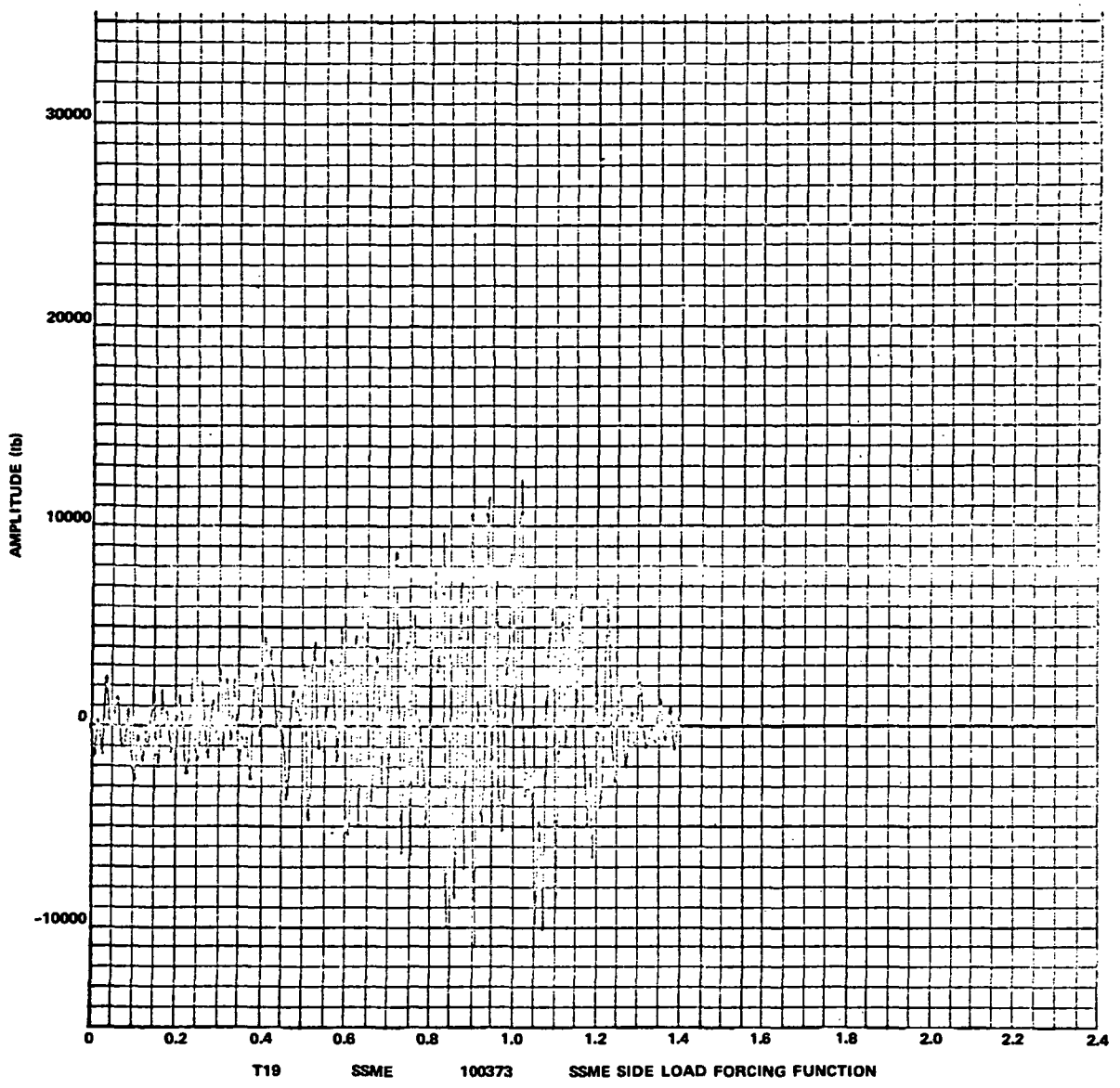

Figure 25. Side load transient no. 19.

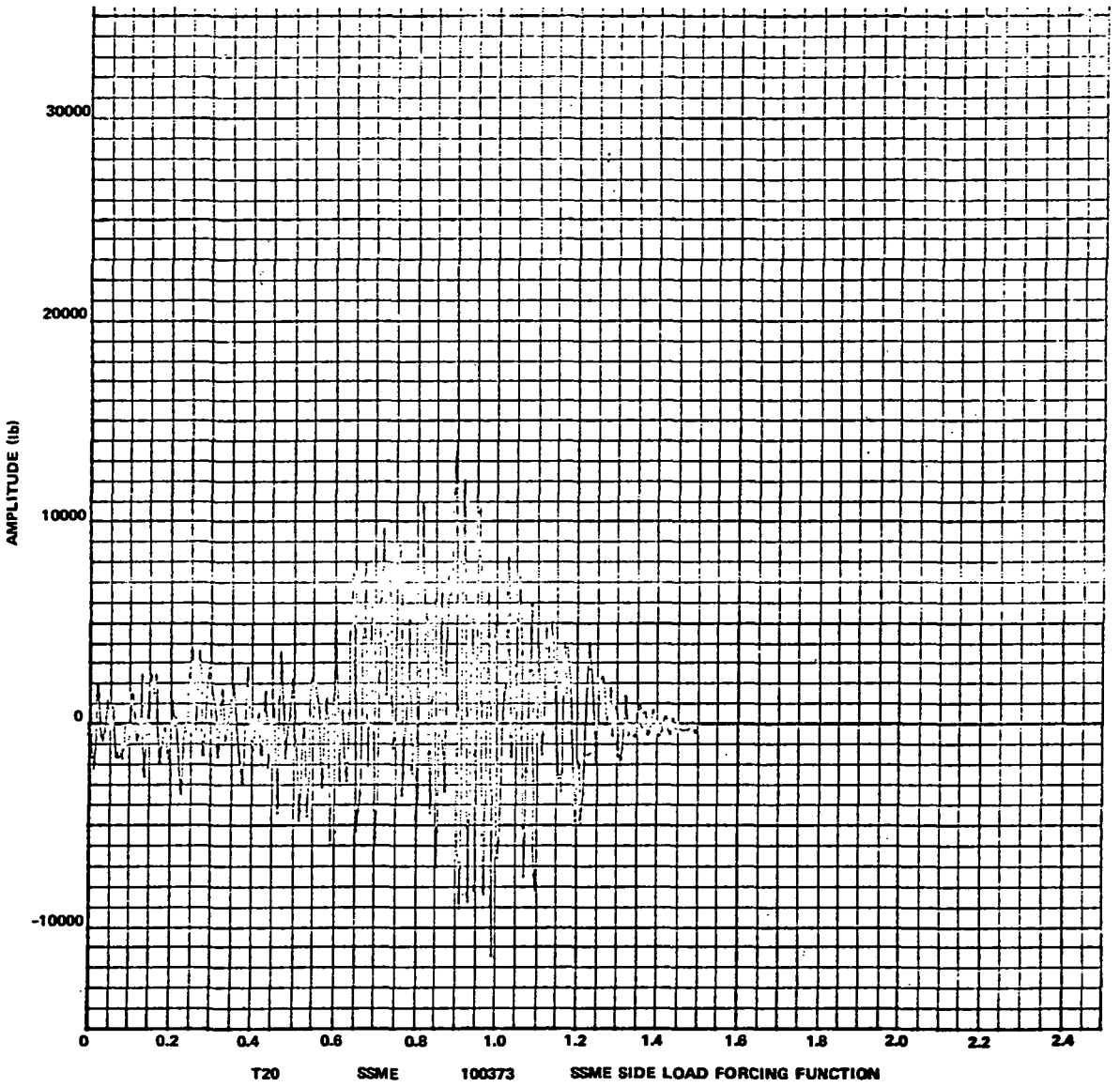

Figure 26. Side load transient no. 20.

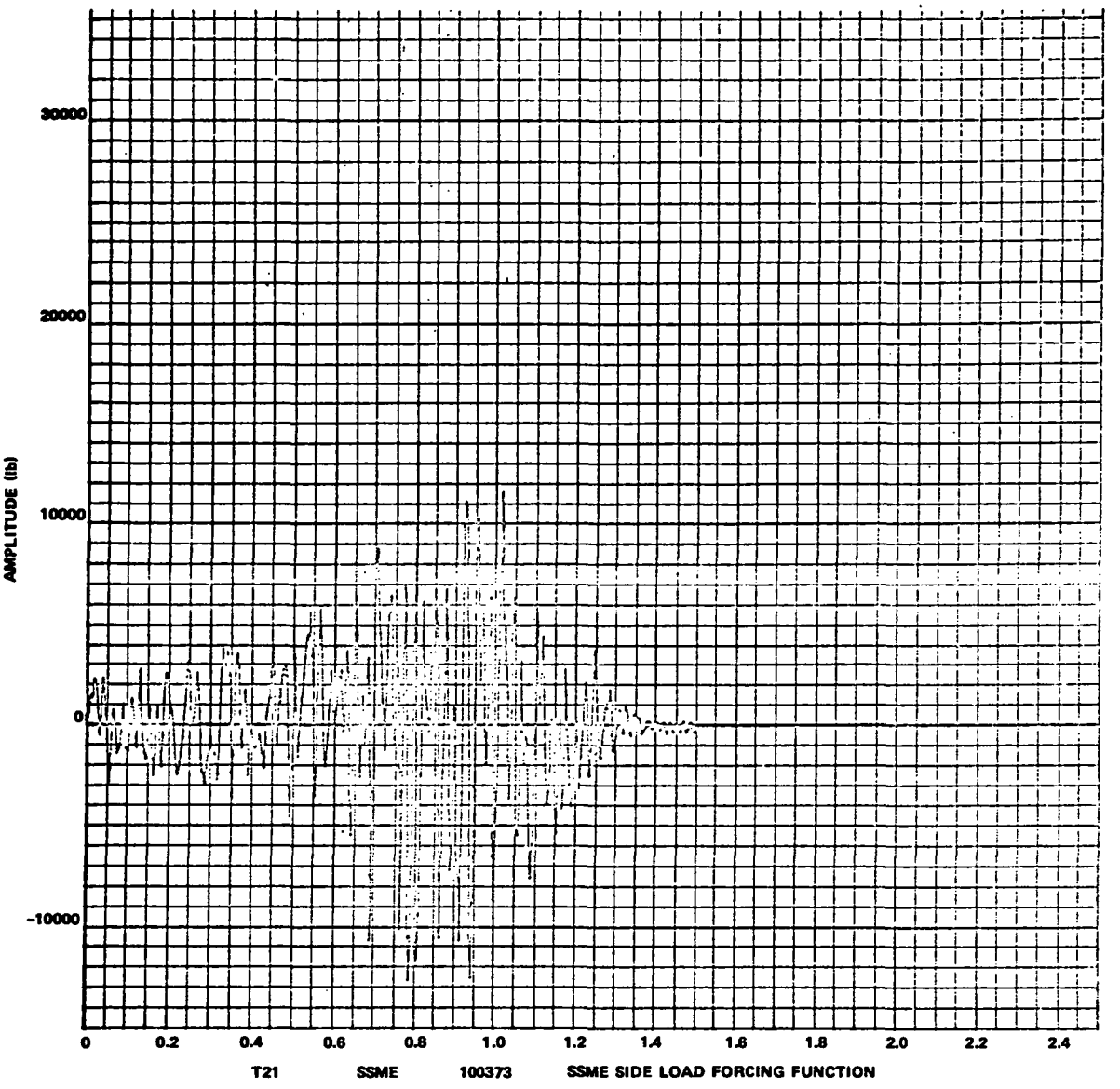

Figure 27. Side load transient no. 21.

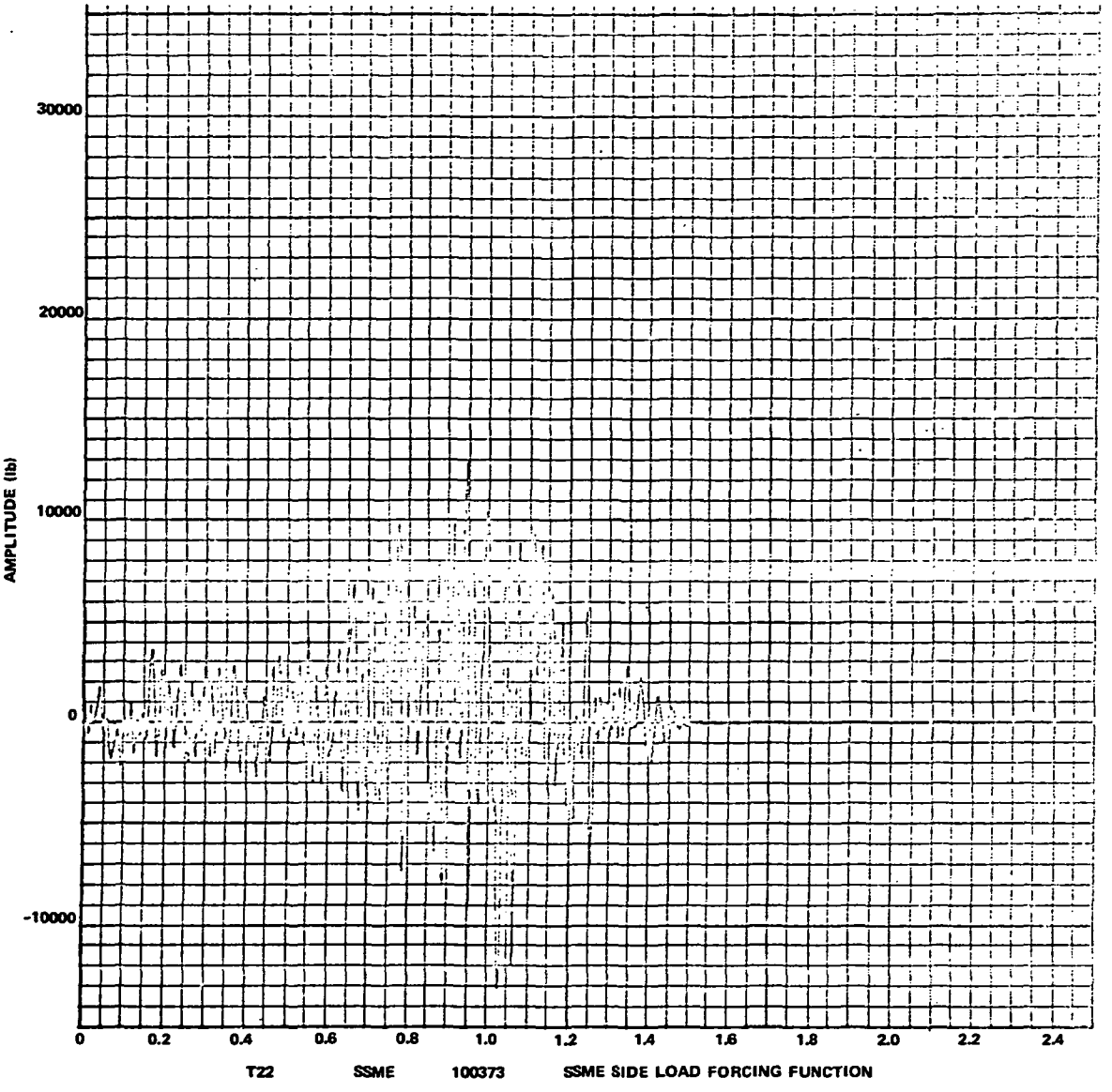

Figure 28. Side load transient no. 22.

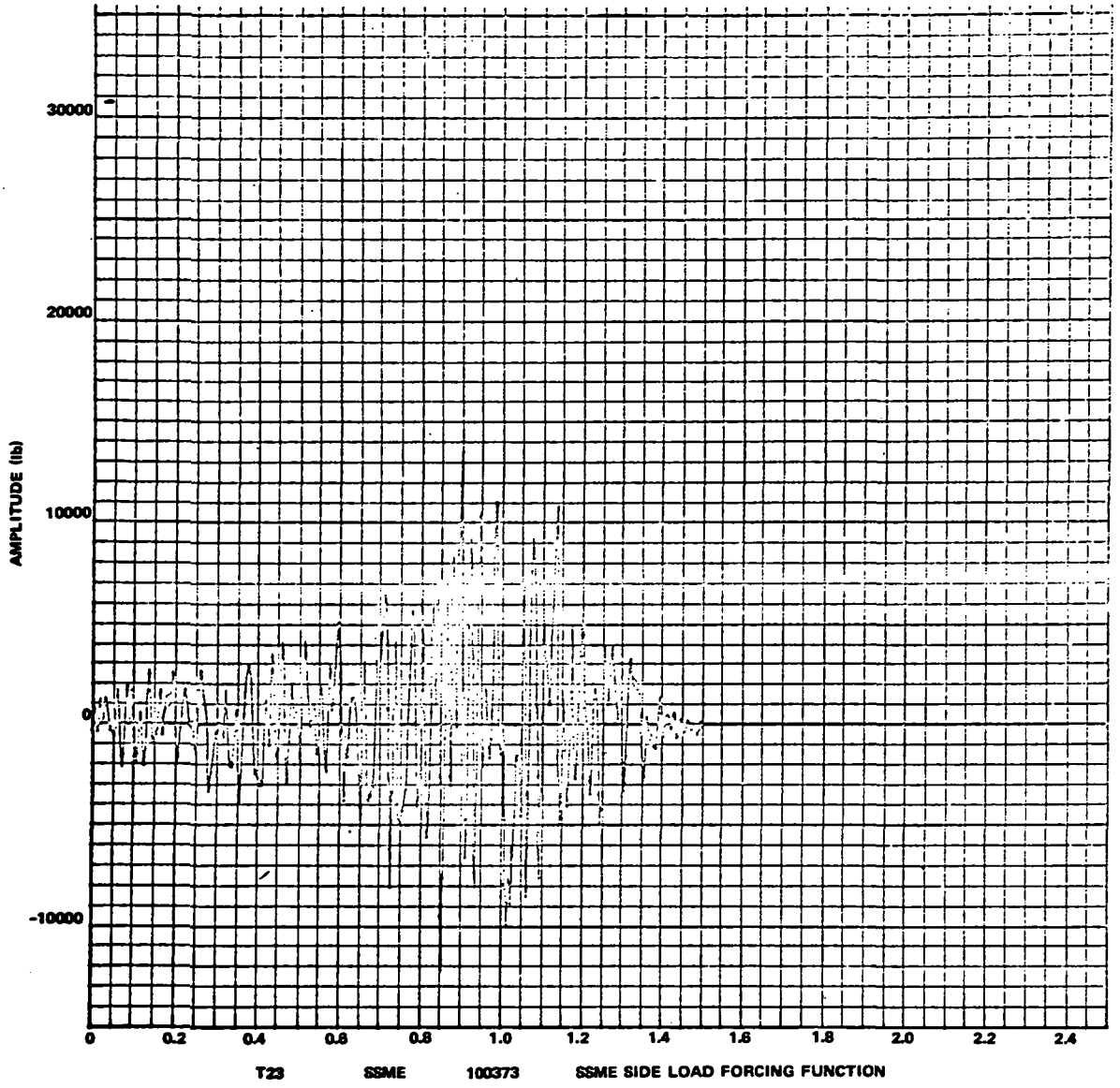

Figure 29. Side load transient no. 23.

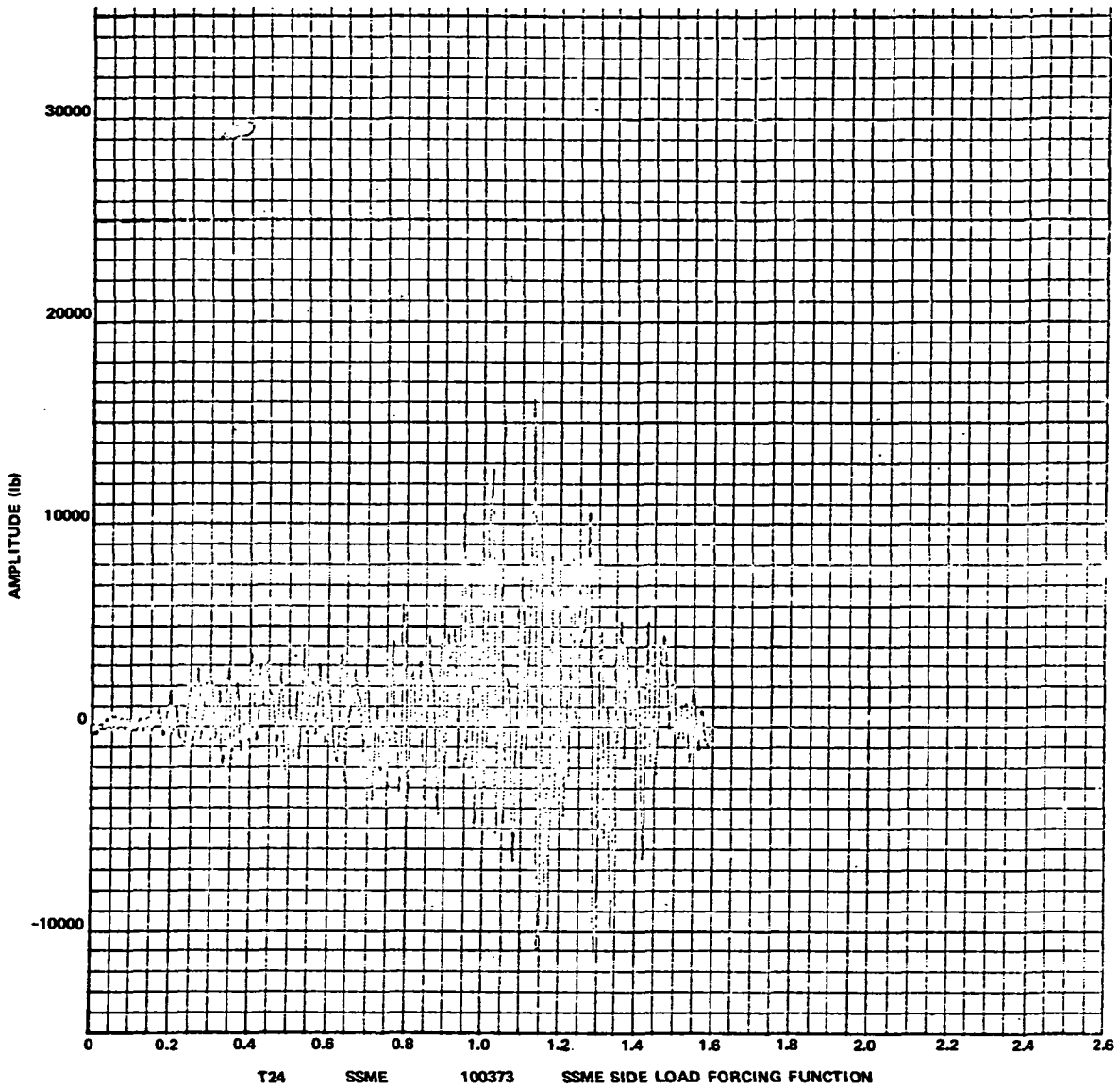

Figure 30. Side load transient no. 24.

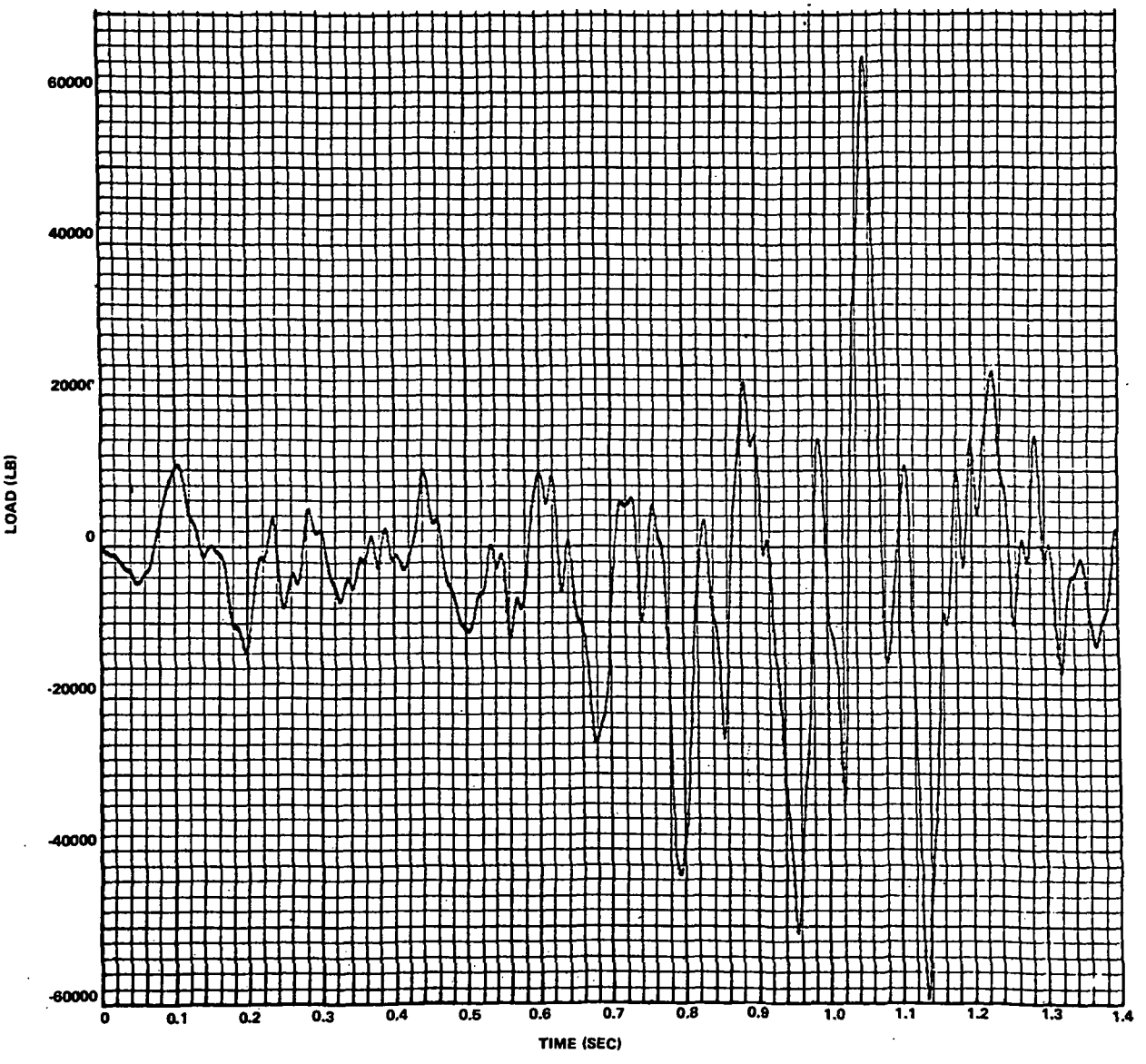

Figure 31. Actuator no. 1 load time history engine 2, start position, excitation case 1 peak side load excitation = 13 613.3 lb.

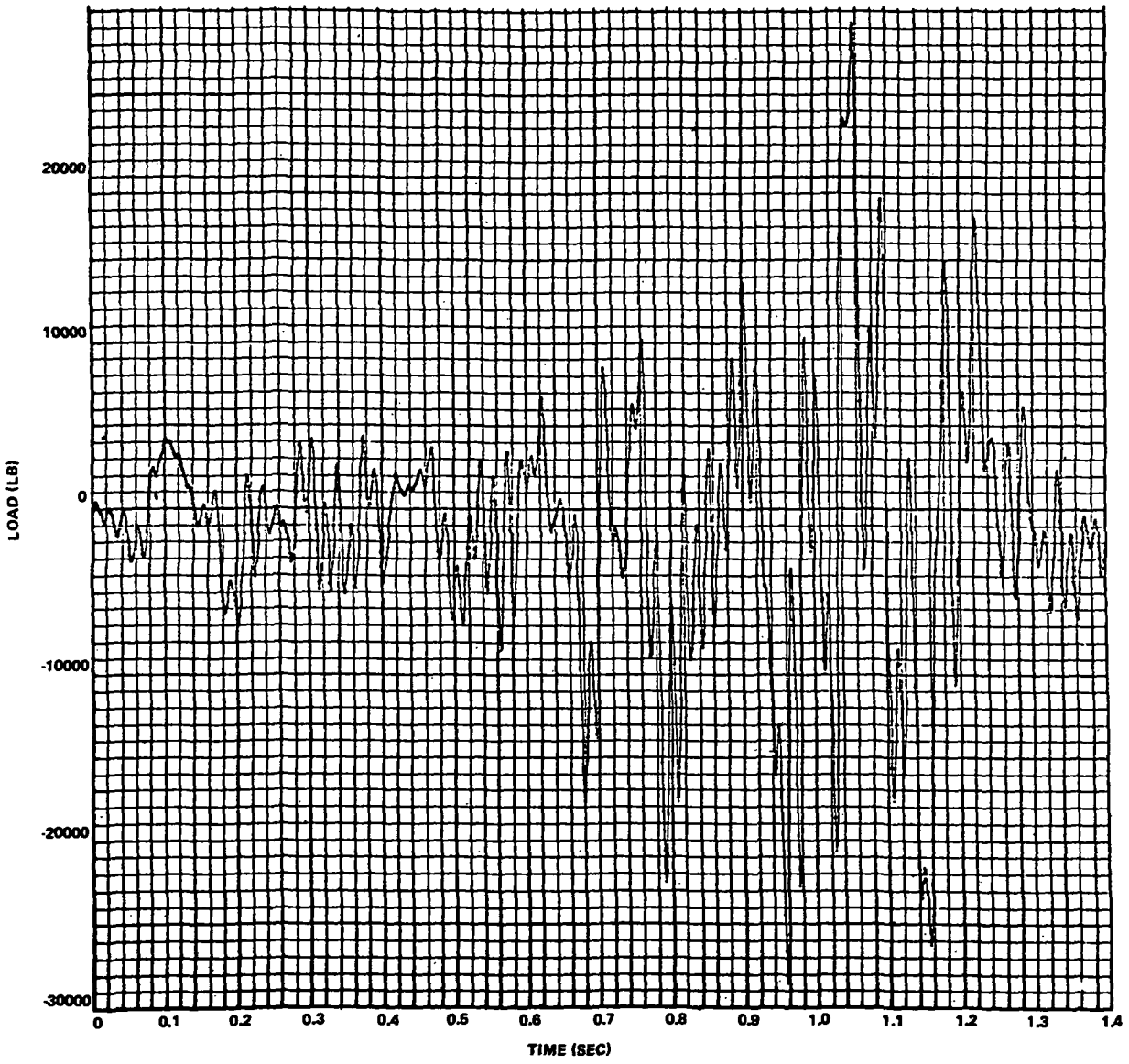

Figure 32. Actuator no. 2 load time history engine 2, start position, excitation case 1 peak side load excitation = 13 613.3 lb.

TABLE 1. DEGREE OF FREEDOM TABLE

NASTRAN Node Number	Degree of Freedom						Node Location (in.)			NASTRAN Coord. System	Node Description
	X	Y	Z	RX	RY	RZ	X	Y	Z		
1	1	2	3	4	5	6	0.0	0.0	0.0	4	Gimbal Point
2	7	8	9	10	11	12	-15.5	0.0	0.0	3	Main Beam/Pumps
3	13	14	15	16	17	18	-27.9	0.0	0.0	3	Thrust Chamber C. L.
4	19	20	21	22	23	24	-39.9	0.0	0.0	3	Throat C. L.
5	25	26	27	28	29	30	-29.4	-19.5	-19.5	3	HPFTP
6	31	32	33	34	35	36	-28.6	18.4	18.4	3	HPOTP
7	37	38	39				10.0	-31.5	0.0	4	Actuator 1/Orbiter
8	40	41	42				10.0	0.0	-31.5	4	Actuator 2/Orbiter
9	43	44	45	46	47	48	-36.0	-25.0	0.0	3	Actuator 1/Struts
10	49	50	51	52	53	54	-36.0	0.0	-25.0	3	Actuator 2/Struts
11	55	56	57	58	59	60	-45.75	0.0	0.0	3	Main Beam/Struts
12	61	62	63	64	65	66	-24.88	-10.72	7.39	3	Strut
13	67	68	69	70	71	72	-24.88	-10.72	-7.39	3	Strut
14	73	74	75	76	77	78	-24.88	7.39	-10.72	3	Strut
15	79	80	81	82	83	84	-24.88	7.39	-10.72	3	Strut
16	85	86	87	88	89	90	-45.75	10.20	-5.89	3	Strut
17	91	92	93	94	95	96	-41.52	-12.12	7.04	3	Strut
18	97	98	99	100	101	102	-41.52	-12.12	-7.04	3	Strut
19	103	104	105	106	107	108	-45.75	-5.89	-10.20	3	Strut
20	109	110	111	112	113	114	-45.75	-10.20	-5.89	3	Strut
21	115	116	117	118	119	120	-41.52	7.04	-12.12	3	Strut
22	121	122	123	124	125	126	-41.52	-7.04	-12.12	3	Strut
23	127	128	129	130	131	132	-45.75	-5.89	10.2	3	Strut
24	133	134	135	136	137	138	-54.0	0.0	0.0	3	Bell C. L.
25	139	140	141	142	143	144	-63.13	0.0	0.0	3	Bell C. L.
26	145	146	147	148	149	150	-74.19	0.0	0.0	3	Bell C. L.
27	151	152	153	154	155	156	-84.99	0.0	0.0	3	Bell C. L.
28	157	158	159	160	161	162	-95.79	0.0	0.0	3	Bell C. L.
29	163	164	165	166	167	168	-106.59	0.0	0.0	3	Bell C. L.
30	169	170	171	172	173	174	-117.59	0.0	0.0	3	Bell C. L.
31	175	176	177	178	179	180	-129.59	0.0	0.0	3	Bell C. L.
32	181	182	183	184	185	186	-142.49	0.0	0.0	3	Bell C. L.
33	187	188	189	190	191	192	-155.59	0.0	0.0	3	Bell C. L. at Exit
34	193	194	195	196	197	198	-20.0	-4.55	9.11	3	Strut
35	199	200	201	202	203	204	-20.0	-4.55	-9.11	3	Strut
36	205	206	207	208	209	210	-20.0	9.11	-4.55	3	Strut
37	211	212	213	214	215	216	-20.0	-9.11	-4.55	3	Strut
38	217	218	219	220	221	222	-34.8	-12.0	26.0	3	Controller C.G.
39	223	224	225	226	227	228	-20.0	0.0	0.0	3	Main Beam/Struts
40	229	230	231	232	233	234	1.5	21.52	-21.26	4	LPOTP
41	235	236	237	238	239	240	-1.71	-21.0	21.0	4	LPFTP
43	241	242	243	244	245	246	10.0	11.0	12.54	3	LPFTP Duct
44	247	248	249	250	251	252	-7.56	-16.3	-16.3	3	LPFTP Duct
45	253	254	255	256	257	258	-8.74	16.68	16.09	3	LPFTP Duct

NOTES: Use Right Hand Rule
Grid Points are identified in Figure 2.

TABLE 2. IDENTIFICATION OF SSME DUCTS

NASTRAN Duct No.	Duct Discription	Nodes Connected By Duct
1	LPFTP Turbine Drive	39, 41
2	LPFTP Discharge	41, 5
3	LPOTP Turbine Drive	40, 6
4	LPOTP Discharge	40, 6
5	LPFTP Turbine Discharge	11, 41, 43, 44, 45

TABLE 3. IDENTIFICATION OF STRUCTURAL ELEMENTS SELECTED FOR LOADS OUTPUT

Element Number	Node At End A	Node At End B	Nodes Defining Plane 1			Type Element
1	1	2	1	2	7	Bar
2	2	39	2	39	7	Bar
3	3	4	3	4	7	Bar
4	4	11	4	11	7	Bar
9	5	2	5	2	3	Bar
10	6	2	6	2	3	Bar
11	39	3	39	3	7	Bar
12	11	24	11	24	7	Bar
13	24	25	24	25	7	Bar

NOTE: Element coordinate system defined in Figure 4.

TABLE 4. SERVOACTUATOR PARAMETERS

Symbol	Units	Value	Description
K_v	cis(in.-lb)	1228	Servovalve flow gain
G_v	-	$\left[\left(\frac{S}{W_v}\right)^2 + \left(\frac{2\zeta_v}{W_v}\right) S+1\right]^{-1}$	Servovalve dynamics
W_v	rad/sec	220	Servovalve natural frequency
ζ_v	-	0.7	Servovalve damping coefficient
A	$in.^2$	24.83	Actuator piston area
K_o	lb/in.	902 800	Oil stiffness
M_p	$(lb\text{-}sec^2)in.$	0.11	Actuator piston equivalent mass
K_p	cis/psi	0.15	Pressure feedback gain
G_p	-	$\frac{T_p S}{T_p S + 1}$	Pressure feedback shaping network
T_p	sec	0.125	Pressure feedback time constant
H	(in.-lb)/in.	0.364	Position feedback gain
f	lb	-	External disturbance load
F_A	lb	-	Actuator developed force
F_B	lb	90 000	Bypass actuating force
X_i	in.	$\frac{1}{A}\int_0^t Q_A dt$	Ideal piston position
X_p	in.	-	Actuator piston position
Q_v	cis	-	Servovalve flow
Q_{dpf}	cis	-	Dynamic pressure feedback flow
Q_B	cis	-	Load bypass flow
Q_A	cis	-	Flow to actuator piston
E	in.-lb	-	Actuating error signal
T_c	in.-lb	-	Command torque

TABLE 5. RANDOMLY SELECTED INPUT DATA

Case	Transient Number	J-2S Side Load Amplitude [lb rms/SQRT (1.6 Hz)]	SSME Scaling Factor	Direction of Transient (deg)
1	22	940.90	1.461	19.03
2	3	337.13	1.474	72.89
3	19	186.18	1.461	1.73
4	6	461.81	1.476	84.95
5	13	463.43	1.508	277.08
6	7	94.91	1.537	336.69
7	16	104.58	1.468	302.16
8	16	778.26	1.571	293.18
9	1	740.72	1.453	282.41
10	16	151.04	1.500	345.91
11	12	106.60	1.556	326.82
12	1	600.96	1.483	231.09
13	15	292.06	1.575	19.38
14	16	872.84	1.589	204.27
15	16	520.91	1.485	206.75
16	22	134.04	1.477	291.12
17	9	554.28	1.454	162.26
18	21	304.70	1.553	134.52
19	3	976.57	1.399	206.06
20	3	594.23	1.426	157.88
21	10	165.28	1.496	61.55
22	16	438.45	1.461	84.68
23	16	107.19	1.419	148.15
24	8	402.82	1.536	214.33
25	24	418.23	1.469	50.16
26	23	154.87	1.451	54.24
27	21	279.96	1.487	282.02
28	15	460.55	1.531	68.09
29	8	375.64	1.505	149.71
30	9	345.75	1.536	60.48
31	4	664.51	1.562	348.47
32	22	450.54	1.531	317.65
33	18	114.74	1.513	216.75
34	1	458.54	1.489	104.65
35	19	415.76	1.575	86.37
36	15	305.61	1.523	35.86
37	18	541.42	1.652	89.02
38	24	263.59	1.521	138.29
39	24	376.66	1.484	98.91
40	3	370.22	1.497	149.95
41	23	703.09	1.415	91.72
42	19	452.00	1.523	29.40
43	19	100.98	1.515	199.83
44	7	308.64	1.556	180.31
45	4	589.17	1.597	103.72
46	23	371.57	1.514	248.78
47	8	449.48	1.518	279.70
48	22	599.09	1.539	354.18
49	11	298.55	1.515	63.83
50	15	895.35	1.577	36.19

TABLE 5. (Concluded)

Case	Transient Number	J-2S Side Load Amplitude [lb rms/SQRT (1.6 Hz)]	SSME Scaling Factor	Direction of Transient (deg)
51	16	203.35	1.414	85.82
52	19	84.97	1.516	40.76
53	15	518.47	1.614	114.89
54	2	728.92	1.489	311.79
55	19	144.89	1.549	317.77
56	3	370.75	1.553	209.77
57	23	532.00	1.526	150.22
58	1	169.76	1.589	70.15
59	9	152.56	1.563	252.67
60	11	604.77	1.535	137.32
61	17	113.44	1.522	332.97
62	18	433.57	1.504	354.49
63	10	310.62	1.552	43.08
64	13	126.22	1.570	116.17
65	20	463.92	1.672	237.58
66	10	406.72	1.489	195.07
67	11	1578.34	1.528	134.12
68	1	509.06	1.582	85.05
69	17	282.84	1.657	134.79
70	18	413.87	1.605	189.57
71	14	336.89	1.581	112.48
72	13	306.77	1.448	351.30
73	2	293.28	1.498	290.42
74	17	221.88	1.484	45.90
75	14	466.38	1.568	126.19
76	14	426.49	1.490	324.48
77	15	125.42	1.525	265.62
78	15	156.58	1.506	306.82
79	12	302.42	1.519	198.07
80	24	437.73	1.580	67.60
81	17	202.84	1.536	314.14
82	15	477.19	1.680	85.61
83	20	201.82	1.554	0.53
84	24	198.89	1.662	337.56
85	4	610.48	1.578	176.72
86	1	397.79	1.589	80.03
87	20	374.13	1.614	264.67
88	12	384.98	1.494	251.20
89	5	88.59	1.518	337.99
90	9	339.63	1.483	164.78
91	21	545.05	1.475	201.36
92	17	528.05	1.570	218.79
93	16	390.83	1.471	56.33
94	10	568.83	1.517	126.21
95	24	134.86	1.549	117.29
96	22	483.47	1.577	112.23
97	20	511.01	1.441	201.66
98	19	385.77	1.504	88.73
99	4	488.68	1.393	93.59
100	13	522.69	1.596	52.67

TABLE 6. PEAK FORCE OF SIDE LOAD TRANSIENTS

Case	Transient Number	Peak Force (lb)	Case	Transient Number	Peak Force (lb)
1	22	13613.3	51	16	2436.9
2	3	4278.9	52	19	1216.3
3	19	2567.4	53	15	9750.6
4	6	7028.9	54	2	10601.6
5	13	7142.1	55	19	2118.8
6	7	1450.7	56	3	4957.2
7	16	1301.3	57	23	8484.3
8	16	10359.3	58	1	2920.5
9	1	11650.1	59	9	2801.6
10	16	1920.3	60	11	10215.3
11	12	1719.2	61	17	2105.7
12	1	9644.3	62	18	6426.8
13	15	5360.0	63	10	5102.1
14	16	11750.0	64	13	2026.3
15	16	6555.0	65	20	8105.8
16	22	1961.0	66	10	6410.3
17	9	10348.7	67	11	26546.8
18	21	4531.5	68	1	8715.9
19	3	11771.2	69	17	5716.3
20	3	7300.4	70	18	6544.2
21	10	2617.2	71	14	4784.1
22	16	5429.1	72	13	4541.5
23	16	1289.4	73	2	4287.7
24	8	5555.5	74	17	4015.8
25	24	7641.3	75	14	6568.9
26	23	2349.2	76	14	5708.4
27	21	3985.2	77	15	2228.6
28	15	8218.1	78	15	2747.6
29	8	5075.8	79	12	4760.2
30	9	6820.0	80	24	8598.9
31	4	11374.7	81	17	3799.1
32	22	6830.3	82	15	9341.3
33	18	1710.9	83	20	3278.0
34	1	7387.9	84	24	4110.6
35	19	6180.7	85	4	10560.8
36	15	5421.6	86	1	6840.8
37	18	8814.9	87	20	6313.5
38	24	4983.0	88	12	5961.9
39	24	6947.8	89	5	1579.3
40	3	4773.7	90	9	6465.8
41	23	10397.9	91	21	7695.2
42	19	6498.0	92	17	10111.6
43	19	1444.5	93	16	4871.9
44	7	4777.3	94	10	9135.9
45	4	10310.5	95	24	2596.6
46	23	5879.5	96	22	7547.6
47	8	6126.6	97	20	7697.0
48	22	9128.5	98	19	5477.1
49	11	4978.0	99	4	7461.5
50	15	16444.3	100	13	8526.4

TABLE 7. IDENTIFICATION OF OUTPUT SET A

Row	Name	Element	End	Plane	Node	Description
1	Act. 1					Actuator 1 Load
2	Act. 2					Actuator 2 Load
3	M1 A1	1	A	1	1	Gimbal Point, Plane 1 Moment
4	M1 A2	1	A	2	1	Gimbal Point, Plane 2
5	M1 A3	1	A	3	1	Gimbal Point, Resultant Moment
6	M1 B1	1	B	1	2	
7	M1 B2	1	B	2	2	
8	M1 B3	1	B	3	2	
9	S1 1	1		1		Gimbal Point, Plane 1 Shear
10	S1 2	1		2		Gimbal Point, Plane 2 Shear
11	S1 3	1		3		Gimbal Point, Resultant Shear
12	A1	1				Gimbal Point, Axial Load
13	T1	1				Gimbal Point, Torsion (-X Side)
14	M2 A1	2	A	1	2	Engine C. L. Loads
15	M2 A2	2	A	2	2	
16	M2 A3	2	A	3	2	
17	M2 B1	2	B	1	39	
18	M2 B2	2	B	2	39	
19	M2 B3	2	B	3	39	
20	S2 1	2		1		
21	S2 2	2		2		
22	S2 3	2		3		
23	A2	2				
24	T2	2				
25	M11 A1	11	A	1	39	
26	M11 A2	11	A	2	39	
27	M11 A3	11	A	3	39	
28	S11 1	11		1		
29	S11 2	11		2		
30	S11 3	11		3		
31	A11	11				
32	T11	11				
33	M3 A1	3	A	1	3	
34	M3 A2	3	A	2	3	
35	M3 A3	3	A	3	3	
36	S3 1	3		1		
37	S3 2	3		2		
38	S3 3	3		3		Engine C. L. Loads

TABLE 7. (Continued)

Row	Name	Element	End	Plane	Node	Description
39	A3	3				Engine C. L. Loads
40	T3	3				Engine C. L. Loads
41	M4 A1	4	A	1	4	Throat, Plane 1 Moment
42	M4 A2	4	A	2	4	Throat, Plane 2 Moment
43	M4 A3	4	A	3	4	Throat, Resultant Moment
44	M4 B1	4	B	1	11	Engine C. L. Loads
45	M4 B2	4	B	2	11	
46	M4 B3	4	B	3	11	
47	S4 1	4		1		
48	S4 2	4		2		
49	S4 3	4		3		
50	A4	4				
51	T4	4				
52	M12A1	12	A	1	11	
53	M12A2	12	A	2	11	
54	M12A3	12	A	3	11	
55	S12 1	12		1		
56	S12 2	12		2		
57	S12 3	12		3		
58	A12	12				
59	T12	12				Engine C. L. Loads
60	M13 A1	13	A	1	24	Bell C. L. Loads
61	M13A2	13	A	2	24	
62	M13A3	13	A	3	24	
63	M13B1	13	B	1	25	
64	M13B2	13	B	2	25	
65	M13B3	13	B	3	25	
66	S13 1	13		1		
67	S13 2	13		2		
68	S13 3	13		3		
69	A13	13				
70	T13	13				Bell C. L. Loads
71	M9 B1	9	B	1	2	HPFTP Beam Loads
72	M9 B2	9	B	2	2	
73	M9 B3	9	B	3	2	
74	S9 1	9		1		
75	S9 2	9		2		
76	S9 3	9		3		HPFTP Beam Loads

TABLE 7. (Concluded)

Row	Name	Element	End	Plane	Node	Description
77	A9	9				HPFTP Beam Loads
78	T9	9				HPFTP Beam Loads
79	M10 B1	10	B	1	2	HPOTP Beam Loads
80	M10 B2	10	B	2	2	
81	M10 B3	10	B	3	2	
82	S10 1	10		1		
83	S10 2	10		2		
84	S10 3	10		3		
85	A10	10				
86	T10	10				HPOTP Beam Loads

NOTES: Prefixes: M = Bending Moment (in.-lb)
S = Shear Load (lb)
A = Axial Load (lb)
T = Torsional Load (in.-lb)

Plane 3 loads are resultant of loads for plane 1 and plane 2; for example: M10B3 = SQRT(M10B1**2 + M10B2**2)

TABLE 8. IDENTIFICATION OF OUTPUT SET B

Row	Name	Node	Description
1	DY33	33	Bell Displacement at Exit
2	DZ33	33	↓
3	DYZ33	33	Bell Displacement at Exit
4	AX1	1	Gimbal Point Accelerations
5	AY1	1	↓
6	AZ1	1	
7	AYZ1	1	
8	RAX1	1	
9	RAY1	1	
10	RAZ1	1	Gimbal Point Accelerations
11	AX2	2	
12	AY2	2	
13	AZ2	2	
14	AYZ2	2	
15	RAX2	2	
16	RAY2	2	
17	RAZ2	2	
18	RAYZ2	2	
19	AX5	5	HPFTP Accelerations
20	AY5	5	↓
21	AZ5	5	
22	AXYZ5	5	
23	RAX5	5	
24	RAY5	5	
25	RAZ5	5	
26	RAXYZ5	5	HPFTP Accelerations
27	AX6	6	HPOTP Accelerations
28	AY6	6	↓
29	AZ6	6	
30	AXYZ6	6	
31	RAX6	6	
32	RAY6	6	
33	RAZ6	6	
34	RAXYZ6	6	HPOTP Accelerations

TABLE 8. (Concluded)

Row	Name	Node	Description
35	AX11	11	
36	AY11	11	
37	AZ11	11	
38	AYZ11	11	
39	RAX11	11	
40	RAY11	11	
41	RAZ11	11	
42	RAYZ11		
43	AX38	38	Controller Accelerations
44	AY38	38	
45	AZ38	38	
46	AXYZ38	38	
47	RAX38	38	
48	RAY38	38	
49	RAZ38	38	Controller Accelerations

NOTES: Prefixes:
- DY = Displacement in Y-Direction
- DZ = Displacement in Z-Direction
- DYZ = Root Sum Square of Displacements, DY, DZ
- AX = Acceleration in X-Direction
- AY = Acceleration in Y-Direction
- AZ = Acceleration in Z-Direction
- AYZ = Root Sum Square of Accelerations, AY, AZ
- AXYZ = Root Sum Square of Accelerations, AX, AY, AZ
- RAX = Rotational Acceleration About X-Axis
- RAY = Rotational Acceleration About Y-Axis
- RAZ = Rotational Acceleration About Z-Axis
- RAYZ = Root Sum Square of Rotational Acceleration, RAY, RAZ.
- RAXYZ = Root Sum Square of Rotational Acceleration, RAX, RAY, RAZ.

Displacements in inches, Translational Accelerations in g, Rotational Accelerations in g/inch

TABLE 9. STATISTICAL VALUES — OUTPUT SET A, ENGINE 1 — START POSITION

ROW	NAME	MAXIMUMS			MINIMUMS		
		MEAN VALUE	STANDARD DEVIATION	STATISTICAL VALUE	MEAN VALUE	STANDARD DEVIATION	STATISTICAL VALUE
1	ACT.1	.1553+05	.1247+05	.5832+05	-.1407+05	.9914+04	-.4807+05
2	ACT.2	.2051+05	.1442+05	.6998+05	-.2096+05	.1518+05	-.7302+05
3	M1 A1	.6249-01	.4546-01	.2184+00	-.6802-01	.5861-01	-.2690+00
4	M1 A2	.1238+00	.7801-01	.3914+00	-.1267+00	.9098-01	-.4387+00
5	M1 A3	.1466+00	.9824-01	.4836+00	.1068-04	.4897-04	-.1573-03
6	M1 B1	.2024+06	.1745+06	.8010+06	-.1891+06	.1472+06	-.6940+06
7	M1 B2	.2308+06	.1845+06	.8638+06	-.2273+06	.1684+06	-.8049+06
8	M1 B3	.3083+06	.2442+06	.1146+07	.1534+02	.6961+02	-.2234+03
9	S1 1	.1220+05	.9497+04	.4477+05	-.1306+05	.1126+05	-.5168+05
10	S1 2	.1466+05	.1086+05	.5193+05	-.1489+05	.1191+05	-.5573+05
11	S1 3	.1989+05	.1576+05	.7394+05	.9896+00	.4491+01	-.1442+02
12	A1	.1605+05	.9479+04	.4856+05	-.1659+05	.1086+05	-.5386+05
13	T1	.1438+06	.9643+05	.4746+06	-.1550+06	.1134+06	-.5440+06
14	M2 A1	.5132+06	.3702+06	.1783+07	-.5083+06	.3646+06	-.1759+07
15	M2 A2	.6317+06	.4540+06	.2189+07	-.6349+06	.4767+06	-.2270+07
16	M2 A3	.7613+06	.5386+06	.2609+07	.6351+02	.2386+03	-.7550+03
17	M2 B1	.5207+06	.3756+06	.1809+07	-.5133+06	.3642+06	-.1763+07
18	M2 B2	.6341+06	.4500+06	.2178+07	-.6384+06	.4786+06	-.2280+07
19	M2 B3	.7664+06	.5300+06	.2584+07	.5207+02	.1815+03	-.5704+03
20	S2 1	.5721+04	.4417+04	.2087+05	-.6346+04	.5274+04	-.2444+05
21	S2 2	.4969+04	.3455+04	.1682+05	-.5257+04	.4380+04	-.2028+05
22	S2 3	.7911+04	.5454+04	.2662+05	.6062+00	.2211+01	-.6979+01
23	A2	.7972+04	.5034+04	.2524+05	-.8601+04	.6126+04	-.2961+05
24	T2	.1858+06	.1349+06	.6486+06	-.2044+06	.1684+06	-.7819+06
25	M11A1	.6036+06	.4506+06	.2149+07	-.5760+06	.3972+06	-.1938+07
26	M11A2	.7501+06	.5260+06	.2554+07	-.7637+06	.5706+06	-.2735+07
27	M11A3	.9122+06	.5998+06	.2969+07	.4391+02	.1423+03	-.4443+03
28	S11 1	.3748+04	.2972+04	.1394+05	-.3607+04	.2585+04	-.1247+05
29	S11 2	.4864+04	.3530+04	.1697+05	-.5034+04	.3878+04	-.1833+05
30	S11 3	.5730+04	.4074+04	.1970+05	.7937+00	.3400+01	-.1087+02
31	A11	.5106+04	.3421+04	.1684+05	-.5164+04	.3485+04	-.1712+05
32	T11	.4847+05	.3244+05	.1598+06	-.5102+05	.3830+05	-.1824+06
33	M3 A1	.5800+06	.4303+06	.2056+07	-.5553+06	.3827+06	-.1868+07
34	M3 A2	.7206+06	.5034+06	.2447+07	-.7315+06	.5475+06	-.2609+07
35	M3 A3	.8782+06	.5730+06	.2844+07	.5148+02	.1897+03	-.5991+03
36	S3 1	.3774+04	.3028+04	.1416+05	-.3595+04	.2557+04	-.1237+05
37	S3 2	.4575+04	.3321+04	.1597+05	-.4742+04	.3737+04	-.1756+05
38	S3 3	.5495+04	.3934+04	.1899+05	.7909+00	.3328+01	-.1062+02
39	A3	.4764+04	.3185+04	.1569+05	-.4818+04	.3247+04	-.1596+05
40	T3	.4847+05	.3244+05	.1598+06	-.5102+05	.3830+05	-.1824+06
41	M4 A1	.5446+06	.3998+06	.1916+07	-.5243+06	.3625+06	-.1768+07
42	M4 A2	.6802+06	.4714+06	.2297+07	-.6888+06	.5106+06	-.2440+07
43	M4 A3	.8317+06	.5367+06	.2672+07	.3781+02	.1317+03	-.4139+03
44	M4 B1	.5258+06	.3845+06	.1845+07	-.5077+06	.3518+06	-.1715+07
45	M4 B2	.6556+06	.4522+06	.2207+07	-.6630+06	.4899+06	-.2343+07

TABLE 9. (Concluded)

46	M4 B3	.8033+06	.5164+06	.2575+07	.3234+02	.1180+03	-.3725+03
47	S4 1	.3786+04	.3054+04	.1426+05	-.3602+04	.2573+04	-.1243+05
48	S4 2	.5070+04	.3568+04	.1731+05	-.5243+04	.4078+04	-.1923+05
49	S4 3	.5971+04	.4266+04	.2060+05	.5073+00	.1980+01	-.6283+01
50	A4	.4420+04	.2949+04	.1453+05	-.4470+04	.3009+04	-.1479+05
51	T4	.4847+05	.3244+05	.1598+06	-.5102+05	.3830+05	-.1824+06
52	M12A1	.5242+06	.3804+06	.1829+07	-.5039+06	.3501+06	-.1705+07
53	M12A2	.6449+06	.4443+06	.2169+07	-.6522+06	.4756+06	-.2284+07
54	M12A3	.7986+06	.5059+06	.2534+07	.3507+02	.1185+03	-.3714+03
55	S12 1	.5620+04	.4168+04	.1992+05	-.5231+04	.3455+04	-.1708+05
56	S12 2	.6807+04	.4864+04	.2349+05	-.7022+04	.5512+04	-.2593+05
57	S12 3	.8442+04	.5766+04	.2822+05	.2597+00	.9672+00	-.3058+01
58	A12	.2807+04	.1922+04	.9398+04	-.2843+04	.1926+04	-.9448+04
59	T12	.6324+05	.4682+05	.2238+06	-.6272+05	.4640+05	-.2219+06
60	M13A1	.4727+06	.3414+06	.1644+07	-.4563+06	.3190+06	-.1551+07
61	M13A2	.5799+06	.3969+06	.1941+07	-.5857+06	.4228+06	-.2036+07
62	M13A3	.7220+06	.4521+06	.2273+07	.3336+02	.1181+03	-.3717+03
63	M13B1	.4232+06	.3049+06	.1469+07	-.4097+06	.2875+06	-.1396+07
64	M13B2	.5191+06	.3534+06	.1731+07	-.5238+06	.3755+06	-.1812+07
65	M13B3	.6483+06	.4030+06	.2031+07	.2771+02	.1084+03	-.3442+03
66	S13 1	.5570+04	.4112+04	.1967+05	-.5239+04	.3522+04	-.1732+05
67	S13 2	.6813+04	.4833+04	.2339+05	-.6991+04	.5394+04	-.2549+05
68	S13 3	.8401+04	.5642+04	.2775+05	.3560+00	.1358+01	-.4301+01
69	A13	.2245+04	.1538+04	.7519+04	-.2274+04	.1541+04	-.7559+04
70	T13	.6066+05	.4508+05	.2153+06	-.6015+05	.4468+05	-.2134+06
71	M9 B1	.3067+06	.2730+06	.1243+07	-.3041+06	.2517+06	-.1167+07
72	M9 B2	.1392+06	.1096+06	.5151+06	-.1417+06	.1198+06	-.5526+06
73	M9 B3	.3249+06	.2770+06	.1275+07	.3251+02	.1247+03	-.3953+03
74	S9 1	.9840+04	.8256+04	.3816+05	-.1005+05	.8860+04	-.4044+05
75	S9 2	.4510+04	.3773+04	.1745+05	-.4421+04	.3446+04	-.1624+05
76	S9 3	.1054+05	.8978+04	.4133+05	.8725+00	.3598+01	-.1147+02
77	A9	.3697+04	.2616+04	.1267+05	-.3660+04	.2400+04	-.1189+05
78	T9	.1551+05	.9882+04	.4940+05	-.1535+05	.9673+04	-.4853+05
79	M10B1	.3408+06	.2575+06	.1224+07	-.3356+06	.2355+06	-.1143+07
80	M10B2	.1655+06	.1474+06	.6712+06	-.1541+06	.1265+06	-.5880+06
81	M10B3	.3770+06	.2576+06	.1260+07	.3003+02	.1140+03	-.3609+03
82	S10 1	.1065+05	.7819+04	.3747+05	-.1075+05	.8417+04	-.3962+05
83	S10 2	.5082+04	.4088+04	.1910+05	-.5505+04	.4962+04	-.2252+05
84	S10 3	.1195+05	.8336+04	.4054+05	.1120+01	.4058+01	-.1280+02
85	A10	.3470+04	.2424+04	.1178+05	-.3492+04	.2318+04	-.1144+05
86	T10	.5820+05	.3669+05	.1840+06	-.5828+05	.3636+05	-.1830+06

TABLE 10. STATISTICAL VALUES — OUTPUT SET B, ENGINE 1 — START POSITION

ROW	NAME	MAXIMUMS			MINIMUMS		
		MEAN VALUE	STANDARD DEVIATION	STATISTICAL VALUE	MEAN VALUE	STANDARD DEVIATION	STATISTICAL VALUE
1	DY33	.4007+00	.3255+00	.1517+01	-.4033+00	.3478+00	-.1596+01
2	DZ33	.4547+00	.2932+00	.1460+01	-.4625+00	.3055+00	-.1510+01
3	DYZ33	.7182+00	.4214+00	.2164+01	.0000	.0000	.0000
4	AX1	.2631+01	.1797+01	.8796+01	-.2662+01	.1802+01	-.8844+01
5	AY1	.4646+01	.3974+01	.1828+02	-.4503+01	.3354+01	-.1601+02
6	AZ1	.5218+01	.4303+01	.1998+02	-.5169+01	.4540+01	-.2074+02
7	AYZ1	.6858+01	.5561+01	.2593+02	.3176-03	.1440-02	-.4621-02
8	RAX1	.3108-01	.2189-01	.1062+00	-.3062-01	.2255-01	-.1080+00
9	RAY1	.3165+00	.2607+00	.1211+01	-.3173+00	.2538+00	-.1188+01
10	RAZ1	.1222+00	.9283-01	.4406+00	-.1251+00	.1151+00	-.5200+00
11	AX2	.2693+01	.1833+01	.8981+01	-.2726+01	.1848+01	-.9066+01
12	AY2	.2936+01	.2604+01	.1187+02	-.2805+01	.2106+01	-.1003+02
13	AZ2	.3461+01	.2825+01	.1315+02	-.3486+01	.2929+01	-.1353+02
14	AYZ2	.4532+01	.3685+01	.1717+02	.2841-03	.1502-02	-.4869-02
15	RAX2	.3427-01	.2342-01	.1146+00	-.3389-01	.2394-01	-.1160+00
16	RAY2	.1451+00	.1180+00	.5497+00	-.1500+00	.1260+00	-.5822+00
17	RAZ2	.1420+00	.1263+00	.5754+00	-.1407+00	.1068+00	-.5071+00
18	RAYZ2	.1914+00	.1407+00	.6739+00	.1655-04	.6969-04	-.2225-03
19	AX5	.5680+01	.5163+01	.2339+02	-.5556+01	.4892+01	-.2233+02
20	AY5	.2777+01	.1977+01	.9557+01	-.2684+01	.1981+01	-.9480+01
21	AZ5	.3400+01	.2392+01	.1161+02	-.3437+01	.2398+01	-.1166+02
22	AXYZ5	.6539+01	.5522+01	.2548+02	.1073-02	.3791-02	-.1193-01
23	RAX5	.3461-01	.2379-01	.1152+00	-.3433-01	.2436-01	-.1179+00
24	RAY5	.2281+00	.1914+00	.8846+00	-.2341+00	.2035+00	-.9323+00
25	RAZ5	.2317+00	.2198+00	.9857+00	-.2275+00	.1932+00	-.8903+00
26	RAXYZ5	.3112+00	.2688+00	.1233+01	.3603-04	.1272-03	-.4004-03
27	AX6	.8569+01	.6565+01	.3109+02	-.8590+01	.6603+01	-.3124+02
28	AY6	.3019+01	.2241+01	.1071+02	-.2906+01	.2133+01	-.1022+02
29	AZ6	.3836+01	.2379+01	.1199+02	-.3925+01	.2650+01	-.1301+02
30	AXYZ6	.9492+01	.6872+01	.3306+02	.1099-02	.3651-02	-.1142-01
31	RAX6	.3915-01	.2775-01	.1343+00	-.3938-01	.2790-01	-.1341+00
32	RAY6	.2179+00	.1798+00	.8345+00	-.2173+00	.1658+00	-.7862+00
33	RAZ6	.2387+00	.2034+00	.9363+00	-.2331+00	.1870+00	-.8744+00
34	RAXYZ6	.3124+00	.2456+00	.1155+01	.4151-04	.1462-03	-.4598-03
35	AX11	.2726+01	.1859+01	.9103+01	-.2761+01	.1871+01	-.9177+01
36	AY11	.1871+01	.1519+01	.7030+01	-.1784+01	.1420+01	-.6655+01
37	AZ11	.2349+01	.1548+01	.7659+01	-.2361+01	.1515+01	-.7559+01
38	AYZ11	.3028+01	.1849+01	.9369+01	.1987-03	.8360-03	-.2669-02
39	RAX11	.2576-01	.1610-01	.8099-01	-.2606-01	.1772-01	-.8686-01
40	RAY11	.1140+00	.1063+00	.4787+00	-.1129+00	.9011-01	-.4219+00
41	RAZ11	.8700-01	.7295-01	.3372+00	-.9087-01	.8013-01	-.3657+00
42	RAYZ11	.1552+00	.1278+00	.5937+00	.6995-05	.3066-04	-.9818-04
43	AX38	.4500+01	.3568+01	.1674+02	-.4533+01	.3437+01	-.1632+02
44	AY38	.2370+01	.1897+01	.8877+01	-.2199+01	.1624+01	-.7769+01
45	AZ38	.2639+01	.1702+01	.8477+01	-.2677+01	.1779+01	-.8778+01
46	AXYZ38	.5415+01	.3570+01	.1869+02	.1067-02	.4061-02	-.1286-01
47	RAX38	.2581-01	.1615-01	.8121-01	-.2611-01	.1778-01	-.8709-01
48	RAY38	.1140+00	.1063+00	.4786+00	-.1129+00	.9015-01	-.4221+00
49	RAZ38	.8703-01	.7295-01	.3373+00	-.9091-01	.8015-01	-.3658+00

TABLE 11. STATISTICAL VALUES — OUTPUT SET A, ENGINE 2 — START POSITION

ROW	NAME	MAXIMUMS			MINIMUMS		
		MEAN VALUE	STANDARD DEVIATION	STATISTICAL VALUE	MEAN VALUE	STANDARD DEVIATION	STATISTICAL VALUE
1	ACT.1	.1658+05	.1165+05	.5655+05	-.1632+05	.1185+05	-.5697+05
2	ACT.2	.1697+05	.1068+05	.5360+05	-.1709+05	.1165+05	-.5703+05
3	M1 A1	.1535+00	.1179+00	.5579+00	-.1619+00	.1415+00	-.6473+00
4	M1 A2	.7601-01	.5841-01	.2764+00	-.7475-01	.5649-01	-.2685+00
5	M1 A3	.1871+00	.1392+00	.6646+00	.6157-05	.3724-04	-.1216-03
6	M1 R1	.2453+06	.2114+06	.9705+06	-.2229+06	.1703+06	-.8069+06
7	M1 R2	.2217+06	.1928+06	.8830+06	-.2150+06	.1681+06	-.7917+06
8	M1 R3	.3221+06	.2321+06	.1118+07	.1157+02	.7197+02	-.2353+03
9	S1 1	.1438+05	.1099+05	.5206+05	-.1583+05	.1364+05	-.6261+05
10	S1 2	.1387+05	.1085+05	.5108+05	-.1430+05	.1244+05	-.5697+05
11	S1 3	.2078+05	.1498+05	.7215+05	.7464+00	.4643+01	-.1518+02
12	A1	.1718+05	.1066+05	.5374+05	-.1741+05	.1110+05	-.5548+05
13	T1	.1752+06	.1161+06	.5733+06	-.1829+06	.1211+06	-.5982+06
14	M2 A1	.4650+06	.3187+06	.1558+07	-.4489+06	.2929+06	-.1453+07
15	M2 A2	.4603+06	.2906+06	.1457+07	-.4533+06	.3319+06	-.1592+07
16	M2 A3	.6426+06	.4155+06	.2068+07	.2487+02	.1785+03	-.5873+03
17	M2 R1	.4742+06	.3291+06	.1603+07	-.4550+06	.2973+06	-.1475+07
18	M2 R2	.4647+06	.2981+06	.1487+07	-.4573+06	.3362+06	-.1611+07
19	M2 R3	.6502+06	.4190+06	.2087+07	.4107+02	.2997+03	-.9868+03
20	S2 1	.5706+04	.3709+04	.1843+05	-.5812+04	.3851+04	-.1902+05
21	S2 2	.4867+04	.2914+04	.1486+05	-.5219+04	.3622+04	-.1764+05
22	S2 3	.7849+04	.4557+04	.2348+05	.1687+00	.1007+01	-.3284+01
23	A2	.7762+04	.5713+04	.2736+05	-.7967+04	.6361+04	-.2979+05
24	T2	.3077+06	.2338+06	.1110+07	-.3078+06	.2373+06	-.1122+07
25	M11A1	.5268+06	.3643+06	.1778+07	-.5079+06	.3247+06	-.1622+07
26	M11A2	.5472+06	.3706+06	.1818+07	-.5430+06	.3955+06	-.1900+07
27	M11A3	.7420+06	.4554+06	.2304+07	.4782+02	.2928+03	-.9565+03
28	S11 1	.3621+04	.2304+04	.1152+05	-.3491+04	.1941+04	-.1015+05
29	S11 2	.3787+04	.2222+04	.1141+05	-.3681+04	.2065+04	-.1077+05
30	S11 3	.4933+04	.2731+04	.1430+05	.1491+00	.1004+01	-.3296+01
31	A11	.5107+04	.3460+04	.1698+05	-.5178+04	.3557+04	-.1738+05
32	T11	.1401+06	.1118+06	.5237+06	-.1416+06	.1138+06	-.5318+06
33	M3 A1	.5204+06	.3665+06	.1778+07	-.4960+06	.3205+06	-.1595+07
34	M3 A2	.5303+06	.3608+06	.1768+07	-.5255+06	.3865+06	-.1851+07
35	M3 A3	.7264+06	.4487+06	.2265+07	.3497+02	.2430+03	-.7984+03
36	S3 1	.3512+04	.2233+04	.1117+05	-.3393+04	.1817+04	-.9626+04
37	S3 2	.3659+04	.2141+04	.1100+05	-.3570+04	.2005+04	-.1045+05
38	S3 3	.4700+04	.2639+04	.1375+05	.1788+00	.1190+01	-.3903+01
39	A3	.4783+04	.3253+04	.1594+05	-.4849+04	.3339+04	-.1630+05
40	T3	.1401+06	.1118+06	.5237+06	-.1416+06	.1138+06	-.5318+06
41	M4 A1	.5090+06	.3706+06	.1780+07	-.4792+06	.3139+06	-.1556+07
42	M4 A2	.5032+06	.3438+06	.1682+07	-.4992+06	.3710+06	-.1772+07
43	M4 A3	.7024+06	.4371+06	.2202+07	.3807+02	.2723+03	-.8958+03
44	M4 R1	.4998+06	.3689+06	.1765+07	-.4681+06	.3079+06	-.1524+07
45	M4 R2	.4836+06	.3322+06	.1623+07	-.4804+06	.3589+06	-.1712+07

TABLE 11. (Concluded)

46	M4 A3	.6837+06	.4277+06	.2149+07	.2037+02	.1270+03	-.4151+03
47	S4 1	.3340+04	.2131+04	.1065+05	-.3288+04	.1784+04	-.9408+04
48	S4 2	.4434+04	.2653+04	.1353+05	-.4361+04	.2577+04	-.1320+05
49	S4 3	.5272+04	.2989+04	.1552+05	.9076-01	.6146+00	-.2017+01
50	A4	.4454+04	.3046+04	.1490+05	-.4519+04	.3120+04	-.1522+05
51	T4	.1401+06	.1118+06	.5237+06	-.1416+06	.1138+06	-.5314+06
52	M12A1	.4986+06	.3691+06	.1765+07	-.4684+06	.3080+06	-.1525+07
53	M12A2	.4726+06	.3171+06	.1560+07	-.4697+06	.3435+06	-.1648+07
54	M12A3	.6790+06	.4177+06	.2112+07	.1784+02	.1018+03	-.3313+03
55	S12 1	.4531+04	.3019+04	.1489+05	-.4416+04	.2655+04	-.1352+05
56	S12 2	.5056+04	.3471+04	.1696+05	-.5038+04	.3526+04	-.1713+05
57	S12 3	.6691+04	.4078+04	.2068+05	.3162+00	.1933+01	-.6315+01
58	A12	.2609+04	.1683+04	.8381+04	-.2643+04	.1772+04	-.8722+04
59	T12	.1771+06	.1479+06	.6820+06	-.1747+06	.1463+06	-.6767+06
60	M13A1	.4585+06	.3431+06	.1635+07	-.4288+06	.2846+06	-.1404+07
61	M13A2	.4245+06	.2814+06	.1390+07	-.4237+06	.3084+06	-.1481+07
62	M13A3	.6211+06	.3806+06	.1927+07	.4049+02	.2576+03	-.8430+03
63	M13H1	.4171+06	.3151+06	.1498+07	-.3876+06	.2602+06	-.1280+07
64	M13R2	.3806+06	.2509+06	.1241+07	-.3809+06	.2764+06	-.1329+07
65	M13R3	.5634+06	.3450+06	.1747+07	.2745+02	.1672+03	-.5459+03
66	S13 1	.4684+04	.3197+04	.1565+05	-.4527+04	.2771+04	-.1403+05
67	S13 2	.5048+04	.3490+04	.1702+05	-.4999+04	.3589+04	-.1731+05
68	S13 3	.6719+04	.4152+04	.2096+05	.3013+00	.2004+01	-.6571+01
69	A13	.2083+04	.1345+04	.6696+04	-.2110+04	.1416+04	-.6968+04
70	T13	.1706+06	.1421+06	.6579+06	-.1683+06	.1412+06	-.6527+06
71	M9 R1	.3002+06	.1864+06	.9394+06	-.2991+06	.1804+06	-.9178+06
72	M9 R2	.1837+06	.1318+06	.6358+06	-.1853+06	.1424+06	-.6739+06
73	M9 R3	.3448+06	.2070+06	.1055+07	.2159+02	.1494+03	-.4907+03
74	S9 1	.9839+04	.5929+04	.3018+05	-.9837+04	.6055+04	-.3061+05
75	S9 2	.5981+04	.4585+04	.2171+05	-.5935+04	.4253+04	-.2052+05
76	S9 3	.1123+05	.6659+04	.3407+05	.4972+00	.3109+01	-.1017+02
77	A9	.5834+04	.4158+04	.2010+05	-.5541+04	.3954+04	-.1910+05
78	T9	.1486+05	.9842+04	.4862+05	-.1491+05	.9297+04	-.4680+05
79	M10R1	.2052+06	.1375+06	.6769+06	-.1932+06	.1127+06	-.5798+06
80	M10R2	.1790+06	.1294+06	.6227+06	-.1813+06	.1346+06	-.6431+06
81	M10R3	.2646+06	.1567+06	.8021+06	.1191+02	.8064+02	-.2647+03
82	S10 1	.6059+04	.3704+04	.1876+05	-.6316+04	.4189+04	-.2068+05
83	S10 2	.6186+04	.4536+04	.2174+05	-.6150+04	.4477+04	-.2151+05
84	S10 3	.8649+04	.5196+04	.2647+05	.2802+00	.1857+01	-.6088+01
85	A10	.5307+04	.4040+04	.1916+05	-.5666+04	.4220+04	-.2014+05
86	T10	.6082+05	.4068+05	.2003+06	-.5998+05	.4157+05	-.2026+06

TABLE 12. STATISTICAL VALUES — OUTPUT SET B, ENGINE 2 — START POSITION

RO#	NAME	MAXIMUMS			MINIMUMS		
		MEAN VALUE	STANDARD DEVIATION	STATISTICAL VALUE	MEAN VALUE	STANDARD DEVIATION	STATISTICAL VALUE
1	DY33	.4013+00	.3388+00	.1563+01	-.4006+00	.3449+00	-.1584+01
2	DZ33	.4490+00	.2916+00	.1449+01	-.4702+00	.3260+00	-.1589+01
3	DYZ33	.7296+00	.4244+00	.2185+01	.0000	.0000	.0000
4	AX1	.2507+01	.1609+01	.8027+01	-.2539+01	.1693+01	-.8344+01
5	AY1	.4800+01	.3309+01	.1615+02	-.4906+01	.3370+01	-.1637+02
6	AZ1	.5081+01	.4108+01	.1917+02	-.4965+01	.3876+01	-.1826+02
7	AYZ1	.6781+01	.4716+01	.2296+02	.1487-03	.8693-03	-.2833-02
8	RAX1	.8141-01	.6200-01	.2941+00	-.8062-01	.6366-01	-.2990+00
9	RAY1	.1045+00	.7602-01	.3652+00	-.1024+00	.6834-01	-.3368+00
10	RAZ1	.9898-01	.6610-01	.3257+00	-.1000+00	.6674-01	-.3289+00
11	AX2	.2539+01	.1627+01	.8120+01	-.2571+01	.1712+01	-.8445+01
12	AY2	.3868+01	.3127+01	.1459+02	-.3796+01	.2948+01	-.1391+02
13	AZ2	.3826+01	.3235+01	.1492+02	-.3717+01	.2998+01	-.1400+02
14	AYZ2	.5511+01	.3993+01	.1921+02	.3523-03	.2100-02	-.6987-02
15	RAX2	.9149-01	.7077-01	.3342+00	-.9084-01	.7157-01	-.3363+00
16	RAY2	.1155+00	.7875-01	.3856+00	-.1217+00	.8274-01	-.4055+00
17	RAZ2	.1098+00	.6492-01	.3325+00	-.1073+00	.6441-01	-.3283+00
18	RAYZ2	.1488+00	.9097-01	.4608+00	.5010-05	.3196-04	-.1046-03
19	AX5	.5358+01	.3396+01	.1701+02	-.5308+01	.3367+01	-.1686+02
20	AY5	.4087+01	.2884+01	.1398+02	-.4014+01	.3095+01	-.1463+02
21	AZ5	.3953+01	.2708+01	.1324+02	-.4000+01	.3026+01	-.1438+02
22	AXYZ5	.7174+01	.4187+01	.2154+02	.6354-03	.4184-02	-.1372-01
23	RAX5	.9497-01	.7408-01	.3491+00	-.9413-01	.7459-01	-.3500+00
24	RAY5	.1748+00	.1124+00	.5603+00	-.1822+00	.1201+00	-.5940+00
25	RAZ5	.1954+00	.1208+00	.6098+00	-.1922+00	.1194+00	-.6018+00
26	RAXYZ5	.2646+00	.1598+00	.8127+00	.1065-04	.6854-04	-.2244-03
27	AX6	.6005+01	.3790+01	.1901+02	-.6207+01	.4080+01	-.2020+02
28	AY6	.4640+01	.3976+01	.1828+02	-.4430+01	.3207+01	-.1557+02
29	AZ6	.4063+01	.2624+01	.1306+02	-.4082+01	.2658+01	-.1320+02
30	AXYZ6	.7982+01	.4875+01	.2470+02	.5888-03	.3488-02	-.1138-01
31	RAX6	.1011+00	.7887-01	.3716+00	-.1007+00	.8033-01	-.3762+00
32	RAY6	.1549+00	.9920-01	.4952+00	-.1605+00	.1013+00	-.5081+00
33	RAZ6	.1442+00	.8889-01	.4491+00	-.1418+00	.8886-01	-.4466+00
34	RAXYZ6	.2175+00	.1244+00	.6441+00	.1380-04	.9197-04	-.3017-03
35	AX11	.2557+01	.1641+01	.8187+01	-.2589+01	.1729+01	-.8521+01
36	AY11	.3402+01	.2971+01	.1359+02	-.3188+01	.2488+01	-.1172+02
37	AZ11	.2310+01	.1603+01	.7807+01	-.2342+01	.1452+01	-.7321+01
38	AYZ11	.4304+01	.2911+01	.1429+02	.1578-03	.9751-03	-.3187-02
39	RAX11	.5546-01	.3968-01	.1916+00	-.5435-01	.3935-01	-.1893+00
40	RAY11	.1090+00	.8551-01	.4023+00	-.1122+00	.8924-01	-.4183+00
41	RAZ11	.5786-01	.3840-01	.1896+00	-.5868-01	.4342-01	-.2076+00
42	RAYZ11	.1276+00	.9174-01	.4422+00	.2173-05	.1337-04	-.4369-04
43	AX38	.4439+01	.3718+01	.1719+02	-.4516+01	.3788+01	-.1751+02
44	AY38	.3687+01	.2911+01	.1367+02	-.3490+01	.2736+01	-.1287+02
45	AZ38	.2639+01	.1774+01	.8723+01	-.2704+01	.1829+01	-.8978+01
46	AXYZ38	.6359+01	.4537+01	.2192+02	.3723-03	.2331-02	-.7624-02
47	RAX38	.5561-01	.3980-01	.1921+00	-.5450-01	.3948-01	-.1899+00
48	RAY38	.1091+00	.8556-01	.4025+00	-.1123+00	.8930-01	-.4186+00
49	RAZ38	.5786-01	.3839-01	.1895+00	-.5868-01	.4342-01	-.2076+00

APPENDIX

METHODOLOGY

The development of the equations used to define the response of the SSME for the side load excitation is presented herein. The formulation is structured to facilitate the application of the Fortran Matrix Analysis (FORMA) system for solution of the problem on the digital computer. FORMA is a library of subroutines coded in Fortran IV for the efficient solution of structural dynamic systems on an electronic digital computer. The FORMA subroutines are in the form of building blocks which can be put together to solve a large variety of structural dynamic problems.

For convenience the methodology development is divided into two sections: (1) transient response analysis and (2) transient loads analysis. The equations of motion and the coordinates used to define the system state are explained in the transient loads analysis section. The transformation equations applied to obtain loads (and displacements and accelerations) from the system state coordinates are explained in the transient loads analysis section.

TRANSIENT RESPONSE ANALYSIS

The transient response analysis involves describing the interaction of the structural model and the actuator models for an externally applied forcing function. The structural model is comprised of both the engine structure and the orbiter thrust structure. The actuators are simulated as a feedback control system, controlling the motion of the engine. The equations of motion for the transient response are obtained by:

1. Developing the equations of motion for the structural model; replacing the actuators with externally applied forces. This matrix equation will be referred to as the structural equations of motion.

2. Expressing the block diagram model of the actuators into a matrix equation. This will be referred to as the actuators equation of motion.

3. Coupling the structure and actuators by applying compatibility relationships to obtain the equations of motion for the coupled system's transient response.

Structural Equations of Motion

The equations of motion for the engine without actuators are developed first. The actuators are replaced with external forces $\{F_a(t)\}$, $\{F_b(t)\}$, $\{F_c(t)\}$, and $\{F_d(t)\}$ applied at the actuators attachment points a, b, c, and d. The side load forcing function $\{F_e(t)\}$ is applied at the centerline of the bell exit plane, point e. These forces are shown in Figure A-1 where

$$\{F_a(t)\} = \begin{Bmatrix} F_x(t) \\ F_y(t) \\ F_z(t) \end{Bmatrix}_a = 3 \times 1 \text{ vector of components of force acting at point a (same notation for other points).}$$

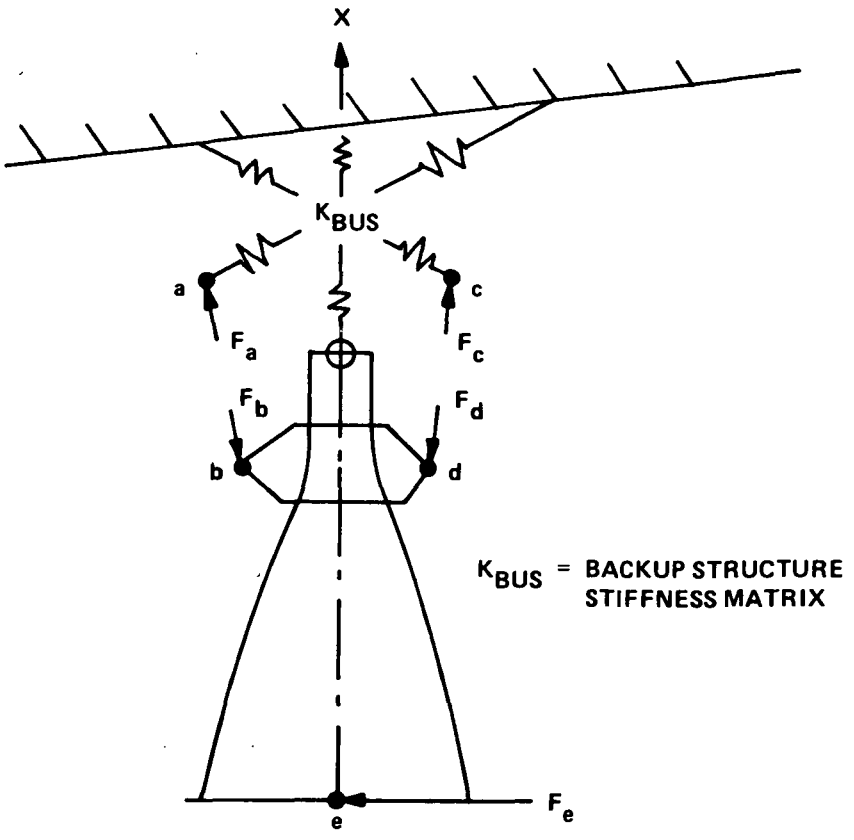

Figure A-1. Applied forces for engine without actuators.

The discrete equations of motion of the engine without actuators included is written as

$$[M]\{\ddot{h}\} + [D]\{\dot{h}\} + [K]\{h\} = \left\{\begin{matrix} \\ F_e(t) \\ \\ \end{matrix}\right\} + \left\{\begin{matrix} F_b(t) \\ F_d(t) \\ F_a(t) \\ F_c(t) \end{matrix}\right\} \quad , \quad (A-1)$$

where $\left\{\begin{matrix} \\ \\ \end{matrix}\right\}$ means a properly positioned matrix and

$\{h\}$ = discrete displacement,
$[M]$ = discrete mass matrix,
$[D]$ = discrete dumping matrix,
$[K]$ = discrete stiffness matrix.

It is extremely convenient to transform the discrete equations into a more practical form. The mode shapes of the dangling engine (engine without actuators) is available from the modal analysis. With these mode shapes one can write the transformation equation

$$\{h\} = [\phi]\{q\} \quad , \quad (A-2)$$

where

$[\phi]$ = modal matrix, each column being a mode shape,
$\{g\}$ = vector of modal coordinates; size $(n \times 1)$,
n = number of modes retained in the transient analysis.

The mode shapes are orthogonal such that

$$[\phi]^T [M][\phi] = \left[Meq\right] , \quad (A-3)$$

where $[Meq]$ = diagonal matrix of equivalent masses. Additionally the modal vectors are energy normalized such that

$$[Meq] = [I], \tag{A-4}$$

where $[I]$ is the identity matrix.

Substituting expression (A-2) into (A-1) and premultiplying by $[\phi]^T$, one obtains

$$[\phi]^T[M][\phi]\{\ddot{q}\} + [\phi]^T[D][\phi]\{\dot{q}\} + [\phi]^T[K][\phi]\{q\} = [\phi]^T \begin{Bmatrix} \\ F_e(t) \\ \\ \end{Bmatrix} + [\phi]^T \begin{Bmatrix} F_b(t) \\ F_d(t) \\ F_a(t) \\ F_c(t) \end{Bmatrix} . \tag{A-5}$$

In view of expressions (A-3) and (A-4), the triple matrix product $[\phi]^T[K][\phi]$ reduces as follows:

$$[\phi]^T[K][\phi] = \left[\omega_i^2\right] , \tag{A-6}$$

where $\left[\omega_i^2\right]$ is the diagonal matrix of modal frequencies squared.

One assumes that the damping matrix is such that

$$[\phi]^T[D][\phi] = \left[2\zeta_i\omega_i\right] , \tag{A-7}$$

where

$\left[2\zeta_i\omega_i\right]$ = diagonal matrix for model damping,

ζ_i = modal damping coefficient for mode i.

With expressions (A-3), (A-4), (A-6), and (A-7), one can write equation (A-5) as

$$\left[I\right]\{\ddot{q}\} + \left[2\zeta_i\omega_i\right]\{\dot{q}\} + \left[\omega_i^2\right]\{q\} = [\phi_1]^T\{F_e(t)\} + [\phi_2]^T\begin{Bmatrix} F_b(t) \\ F_d(t) \\ F_a(t) \\ F_c(t) \end{Bmatrix} \quad , (A\text{-}8)$$

where

$[\phi_1]$ = modal matrix whose rows correspond to the X, Y, Z displacements at point e; size (3 × n),

$[\phi_2]$ = modal matrix whose rows correspond to the X, Y, Z displacements at points b, d, a, and c, respectively; size (12 × n).

Expression (A-8) is the equation of motion in modal coordinates for the structural model with the actuators replaced by the applied forces; $\{F_a(t)\}$, $\{F_b(t)\}$, $\{F_c(t)\}$, and $\{F_d(t)\}$. These forces are unknowns at this point in the analytical development and must be eliminated.

Actuators Equations of Motion

The block diagram representation of an actuator is shown on Figure 5. This block diagram represents the actuator grounded at one end with an external force applied at the free piston end. For the analysis here, the actuator connecting points a and b are referred to as actuator no. 1; actuator no. 2 connects points c and d (see Figure A-1). Let points a and c correspond

to the grounded ends of the actuators. It will be necessary to remove these "ground" constraints since points a and c are points on the flexible thrust structure.

Each block in the diagram contains the Laplace representation of a transfer function of the form

$$E_{out} = \frac{N(s)}{D(s)} E_{in} \quad ,$$

where $D(s)$ is of quadratic or lower order and the order of $N(s)$ cannot exceed the order of $D(s)$. This expression is written in matrix form as

$$[D(s) \; -N(s)] \begin{Bmatrix} E_{out} \\ E_{in} \end{Bmatrix} = \{0\} \quad .$$

The several transfer functions involved in the block diagram can be stacked in one matrix expression of the form:

$$[H]\{E\} = \{0\} \quad . \qquad (A-9)$$

The blocks are connected by applying the compatibility relations which exist between various input-output coordinates in $\{E\}$ as defined by the block diagram. These compatibility relations are expressed in a transformation equation as

$$\{E\} = [CT]\{\delta\} \quad , \qquad (A-10)$$

where

$[CT]$ = coordinate transformation matrix,

$\{\delta\}$ = coordinates chosen to represent the system block diagram equations; size $(m \times 1)$,

m = number of block diagram coordinates.

Substituting expression (A-10) into (A-9), one obtains a matrix equation for the block diagram as

$$[G]\{\delta\} = \{0\} \quad , \tag{A-11}$$

where

$$[G] = [H][CT] \quad ,$$

$$G(I, J) = \alpha_{ij} S^2 + \beta_{ij} S + \gamma_{ij} \quad .$$

Then equation (A-11) can be expressed in a more convenient form as

$$[\alpha]\{\ddot{\delta}\} + [\beta]\{\dot{\delta}\} + [\gamma]\{\delta\} = \{0\} \quad . \tag{A-12}$$

Now, a procedure by which a block diagram model can be expressed in a matrix equation which has the same form as the structural equations of motion (A-8) has been outlined. This procedure was applied to the block diagram of the actuators. The equations for both actuators are stacked in one matrix equation of the same form as equation (A-12). The bypass load limiter loop is omitted for this analysis. The matrix expression obtained for the actuators equations of motion is as follows:

$$
[\alpha] \qquad \{\ddot{\delta}\}
$$

$$
\begin{bmatrix}
0 & 0 & 0 & 0 & 0 & 0 & 0 & 0 & 0 & 0 \\
0 & 0 & 0 & 0 & 0 & 0 & 0 & 0 & 0 & 0 \\
0 & 0 & M_p(1) & 0 & 0 & 0 & 0 & 0 & 0 & 0 \\
0 & 0 & 0 & 1 & 0 & 0 & 0 & 0 & 0 & 0 \\
0 & 0 & 0 & 0 & A(1)T_p(1) & -K_p(1)T_p(1)K_o(1) & 0 & 0 & 0 & 0 \\
0 & 0 & 0 & 0 & 0 & A(1) & 0 & 0 & 0 & 0 \\
0 & 0 & 0 & 0 & 0 & 0 & M_p(2) & 0 & 0 & 0 \\
0 & 0 & 0 & 0 & 0 & 0 & 0 & 1 & 0 & 0 \\
0 & 0 & 0 & 0 & 0 & 0 & 0 & 0 & A(2)T_p(2) & -K_p(2)T_p(2)K_o(2) \\
0 & 0 & 0 & 0 & 0 & 0 & 0 & 0 & 0 & A(2)
\end{bmatrix}
\begin{Bmatrix}
\ddot{f}(1) \\ \ddot{f}(2) \\ \ddot{X}_p(1) \\ \ddot{Q}_v(1) \\ \dot{Q}_{dpf}(1) \\ \dot{X}_i(1) \\ \ddot{X}_p(2) \\ \ddot{Q}_v(2) \\ \dot{Q}_{dpf}(2) \\ \dot{X}_i(2)
\end{Bmatrix}
$$

$$
[\beta]
$$

$$
+
\begin{bmatrix}
0 & 0 & 0 & 0 & 0 & 0 & 0 & 0 & 0 & 0 \\
0 & 0 & 0 & 0 & 0 & 0 & 0 & 0 & 0 & 0 \\
0 & 0 & 0 & 0 & 0 & -K_o(1) & 0 & 0 & 0 & 0 \\
0 & 0 & 0 & 2\zeta_v(1)\omega_v(1) & 0 & 0 & 0 & 0 & 0 & 0 \\
0 & 0 & K_p(1)T_p(1)K_o(1) & 0 & A(1) & 0 & 0 & 0 & 0 & 0 \\
0 & 0 & 0 & 0 & 1 & 0 & 0 & 0 & 0 & 0 \\
0 & 0 & 0 & 0 & 0 & 0 & 0 & 0 & 0 & -K_o(2) \\
0 & 0 & 0 & 0 & 0 & 0 & 0 & 2\zeta(2)\omega_v(2) & 0 & 0 \\
0 & 0 & 0 & 0 & 0 & 0 & K_p(2)T_p(2)K_o(2) & 0 & A(2) & 0 \\
0 & 0 & 0 & 0 & 0 & 0 & 0 & 0 & 1 & 0
\end{bmatrix}
$$

$$
\{\dot{\delta}\} \qquad [\gamma] \qquad \{\delta\}
$$

$$
\times
\begin{Bmatrix}
\dot{f}(1) \\ \dot{f}(2) \\ \dot{X}_p(1) \\ \dot{Q}_v(1) \\ \dot{Q}_{dpf}(1) \\ \dot{X}_i(1) \\ \dot{X}_p(2) \\ \dot{Q}_v(2) \\ Q_{dpf} \\ X_i(2)
\end{Bmatrix}
+
\begin{bmatrix}
0 & 0 & 0 & 0 & 0 & 0 & 0 & 0 & 0 & 0 \\
0 & 0 & 0 & 0 & 0 & 0 & 0 & 0 & 0 & 0 \\
-1 & 0 & K_o(1) & 0 & 0 & 0 & 0 & 0 & 0 & 0 \\
0 & 0 & H(1)K_v(1)\omega_v^2(1) & \omega_v^2(1) & 0 & 0 & 0 & 0 & 0 & 0 \\
0 & 0 & 0 & 0 & 0 & 0 & 0 & 0 & 0 & 0 \\
0 & 0 & 0 & -1 & 0 & 0 & 0 & 0 & 0 & 0 \\
0 & -1 & 0 & 0 & 0 & 0 & K_o(2) & 0 & 0 & 0 \\
0 & 0 & 0 & 0 & 0 & 0 & H(2)K_v(2)\omega_v^2(2) & \omega_v^2(2) & 0 & 0 \\
0 & 0 & 0 & 0 & 0 & 0 & 0 & 0 & 0 & 0 \\
0 & 0 & 0 & 0 & 0 & 0 & 0 & -1 & 0 & 0
\end{bmatrix}
\begin{Bmatrix}
f(1) \\ f(2) \\ X_p(1) \\ Q_v(1) \\ \text{DUMMY} \\ \text{DUMMY} \\ X_p(2) \\ Q_v(2) \\ \text{DUMMY} \\ \text{DUMMY}
\end{Bmatrix}
=
\begin{Bmatrix}
0 \\ 0 \\ 0 \\ 0 \\ 0 \\ 0 \\ 0 \\ 0 \\ 0 \\ 0
\end{Bmatrix}
$$

(A-13)

In the above expression the index (1) indicates that the parameter is for actuator no. 1 and an index (2) indicates actuator no. 2. The block diagram parameters are described in Table 4.

Coupled Actuators/Structure Equations of Motion

In the previous sections the equations of motion have been developed for (1) the structural model without actuators and (2) the actuators with one end grounded, the other end free. Now these systems will be coupled and the equations of motion for the combined system will be obtained. In order to accomplish this, compatibility conditions between the two systems involving force relationships and displacement relationships must be enforced.

One knows that, if one neglects the mass of the actuator, the forces applied at the attachment points are opposite in direction and equal in magnitude. Then for actuator no. 1,

$$\vec{F}_a = -\vec{F}_b = f(1)\ \vec{U}_1 \quad ,$$

where $\vec{U}_1$ is a unit vector along the actuator axis directed from point b toward point a. Similarly, for actuator no. 2,

$$\vec{F}_c = -\vec{F}_d = f(2)\ \vec{U}_2 \quad ,$$

where $\vec{U}_2$ is a unit vector along the actuator axis directed from point d toward point c.

One can express the above force compatibility conditions in a matrix form as

$$\begin{Bmatrix} \{F_b\} \\ \{F_d\} \\ \{F_a\} \\ \{F_c\} \end{Bmatrix} = [TFf]\{f\} \quad , \qquad \text{(A-14)}$$

where

$$[TFf] = \begin{bmatrix} -\{U_1\} & \{0\} \\ \{0\} & -\{U_2\} \\ \{U_1\} & \{0\} \\ \{0\} & \{U_2\} \end{bmatrix}$$

and

$$\{f\} = \begin{Bmatrix} f(1) \\ f(2) \end{Bmatrix} \quad .$$

Substituting equation (A-14) into equation (A-8), one obtains the expression

$$\left[I\right]\{\ddot{q}\} + \left[2\zeta_i\omega_i\right]\{\dot{q}\} + \left[\omega_i^2\right]\{q\} = [\phi_1]^T\{F_e(t)\} + [\phi_2]^T[TFf]\{f\} \quad .(A-15)$$

Since the actuator forces, $\{f\}$, are unknowns, one chooses to rewrite equation (A-15) with the actuator forces on the left-hand side to obtain the following expression for the structural equations of motion:

$$\begin{bmatrix} \left[I\right] & [0] \\ \left[0\right] & [0] \end{bmatrix} \begin{Bmatrix} \{\ddot{q}\} \\ \{\ddot{f}\} \end{Bmatrix} + \begin{bmatrix} \left[2\zeta_i\omega_i\right] & [0] \\ [0] & [0] \end{bmatrix} \begin{Bmatrix} \{\dot{q}\} \\ \{\dot{f}\} \end{Bmatrix} + \begin{bmatrix} \left[\omega_i^2\right] & \left[-[\phi_2]^T[TFf]\right] \\ [0] & [0] \end{bmatrix} \begin{Bmatrix} \{q\} \\ \{f\} \end{Bmatrix}$$

$$= \begin{bmatrix} [\phi_1]^T \\ [0] \end{bmatrix} \{F_e(t)\} \quad . \qquad (A-16)$$

Now, the structural model equations of motion, (A-16), and the actuator models equations of motion, (A-12), can be stacked in one matrix expression as follows:

$$\begin{bmatrix} [I] & [0] \\ [0] & [\alpha] \end{bmatrix} \begin{Bmatrix} \{\ddot{q}\} \\ \{\ddot{\delta}\} \end{Bmatrix} + \begin{bmatrix} [2\zeta_i\omega_i] & [0] \\ [0] & [\beta] \end{bmatrix} \begin{Bmatrix} \{\dot{q}\} \\ \{\dot{\delta}\} \end{Bmatrix} + \begin{bmatrix} [\omega_i^2] & [D_2] \\ [0] & [\gamma] \end{bmatrix} \begin{Bmatrix} \{q\} \\ \{\delta\} \end{Bmatrix} = [D_1]\{F_e(t)\} \quad , \tag{A-17}$$

where

$$[D_1] = \begin{bmatrix} [\phi_1]^T \\ [0] \end{bmatrix} \begin{matrix} \} n \\ \} m \end{matrix}$$
$$\quad 3$$

and

$$[D_2] = \begin{matrix} \quad\quad 2 \quad\quad\quad (m-2) \\ \end{matrix} \begin{bmatrix} -[\phi_2]^T [TFf] & [0] \end{bmatrix} \} n \quad .$$

The force compatibility conditions, (A-14), are contained in equation (A-17); however, there are displacement relationships yet to be included. The ground constraints for the actuators are relieved and deflection compatibility conditions are implemented by a transformation which will be applied to equation (A-17).

Consider actuator 1 only for the time being and let the vectors $\vec{\rho}_a$ and $\vec{\rho}_b$ denote the displacements of ends a and b, respectively. These vectors are shown on Figure A-2. Then, take components of $\vec{\rho}_a$ and $\vec{\rho}_b$ along the undeformed actuator as follows

$$\vec{\delta}_a = (\vec{\rho}_a \cdot \vec{U}_1)\,\vec{U}_1$$

and

$$\vec{\delta}_b = (\vec{\rho}_b \cdot \vec{U}_1)\vec{U}_1 \quad . \tag{A-18}$$

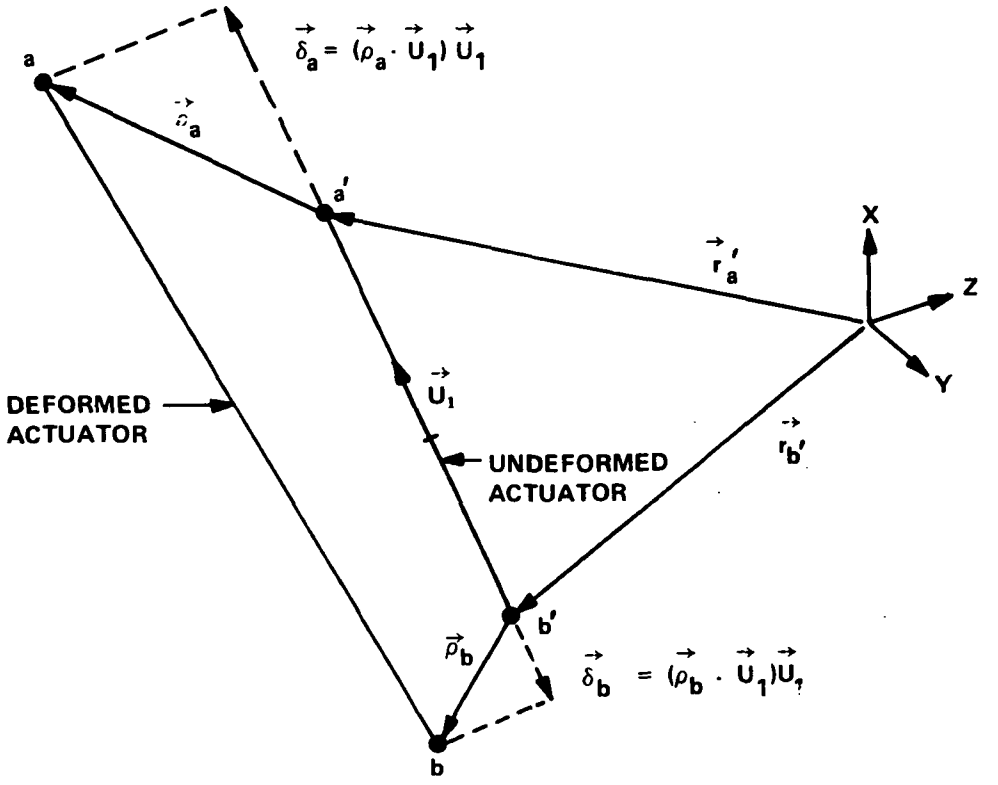

Figure A-2. Actuator geometry.

One assumes that the deflections will be small and relieve the ground constraint at point a by applying the expression

$$\vec{\delta}_b = \vec{\delta}_a + X_p(1)\,\vec{U}_1 \quad . \tag{A-19}$$

Substituting expressions (A-18) into (A-19) and solving for $X_p(1)$, one obtains

$$X_p(1) = \vec{U_1} \cdot (\vec{\rho_b} - \vec{\rho_a}) \quad . \tag{A-20}$$

The displacements at the actuator ends are equal to the displacement of the structural model (engine and backup structure). Using the mode shapes of the structural model to define the deflections of the structural model, one applies equation (A-2) and expresses the displacement compatibility conditions as:

$$\vec{\rho_a} = \{\rho_a\} = [\phi_a]\{q\}$$

and (A-21)

$$\vec{\rho_b} = \{\rho_b\} = [\phi_b]\{q\} \quad ,$$

where

$[\phi_a]$ = modal matrix whose rows correspond to the X, Y, Z displacements at point a,

$[\phi_b]$ = modal matrix whose rows correspond to the X, Y, Z displacements at point b.

Substituting expressions (A-21) into (A-20), one obtains

$$X_p(1) = [TXP1Q]\{q\} \quad , \tag{A-22}$$

where

$$[TXP1Q] = \{U_1\}^T \left([\phi_b] - [\phi_a]\right) \quad .$$

In a similar manner, the following expression is obtained for actuator 2:

$$X_p(2) = [TXP2Q]\{q\} \quad , \tag{A-23}$$

where

$$[TXP2Q] = \{U_2\}^T \left([\phi_d] - [\phi_c]\right) \quad .$$

Using equations (A-22) and (A-23), one can write the following transformation:

$$\begin{Bmatrix} \{q\} \\ \hline f(1) \\ f(2) \\ X_p(1) \\ Q_v(1) \\ \text{Dummy} \\ \text{Dummy} \\ X_p(2) \\ Q_v(2) \\ \text{Dummy} \\ \text{Dummy} \end{Bmatrix} = \left[\begin{array}{c|c} [I] & [0] \\ \hline \begin{bmatrix} 0 \\ 0 \\ [TXP1Q] \\ 0 \\ 0 \\ 0 \\ [TXP2Q] \\ 0 \\ 0 \\ 0 \end{bmatrix} & \begin{bmatrix} 1 & 0 & 0 & 0 & 0 & 0 & 0 & 0 \\ 0 & 1 & 0 & 0 & 0 & 0 & 0 & 0 \\ 0 & 0 & 0 & 0 & 0 & 0 & 0 & 0 \\ 0 & 0 & 1 & 0 & 0 & 0 & 0 & 0 \\ 0 & 0 & 0 & 1 & 0 & 0 & 0 & 0 \\ 0 & 0 & 0 & 0 & 1 & 0 & 0 & 0 \\ 0 & 0 & 0 & 0 & 0 & 0 & 0 & 0 \\ 0 & 0 & 0 & 0 & 0 & 1 & 0 & 0 \\ 0 & 0 & 0 & 0 & 0 & 0 & 1 & 0 \\ 0 & 0 & 0 & 0 & 0 & 0 & 0 & 1 \end{bmatrix} \end{array}\right] \begin{Bmatrix} \{q\} \\ \hline f(1) \\ f(2) \\ Q_v(1) \\ \text{Dummy} \\ \text{Dummy} \\ Q_v(2) \\ \text{Dummy} \\ \text{Dummy} \end{Bmatrix} ,$$

or, more concisely,

$$\begin{Bmatrix} \{q\} \\ \{\delta\} \end{Bmatrix} = [\psi] \begin{Bmatrix} \{q\} \\ \{\xi\} \end{Bmatrix} \quad . \tag{A-24}$$

Substituting equation (A-24) into equation (A-17) and premultiplying by $[\psi]^T$, one obtains the equations of motion for the combined structural and actuator systems as

$$[A^*] \begin{Bmatrix} \{\ddot{q}\} \\ \{\ddot{\xi}\} \end{Bmatrix} + [B^*] \begin{Bmatrix} \{\dot{q}\} \\ \{\dot{\xi}\} \end{Bmatrix} + [C^*] \begin{Bmatrix} \{q\} \\ \{\xi\} \end{Bmatrix} = [D^*]\{F_e(t)\} \quad , \tag{A-25}$$

where

$$[A^*] = [\psi]^T \begin{bmatrix} [I] & [0] \\ [0] & [\alpha] \end{bmatrix} [\psi] \quad ,$$

$$[B^*] = [\psi]^T \begin{bmatrix} [2\xi_i\omega_i] & [0] \\ [0] & [\beta] \end{bmatrix} [\psi]$$

$$[C^*] = [\psi]^T \begin{bmatrix} [\omega_i^2] & [D_2] \\ [0] & [\gamma] \end{bmatrix} [\psi] \quad ,$$

$$[D^*] = [\psi]^T [D_1] \quad .$$

It can be shown that the rows and columns of [A*], [B*], and [C*] which correspond to f(1) and f(2) must necessarily be zero. Likewise the rows of [D*] corresponding to f(1) and f(2) must necessarily be zero. [The coupling procedure could have been accomplished by solving equation (A-13) for f(1), f(2) and inserting into equation (A-15), thus eliminating f(1), f(2)]. As an error check, the rows and columns corresponding to f(1) and f(2) are examined for nullness in the computer program. By collapsing the null rows and columns from the matrices, one obtains the equations of motion for the transient response as:

$$[A]\begin{Bmatrix}\{\ddot{q}\}\\ \{\ddot{p}\}\end{Bmatrix}+[B]\begin{Bmatrix}\{\dot{q}\}\\ \{\dot{p}\}\end{Bmatrix}+[C]\begin{Bmatrix}\{q\}\\ \{p\}\end{Bmatrix}=[D]\{F_e(t)\} \quad , \tag{A-26}$$

where

$$\{\ddot{p}\}\begin{Bmatrix}\ddot{Q}_v(1)\\ \dot{Q}_{dpf}(1)\\ \dot{X}_i(1)\\ \ddot{Q}_v(2)\\ \dot{Q}_{dpf}(2)\\ X_i(2)\end{Bmatrix};\ \{\dot{p}\}=\begin{Bmatrix}\dot{Q}_v(1)\\ Q_{dpf}(1)\\ X_i(1)\\ \dot{Q}_v(2)\\ Q_{dpf}(2)\\ X_i(2)\end{Bmatrix};\ \{p\}=\begin{Bmatrix}Q_v(1)\\ \text{Dummy}\\ \text{Dummy}\\ Q_v(2)\\ \text{Dummy}\\ \text{Dummy}\end{Bmatrix}$$

and [A], [B], [C], [D] are obtained from [A*], [B*], [C*], [D*] by removing the null rows and columns corresponding to f(1), f(2).

The transient response equation (A-26) is solved numerically for

$$\begin{Bmatrix}\{\ddot{q}\}\\ \{\ddot{p}\}\end{Bmatrix},\begin{Bmatrix}\{\dot{q}\}\\ \{\dot{p}\}\end{Bmatrix} \quad , \text{ and } \begin{Bmatrix}\{q\}\\ \{p\}\end{Bmatrix}$$

at incremental times using FORMA subroutine TR2. This subroutine uses a third-order Newmark-Chan-Beta numerical integration procedure.[5] The transient response solution is saved and used in load transformation equations to obtain the transient loads experienced by the system.

TRANSIENT LOADS ANALYSIS

The equations used to obtain internal loads (shear, bending moment, torsion, etc.) are developed herein. A loads transformation matrix, [LTM], is available from the vibration analysis. This matrix transforms the total force acting at some time, t, to the internal loads, thus:

$$\{L(t)\} = [LTM]\{F(t)\} \quad , \tag{A-27}$$

where

$\{L(t)\}$ = vector of internal loads,

$[LTM]$ = force loads transformation matrix,

$\{F(t)\}$ = total force vector, (includes inertial and applied forces).

We know that the total force acting on a structural system can be determined from the displacement as follows:

$$\{F(t)\} = [K]\{h(t)\} \quad . \tag{A-28}$$

5. Chan, S. P.; Cox, H. L.; and Benefield, W. A.: Transient Analysis of Forced Vibrations of Complex Structural-Mechanical Systems. J. Roy. Aeron. Soc., July 1962.

Substituting equation (A-1) into equation (A-28) yields

$$\{F(t)\} = -[M]\{\ddot{h}(t)\} - [D]\{\dot{h}(t)\} + \{F_e(t)\} + \begin{Bmatrix} F_b(t) \\ F_d(t) \\ F_a(t) \\ F_c(t) \end{Bmatrix} . \quad (A-29)$$

Now, neglect the dissipative forces (generally conservative assumption) and substitute equation (A-2) into equation (A-29) and obtain

$$\{F(t)\} = -[M][\phi]\{\ddot{q}(t)\} + \{F_e(t)\} + \begin{Bmatrix} F_b(t) \\ F_d(t) \\ F_a(t) \\ F_c(t) \end{Bmatrix} . \quad (A-30)$$

Substituting equation (A-30) into equation (A-27) yields the following expression for internal loads:

$$\{L(t)\} = -[LTM][M][\phi]\{\ddot{q}(t)\} + [LTM1]\{F_e(t)\} + [LTM2]\begin{Bmatrix} F_b(t) \\ F_d(t) \\ F_a(t) \\ F_c(t) \end{Bmatrix} \quad (A-31)$$

where

[LTM1] = submatrix of [LTM] whose columns correspond to X, Y, Z forces at point e,

[LTM2] = submatrix of [LTM] whose columns correspond to X, Y, Z forces at points b, d, a, and c, respectively.

Substituting equation (A-14) into equation (A-31) yields

$$\{L(t)\} = -[LTMMP]\{\ddot{q}(t)\} + [LTM1]\{F_e(t)\} + [LTM2][TFf]\{f(t)\} \quad , \tag{A-32}$$

where

$$[LTMMP] = [LTM]\,[M]\,[\phi] \quad .$$

Now referring to Figure 5, the actuators forces f(1), f(2) can be written as

$$\begin{aligned} f(1) &= M_p(1)\,\ddot{X}_p(1) - K_o(1)\,X_i(1) + K_o(1)\,X_p(1) \\ f(2) &= M_p(2)\,\ddot{X}_p(2) - K_o(2)\,X_i(2) + K_o(2)\,X_p(2) \end{aligned} \quad . \tag{A-33}$$

We know from equation (A-26) that

$$\begin{aligned} X_i(1) &= \dot{p}(3) \\ X_i(2) &= \dot{p}(6) \end{aligned} \quad .$$

Then using equations (A-22) and (A-23), one can write expressions (A-33) in matrix form as follows:

$$\{f(t)\} = \begin{Bmatrix} f(1) \\ f(2) \end{Bmatrix} = \begin{bmatrix} M_p(1) & 0 \\ 0 & M_p(2) \end{bmatrix} \begin{bmatrix} \lfloor TXP1Q \rfloor \\ \lfloor TXP2Q \rfloor \end{bmatrix} \{\ddot{q}\}$$

$$+ \begin{bmatrix} -K_o(1) & 0 \\ 0 & -K_o(2) \end{bmatrix} \begin{Bmatrix} \dot{p}(3) \\ \dot{p}(6) \end{Bmatrix} + \begin{bmatrix} K_o(1) & 0 \\ 0 & K_o(2) \end{bmatrix} \begin{bmatrix} \lfloor TXP1Q \rfloor \\ \lfloor TXP2Q \rfloor \end{bmatrix} \{q\} \quad . \text{(A-34)}$$

A more convenient form of equation (A-34) is expressed as follows:

$$\{f(t)\} = [a] \begin{Bmatrix} \{\ddot{q}\} \\ \{\ddot{p}\} \end{Bmatrix} + [b] \begin{Bmatrix} \{\dot{q}\} \\ \{\dot{p}\} \end{Bmatrix} + [c] \begin{Bmatrix} \{q\} \\ \{p\} \end{Bmatrix} \quad , \qquad \text{(A-35)}$$

where

$$[a] = \left[\begin{array}{c|cccccc} \multicolumn{1}{c|}{\overleftarrow{\quad n \quad}} & \multicolumn{6}{c}{\overrightarrow{\quad\quad 6 \quad\quad}} \\ M_p(1)\lfloor TXP1Q \rfloor & 0 & 0 & 0 & 0 & 0 & 0 \\ M_p(2)\lfloor TXP2Q \rfloor & 0 & 0 & 0 & 0 & 0 & 0 \end{array}\right] ,$$

$$[b] = \left[\begin{array}{c|ccccccc} 0 & 0 & 0 & -K_o(1) & 0 & 0 & 0 & 0 \\ 0 & 0 & 0 & 0 & 0 & 0 & -K_o & 2 \end{array}\right] ,$$

$$[c] = \left[\begin{array}{c|cccccc} K_o(1)\lfloor TXP1Q \rfloor & 0 & 0 & 0 & 0 & 0 & 0 \\ K_o(2)\lfloor TXP2Q \rfloor & 0 & 0 & 0 & 0 & 0 & 0 \end{array}\right] .$$

Substituting equation (A-35) into equation (A-32) yields the following expression:

$$\{L(t)\} = -[LTMMP]\{\ddot{q}(t)\} + [LTM1]\{F_e(t)\} + [LTM2][TFf][a]\begin{Bmatrix}\{\ddot{q}\}\\ \{\ddot{p}\}\end{Bmatrix}$$

$$+ [LTM2][TFf][b]\begin{Bmatrix}\{\dot{q}\}\\ \{\dot{p}\}\end{Bmatrix} + [LTM2][TFf][c]\begin{Bmatrix}\{q\}\\ \{p\}\end{Bmatrix} . \qquad (A-36)$$

Finally, one can express equation (A-36) in a form convenient for solution using the FORMA library as

$$\{L(t)\} = [AA]\begin{Bmatrix}\{\ddot{q}\}\\ \{\ddot{p}\}\end{Bmatrix} + [BB]\begin{Bmatrix}\{\dot{q}\}\\ \{\dot{p}\}\end{Bmatrix} + [CC]\begin{Bmatrix}\{q\}\\ \{p\}\end{Bmatrix} + [DD]\{F_e\} \quad , \qquad (A-37)$$

where

$$[AA] = \left(\left[-[LTMMP]\,\vdots\,[0]\right] + [LTM2][TFf][a]\right) \quad ,$$

$$[BB] = [LTM2][TFf][b] \quad ,$$

$$[CC] = [LTM2][TFf][c] \quad ,$$

$$[DD] = [LTM1] \quad .$$

The solution of the transient response equation (A-26) applied in equation (A-37) yields the transient-internal loads. Acceleration and displacement responses can be obtained directly by solving equation (A-2). That is, displacements are computed as

$$\{h(t)\} = [\phi]\{q(t)\}$$

and accelerations are computed as

$$\{\ddot{h}(t)\} = [\phi]\{\ddot{q}(t)\} \quad .$$

APPROVAL

SSME/SIDE LOADS ANALYSIS FOR FLIGHT CONFIGURATION

By Wayne Holland

The information in this report has been reviewed for security classification. Review of any information concerning Department of Defense or Atomic Energy Commission programs has been made by the MSFC Security Classification Officer. This report, in its entirety, has been determined to be unclassified.

This document has also been reviewed and approved for technical accuracy.

R. S. RYAN
Chief, Structural Dynamics Division

for J. A. LOVINGOOD
Director, Systems Dynamics Laboratory

☆U.S. GOVERMENT PRINTING OFFICE 1974 – 640-447 / 133 REGION NO. 4